POLISH ACADEMY OF SCIENCE
COMMITTEE FOR ELECTRONICS AND TELECOMMUNICATIONS

ELECTRONICS AND TELECOMMUNICATIONS QUARTERLY

KWARTALNIK ELEKTRONIKI I TELEKOMUNIKACJI

VOLUME 54 – No 2

WARSAW 2008

Addres of Editorial Office
00-665 Warszawa, ul. Nowowiejska 15/19 Politechnika, pok. 470
Instytut Telekomunikacji, Gmach im. prof. JANUSZA GROSZKOWSKIEGO

Editor-on-duty
Mondays and Wednesdays
From 2pm to 4pm
Phone number: (022) 234 77 37

Telephone numbers
Editor-in-Chief: (022) 825 15 80; (022) 234 73 30
Responsible Secretary: 0500044131
www.tele.pw.edu.pl/keit

Ark. wyd. 10,25 Ark. druk. 8,25	Podpisano do druku w lipiec 2008 r.
Papier offset, kl. III 80 g. B-1	Druk ukończono w lipiec 2008 r.

Publishing
Warszawska Drukarnia Naukowa PAN
00-656 Warszawa, ul. Śniadeckich 8
Tel./fax 628-87-77

IMPORTANT MESSAGE FOR THE AUTHORS

The Editoral Board during their meeting on the 18th of January 2006 authorized the Editoral Office to introduce the following changes:

1. PUBLISHING THE ARTICLES IN ENGLISH LANGUAGE ONLY

Starting from No 1'2007 of E&T Quarterly, all the articles will be published in English only.

Each article prepared in English must be supplemented with a thorough summary in Polish (e.g. 2 pages), including the essential formulas, tables, diagrams etc. The Polish summary must be written on a separate page. The articles will be reviewed and their English correctness will be verified.

2. COVERTING THE PUBLISHING EXPENSES BY AUTHORS

Starting from No'2007 of E&T Quarterly, a principle of publishing articles against payment is introduced, assuming non-profit making editorial office. According to the principle the authors or institutions employing them, will have to cover the expenses in amount of 760 PLN for each publishing sheet. The above amount will be used to supplement the limited financial means received from PAS for publishing; particularly to increase the capacity of next E&T Quarterly volumes and verify the English correctness of articles. It is neccessary to increase the capacity of E&T Quarterly volumes due to growing number of received articles, which delays their publishing.

In case of authors written request to accelerate the publishing of an article, the fee will amount to 1500 PLN for each publishing sheet.

In justifiable cases presented in writting, the editorial staff may decide to relieve authors form basic payment, either partially or fully. The payment must be made by bank transfer into account of Warsaw Science Publishers The account number: Bank Zachodni WBK S.A. Warszawa Nr 94 1090 1883 0000 0001 0588 2816 with additional note: "For Electronics and Telecommunications Quarterly".

Editors

Dear Authors,

Electronics and Telecommunications Quarterly continues tradition of the "Rozprawy Elektrotechniczne" quarterly established 54 years ago.

The E&T Quarterly is a periodical of Electronics and Telecommunications Committee of Polish Academy of Science. It is published by Warsaw Science Publishers of PAS. The Quarterly is a scientific periodical where articles presenting the results of original, theoretical, experimental and reviewed works are published. They consider widely recognised aspects of modern electronics, telecommunications, microelectronics, optoelectronics, radioelectronics and medical electronics.

The authors are outstanding scientists, well-known experienced specialists as well as young researchers – mainly candidates for a doctor's degree.

The articles present original apporaches to problems, interesting research results, critical estimation of theories and methods, discuss current state or progress in a given branch of technology and describe development prospects. The manner of writing mathematical parts of articles complies with IEC (International Electronics Commision) and ISO (International Organization of Standardization) standards.

All the articles published in E&T Quarterly are reviewed by knows, domestic specialists which ensures that the publications are recognized as author's scientific output. The publishing of research work results completed within the framework of *Ministry of Science and Higher Education* GRANT's meets of the requirements for those work.

The periodical is distributed among all thóse who deal with electronics and telecommunications in national scientific centres, as well as in numeral foreign institutions. Moreover it is subscribed by many specialists and libraries.

Each author is entitled to free of charge 20 copies of article, which allows for easier distribution to persons and institutions domestic and abroad, individually chosen by the author. The fact that the articles are published in English makes the quarterly even more accessible.

The articles received are published within half a year if the cooperation between author and the editorial staff is efficient. Instructions for authors concerning the form of publications are included in every volume of the quarterly; they may also be otained in editorial office.

The articles may be submitted to the editorial office personally or by post; the editorial office address is shown on editorial page in each volume.

Editors

CONTENTS

The a
fiber
resear
societ
that t
of the
streng
back
meani
count
profes
and e
proce

S
resear
–The
1988,
the ye

Photonics Society of Poland established

Warsaw, June 2008

Each bigger research and technical community in this country and elsewhere has its own representation inside the social space in a form of a professional society. Either the society has a broad topical extent covering the whole community activities or it is a number of narrow topical societies each active in their own fields. The subject of activity of a professional society is usually: expertise in the field, training, social, publishing, cooperation and integration, information, etc. The above concerns also the national research and technical community of optics, optical fiber communications, laser technology, optoelectronics and photonics. Some time ago, the research, technical and industrial communities in this country were organized in professional societies within a formal framework of the Federation of Engineering Associations. Since that time the federation has never regained its high administrative meaning. The president of the federation was at that time a deputy prime minister of the country. Today, such a strengthening of research, technical and hi-tech communities and industries, through giving back this high role for a renewed Federation of Engineering Associations might have other meaning, other influence and would give other possibilities. There is a clear need in this country for strong consolidation and rebuilding of the self-organization of the technical professional communities. They have to accommodate themselves to the dynamic changes and evolutions of the contemporary society of knowledge. A clear reflection of these vivid processes is a formation of the Photonics Society of Poland (PSP).

TRANSFORMATION OF SPIE POLAND CHAPTER TO PSP

Since the first half of 2007, there have been carried out formal endeavors by the national research and technical communities of photonics to transform the Poland Chapter of SPIE –The International Society for Optical Engineering (SPIE-PL) [www.spie.pl], existing since 1988, into the Photonics Society of Poland (PSP) [www.photonics.pl]. During the turn of the year 2007/2008 and at the beginning of 2008, the Administrative Court for Warsaw, after

some changes and improvements in the bylaws and after two plenary meetings of the Society members approved the change in the name and the new bylaws of the new (transformed) research and technical Society. Prof. T. Woliński of WUT [www.if.pw.edu.pl/~opto] ws elected the first president of PSP. The headquarters of PSP is the Faculty of Physics, Warsaw University of Technology [www.if.pw.edu.pl]. The PSP has applied to the court for the right to start and run business activities. It will soon apply to be elevated to the status of a society of a higher public service. PSP has now more than 200 members, mainly from the academic world and from governmental institutes, and still too small number of members from industrial, business and administration communities. The PSP members originate from the whole country but the majority come from the following large academic centers: Warsaw, Wroclaw, Poznan, Lublin, Bialystok, Krakow, Gdansk, High Silesia, Szczecin, Rzeszow, Lodz. The PSP is open for international and corporate members. The aim of the PSP is integration of the national research and technical community of photonics and undertaking important actions, from the point of research, technical, financial, organizational, business and political point of view, in the name and on behalf of the whole national professional photonics community in relation to the industry, local and national administration, international partners, European programs, consortia and technological platforms, etc.

INTEGRATION ACTIVITIES OF THE NATIONAL RESEARCH AND TECHNICAL COMMUNITY OF OPTICS AND OPTOELECTRONICS

Establishment of the Photonics Society of Poland is a crowning achievement in a long lasting organization, technical and research activity of the national community of optics, optoelectronics and photonics in order to coordinate common endeavors in this country. At the beginning of the 80s there were undertaken in this country some attempts, by INOS – Institute of Applied Optics, PTF – Polish Physical Society and WUT – Warsaw University of Technology, to establish an Optical Society of Poland. These trials were, at that time, not successful enough. In the middle of the 70s, the Committee of Electronics and Communications [keit.pan.pl] of Polish Academy of Sciences has established a Section of Optoelectronics with Working Groups on Optical Fiber Technology, Integrated Optics and Optoelectronic Sensors. This body organized during the years of 1976, 1979, 1982 (shifted to 1983), 1986 the first, second third and the fourth National Symposia on "Optical Fibers and Their Applications" in Jabłonna. The Section of Optoelectronics organized also the National Symposia on Laser Technology in Szczecin/Świnoujście. The SPIE was present during all of these conferences in a form of tabletop SPIE literature exhibits organized from the beginning by SPIE sympathizers and next members. The Polish Optoelectronics Committee (PKOpto) of SEP – Association of Polish Electrical Engineers was established in 1985 [ww.sep.com.pl]. There were only few members of international optical organizations, in this country, at the beginning of the 80s, like SPIE [spie.org], OSA -Optical Society of America [www.osa.org], LIA – Laser Institute of America [www.laserinstitute.org], IEEE – LEOS-Laser and Electro-Optics Society [www.ieee.org/portal/site/leos/], and later EOS – European Optical

Society [www.europeanopticalsociety.org]. A very concrete results emerged from the initial talks and technical, research and organization activities between Polish researchers and SPIE, Bellingham, WA, USA. These difficult contacts were carried out done at conditions of incompatibility of the currencies.

Individual contacts with SPIE of persons from academic and governmental institutes in this country go back as far as to 1976. More official talks, between professional societies of SPIE and SEP started in 1982. During the years 1982-1985 the talks resulted in formation in this country of a Polish Group of SPIE Members, gathering above 10 persons. The activity of this Group resulted in participation of a number of persons from Poland in SPIE conferences in Los Angeles (1982), Stuttgart (1984), Boston, San Diego, Paris, Hague, Hamburg, organization of small exhibits during some of SPIE symposia, publishing of the first papers from Polish optical research community in the Proceedings of SPIE (vols. 403-404 from 1983), publishing of the first „Polish" volume of Proc.SPIE (vol 670 from 1986), the first visit of SPIE representatives from the SPIE headquarters with executive secretary Joseph Yaver in Poland. The Polish Group of SPIE Members was officially affiliated with the PKOpto, SEP in 1985 and approved by the Boards of both societies SPIE and SEP. During this period, the Polish Group of SPIE Members, chaired by the late professor Adam Smoliński, was reporting periodically, two times a year, about their activities at the plenary meetings of PKOpto SEP, then very frequently attended by the professional optics community.

ACTIVITY OF SPIE POLAND CHAPTER

The Polish Group of SPIE Members was transformed into SPIE Poland Chapter in 1988 (SPIE-PL). A legal technical association under the name of Polish Chapter of the International Society for Optical Engineering was registered then by the administrative court [www.spie.pl]. During the first period the SPIE-PL was chaired by prof A.Smoliński and then by prof.M.Pluta. The SPIE headquarters were situated in the Institute of Applied Optics, during the period of 1990-2002. During the period of 1986-2008, the Polish Group of SPIE Members, then SPIE-PL and now PSP published over 200 volumes of Proc. SPIE. In 2005, the SPIE-PL in cooperation with SPIE headquarters organized a large Middle-European Congress on Optics and Optoelectronics at Warsaw University of Technology. The congress consisted of 14 combined topical conferences. It was well attended by more than 700 professionals from all over the world. Long lasting, very active, profitable for all sides and frank contacts of the Polish photonics community, since 1988 organized in SPIE-PL, with the SPIE headquarters, were one of the major foundations of nomination for prof. Malgorzata Kujawinska of WUT in 2005 for the first woman and the first non-American president of the SPIE. During her presidency prof. M.Kujawinska wrote her name down in golden letters in the history of this great engineering society of global extent

A number of professionals from Poland were awarded, during these years, the prestigious titles of the Fellow of SPIE. These important professional distinction titles stem definitely from

the individual virtues of the awarded researchers but there was also a strong supporting factor caused by unprecedented and incomparable activity of the SPIE-PL. Fellowship in the society is awarded for individual scientific achievements and the process goes through a few international reviewers. The Polish SPIE Fellows are professors: Maksymilian Pluta-INOS (1992), Ryszard Romaniuk-WUT (1993), Antoni Rogalski-MUT (1995), Romuald Jóźwicki-WUT (1995), Małgorzata Kujawińska-WUT (1997), Krzysztof Patorski-WUT (1998), Tadeusz Kryszczyński-INOS (2001), Katarzyna Chałasińska-Macukow-WU (2003), Leszek Jaroszewicz-MUT (2003), Andrzej Domański-WUT (2004), Tomasz Woliński-WUT (2004), Tomasz Szoplik-WU (2006), Wacław Urbańczyk-WrUT (2007).

ACTIVITY PLANS OF PHOTONICS SOCIETY OF POLAND FOR NATIONAL AND REGIONAL PROFESSIONAL COMMUNITY

It seems that in the circumstances, which the science is now in this country, the Photonics Society of Poland has to fulfill important function for the integration, efficiency increase and reconfiguration of the local research, technical, business and administration communities in photonics. In the framework of this policy the PSP has undertaken recently a number of initiatives. Some of them are continuation of the activities of SPIE-PL and some of them are quite new. Some of these ideas are described below. They embrace endeavors in the field of European cooperation, industrial, academic, educational, conferences, continuous training, publishing, organizational and lobbying.

NATIONAL COOPERATION

The most important foundation of PSP existence is domestic activity and cooperation. It seems that by gathering relevant representatives of all national communities, the PSP has a chance to work out a common platform for the constructive actions of such organizations in the similar fields (with their permission) like: Polish Committee of Optoelectronics of SEP (chair prof W.L.Wolinski-WUT), Section of Optoelectronics, Committee of Electronics and Telecommunications PAS (chair prof T.R.Wolinski-WUT), Section of Optics, Polish Physical Society (chair prof. Henryk Kasprzak-WrUT), Section of Metrology (previously also Section of Optics) SIMP – Polish Association of Mechanical Engineers [www.simp.pl], Polish Association of Synchrotron Radiation [www.synchrotron.org.pl/], Polish Association of Sensor Technology [www.ptts.pl], IEEE-LEOS Chapter Poland (chair. prof. Sergiusz Patela-WrUT), OSA Member Group in Poland, Student Chapters of SPIE, OSA and IEEE in Poland, Polish Technological Platforms (Advanced Materials – IWC PAN, Opto and Nanoelectronics – NOT), Consortium of Polish Optoelectronics – ITME [www.optoelektronika.com.pl], NOT – Federation of Engineering Associations , and others. The proposed platform of cooperation concerns mainly building of a practical industrial coalition in this country in the frames of operational programs, structural, topical, ordered and other European ones.

INTERNATIONAL COOPERATION

The international cooperation of the Photonics Society of Poland embraces primarily the SPIE Institute. It is also directed towards other societies of global extent like: OSA, IEEE, LEOS, EOS, national associations of optics, optoelectronics and photonics like: DGaO – Deutsche Gesellschaft fur angewandte Optik [www.dgao.de], analogous associations in the UK, France, Russia and in all neighboring countries. The international cooperation includes also optics industry active in the European scale as European Technology Platform Photonics 21 [www.photonics21.org], and others.

COOPERATION WITH SPIE

A special meaning for the Photonics Society of Poland is close cooperation with SPIE. PSP extends its activities beyond the boundaries of its own country, especially to the neighboring regions. Despite that it remains a local association representing the profession in this country and this geographical region. The Institutes like IEEE, SPIE, OSA have different duties to fulfill, but to a large extent complementary to the duties of local societies like PSP. Speaking of any competition between global and local societies, as it is put forward by some opponents of cooperation and globalization, is a complete misunderstanding. An important role of PSP may be supporting SPIE in building a global network or federation of local professional societies in optics, optoelectronics, photonics and related fields. As for now there does not exist such a global federation. This is caused probably by various reasons, and among others, by misunderstanding the difference in the character of activity scales on the global and local levels. It is clearly seen that there are a lot chances for the global community integration. The closest to this global character is perhaps the IEEE, however, not due to its federation character but the size. If the SPIE Institute is going to be brave enough to undertake this difficult, challenging and looking far into the future endeavor, to start building a global professional federation of photonics (because this is a duty for one of the global societies, which has to fill a role of a crystallization triggering center for the process), the PSP would be more than ready, with all its strength and devotion, to participate in this important process of reconfiguration of the professional intellectual resources of the world. In some foreseeable future, without this kind of consolidation, the progress may be slowed down or endangered.

RAPID INTERNET PUBLICATION – PHOTONICS LETTERS

One of the main intentions of the Photonics Society of Poland is to launch, in close cooperation with SPIE a rapid Internet publication: Photonics Letters (PL) – A publication of the PSP. The simplest way to start the journal would be by using the existing infrastructure like MYSPIE paper management and publication web engine [myspie.org] and a large publication database SPIEDL [spiedl.org]. These systems are analogous to other interactive publication

databases run by other societies like: OpticsInfoBase by OSA and Xplore by the IEEE, but also Versita Internet publications. A totally Internet based publication, without accompanying printed version, identified by on-line ISSN ID, would publish very fast, initially faster than a month, very short, four pages long, research and technical letters, of the internal structure of the full length paper. Photonics Letter would not compete with any international journal issued locally and indexed by the ISI Thomson Scientific like: Optica Applicata – published by Wroclaw Uni.Technology [www.if.pwr.wroc.pl/~optappl] and Opto-Electronics Review – published by MUT in cooperation with Versita and Springer [www.versita.com/science/physics/oer/], [www.springerlink.com/content/120191/]. Photonics Letters would supplement these regular journals initially in the local scale and then perhaps more widely. Photonics Letters would be more similar to the kind of publication represented by global and very successful Optics Express run by OSA [www.opticsexpress.org].

The PSP has nominated Editorial Board of a new rapid Internat publication. Each person in the EB of Photonics Letters is responsible for a narrow subject, coherent with the scientific expertise of a particular person. The EB of Photonics Letters consists of the following photonics experts, university professors: Krzysztof Abramski, WrUT, (laser photonics A); Rajmund Bacewicz, WUT (photovaltaice); Anna Cysewska-Sobusiak, PUT (photonics applications); Roman Dąbrowski, MUT (liquid crystal photonics); Andrzej Domański, WUT (polarization photonics); Jan Dorosz, BUT, (nontelecom photonics, lighting); Leszek Jaroszewicz, MUT, (photonic sensors); Zbigniew Jaroszewicz, INOS, (diffraction photonics); Mirosław Karpierz, WUT, (nonlinear and integrated photonics); Bogdan Kosmowski, GUT, (dispay photonics); Andrzej Kowalczyk, UMK, (biomedical and image photonics), Małgorzata Kujawińska, WUT, (interferometry and photonics metrology); Jan Rayss, UMCS, (photonic matetrials); Antoni Rogalski, MUT, (infrared photonics); Ryszard Romaniuk, WUT, editor-in-chief, (optical fiber photonics, high energy photonics); Tomasz Szoplik, WU, (metamaterial photonics; Andrzej Zając, BUT and MUT, (laser photonics B). The International Advisory Board of Photonics Letters, is under establishment. It is chaired by prof. T.R.Woliński. The aim of the IAB is to help the Photonics Letters in international field.

EDITORIAL SERIES "PROCEEDINGS OS SPIE"

Photonics Society of Poland would maintain good and long lasting tradition (since 1986) to cooperate with SPIE publications. The editorial series of SPIE Proceedings embraces nearly 8000 volumes and nears fast to a magic number of 500000 papers. The annual rate of the increase in the number of volumes is 350-450 with average contents of a volume reaching over 60. It is decisively one of the most frequently cited optics, optoelectronics and photonics publication series in the world. Proc. SPIE are indexed by all major research and technical publication databases. During the last years, a few Proc. SPIE volumes annually were published from national and international photonics conferences, which originated from Poland. During the most intense period of prof. M. Pluta activities as a chair of SPIE-PL, the number of volumes per year was well over ten. The series of Proc SPIE is, however, not a journal, thus, it is not

indexed by Master Journal List of ISI Thomson Scientific. A consequence in this country is that the Ministry of Science and Higher Education (MNiSW) values the papers published there only for two categorization points (previous edition of this list had four points for Proc.SPIE). This evaluation is not adequate to the objective meaning and weight of this publication series in the world photonics literature. The PSP undertakes relevant activities on the ministerial level trying to change this situation. Keeping the official evaluation on this low level would mean a complete withdrawal of Proc. SPIE from the local market of conference paper publications. The withdrawal of the most popular, the widest extent and technical impact, photonics publication series in the world, from the local market, would mean a major intentional step back in the development of the whole local photonics community.

CONFERENCES

A traditional area of SPIE-PL activity, and its follower the Photonics Society of Poland is organization, co-organization and sponsoring of scientific and technical conferences in the fields of optics, optoelectronics and photonics and related fields like: physics, simulation and design of components, metrology, construction of equipment, sensors, materials research, applications, etc. Inside an area of interest for the PSP, there are the following traditional conferences of the local photonics community: Optical Fibers and Their Applications, organized on exchange basis by Bialystok Uni.Technology and Lublin Uni.Technology as well as Optical Fiber Technology Lab. of Maria Curie-Skłodowska Uni. in Lublin; Laser Technology Symposium organized by Szczecin Uni.Technology in Świnoujście; Optoectronic and Electronic Sensors organized by the Polish Society of Sensor Technology [www.ptts.pl], Photonics Metrology Symposia series organized by the Institute of Applied Optics; traditional Polish-Czech-Slovak Symposium on Contemporary Optics; Photonics Symposium of Young Researchers WILGA organized by WUT in WILGA. The PSP would try to continue to organize, in cooperation with SPIE and relevant photonics societies in the neighboring countries, the cyclic, large Middle and East European Congresses on Optics and Optoelectronics.

RESEARCH PROGRAMS

One of the most important tasks for the Photonics Society of Poland is to initiate the executive consortia, technological platforms, industrial groups, and participation in the realization of research and industrial programs financed from the national and European funds in the area of photonics. There are some undertaken initiatives, concerning continuation of currently realized programs and new actions for future programs in the area of: optoelectronics for industry, environment protection, medicine and homeland security. The single aim is to look for concrete industrial results which stem from and then strongly rest on the local research efforts. The SPIE-PL and now PSP participates in a number of such programs of national, European and global extent, like: LEAP – Linking Europe and Asia in Photonics, NEMO – Network of Excellence in

Micro-Optics, and other. The task of PSP is to trace the developments in the ERA – European Research Area of all initiatives concerning the field of photonics. The aim is to activate the community and actively participate in these programs.

COOPERATION WITH SMALL AND MEDIUM ENTERPRISES

The area which can not be omitted in the activity of the Photonics Society of Poland as an effective professional association which serves well its community is technical expertise, business activities, cooperation with industry, linking university industry, cooperation with administration on various levels. Together with the development of the PSP an establishment of the Chamber of Photonics Experts is considered, if there is a demand for such services. The main concern is cooperation with relevant chambers of commerce, industry and trade. The PSP continues a more in-depth recognition of the domestic market for photonics products and services. The PSP prepared a questionnaire concerning the status of national photonics and sent it to more than 200 institutions including academic, governmental, administration, business and industrial ones. Till now, more than 70 answers were gathered. It shows the status of community integration and reveals some reserve for taking common decisions and actions of a wider extent. Certain lack of faith to take common actions on behalf of the whole community is observed, which stems from the recent changes in the role of universities, governmental laboratories, and primarily from large changes in the industry. There is not yet observed in this country a strong and active process of formation of small and medium businesses in narrowly defined and highly advanced technologies. PSP, via observation and analysis of these photonics market changes would try to support the favorable components of these complex processes. PSP would try to be an active participant and a sort of intermediary between academia, where young photonics experts are generated and business and industry worlds, where they are to be efficiently and creatively employed. The aim is to provide innovative photonic products needed on to the market.

M.SC. AND PH.D STUDENTS SECTIONS

Photonics Society of Poland is very close to all affairs combined with students and young researchers studying and developing photonics. PSP would always try to support students and young researchers by offering them fellowships, research awards, creating employment possibilities, etc. There will be continued a fruitful cooperation with Student Chapters of SPIE, OSA, IEEE. There are ideas to built own students organization. PSP stands for extending of the university curricula in photonics and related fields of nanotechnologies. It seems to be necessary to increase the number of promoted Ph.D. students in photonics in this country. There are now practical possibilities to internationalize considerably the educational models for Ph.D. students in such an advanced branch as the photonics.

INAUGURATION SYMPOSIUM OF PHOTONICS SOCIETY OF POLAND

The ceremonial Inauguration Symposium of the Photonics Society of Poland was held on 30th May – 1st June 2008. On 30th May there was organized a working meeting between the representatives of both cooperating societies SPIE and PSP. A draft of the memorandum of understanding was discussed during this meeting. The main symposium sessions were held in the Faculty of Physics on 31th May. The scientific program of the symposium embraced a number of plenary presentations delivered by the key experts in some of the most current fields of photonics: Philip Russel, Max Planck Inst., Nanoscale photonic structures in fibre form; Brian Culshaw, Strathclyde Univ., Fibre optic sensors, a perspective on science, technology and application; Allan Boardman, Univ. of Salford, Metamaterials: from concepts to applications; Andrzej Kowalczyk, Nicolaus Copernicus Univ., Optical coherence tomography in ophthalmology and art conservation. The technical program of the symposium embraced a couple presentations on the photonics community organization in Europe and in Poland: Małgorzata Kujawińska, PW, Photonics 21 – Advocating for optics and photonics in Europe; Ryszard Romaniuk, PW, Photonics Letters: Publication of the Photonics Society of Poland; Tomasz Woliński, PW Photonics and optical technologies in Poland. After the plenary sessions, there was an award ceremony and a reception. PSP awarded a few key persons from SPIE for promoting the long lasting and fruitful cooperation. The following persons were awarded: Joseph Yaver, previous Executive Director of SPIE; dr Emery Moore, 1990 SPIE President, prof Brain Culshaw, 2007 SPIE President, prof. Mieczysław Szustakowski, MUT, a member of the first Board of SPIE-PL in 1988. On 1 June, a delegation of both societies participated in a special student paper competition session in WILGA. The session was organized during the annual WILGA conference on Photonics and Web Engineering [wilga.ise.pw.edu.pl]. The awards for students were funded by SPIE.

COOPERATION OFFER

Photonics Society of Poland is ready to undertake a cooperation with every organization of public benefit, including local and national administration, industrial, business and lobbying, which has an aim of science and hi-tech industry development in Poland. The science development for the PSP means: chances for young, gifted people to fulfill successfully their own research career, creation of good working condition for the researchers, building of the modern research infrastructure, timely renewing of this infrastructure, creation of real and strong mechanisms of industry development, this industry which uses actively the results of applied research. PSP encourages individual persons working or interested in optics, optoelectronics and photonics to enroll.

Tomasz R. Woliński, Ryszard S. Romaniuk, on behalf of the psp board

Ceremonial Inauguration Symposium of the Photonics Sociaty of Poland. Faculty of Physics, Warsaw University of Technology, 31 May 2008; (L) there are standing l to r professors: A.Domański, L.Jaroszewicz, S.Kłosowicz, T.Kidger, E.Moore, M.Kujawińska, B.Culshaw, R.Romaniuk, T.Woliński; (P) Ms Krisinda Plenkovich from SPIE headquarters presents to prof. T.Woliński a commemorative plaque for the inauguration of PSP, in the presence of prof.B.Culshaw of Strathclyde Univ. in Glasgow.

ELECTRONICS AND TELECOMMUNICATIONS QUARTERLY, 2008, 54, no 2, pp. 107–111

XXII Symposium WILGA 2008 Web Engineering and Advanced Applications of Photonic and Electronic Systems

RYSZARD S. ROMANIUK

Warsaw University of Technology
Institute of Electronic System
R.Romaniuk@ise.pw.edu.pl

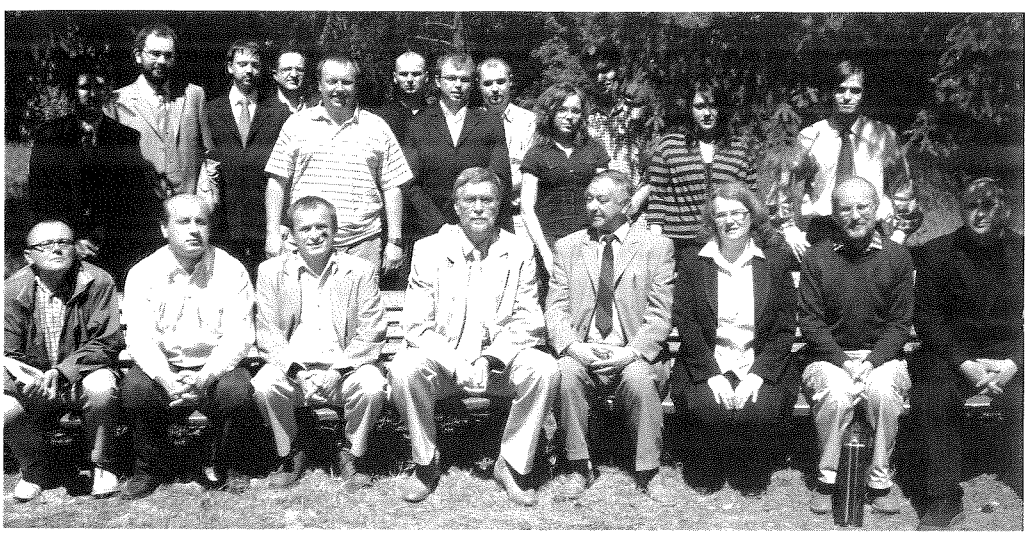

Friday 30 May 2008, WILGA, Warsaw University of Technology Resort; there are sitting (l to r): dr Robert Nietubyć – IPJ Świerk; Grzegorz Kasprowicz – CERN and ISE PW; Tomasz Pławski – Thomas Jefferson Laboratory, Newport News, VA, USA; dr Michał Borecki (standing), IMiO PW; prof. R.Romaniuk – ISE PW, WILGA Symposium Chaire; prof. T.Morawski – IR PW, palindromist; Katarzyna Rapacka, SPECTROPOL; dr J.Kalenik – IMiO PW; Dominik Rybka – ISE PW and IPJ Świerk, Chair of the Organization Committee of WILGA 2008 Symposium.

From 29th May till 1st June, in WILGA near Warsaw, there was held an annual Symposium on Web Engineering and Advanced Applications of Photonic and Electronic Systems. The Symposium was held this year for the first time under the auspices of a newly established Photonics Society of Poland PSP [www.photonics.pl] and cooperating organizations – Polish Committee of Optoelectronics PKOpto, Association of Polish Electrical Engineers SEP [www.sep.org.pl] and Section of Optoelectronics, Committee of Electronics and Telecommunications

Sunday 1 June 2008, WILGA, there are sitting (l to r): prof. Andrzej W.Domański – Treasurer of the Photonics Society of Poland PSP [photonics.pl], Faculty of Physics WUT, SPIE Fellow; prof Brian Culshaw – SPIE President 2007, Univ. of Strathclyde, Glasgow; dr R.Kossowski (standing) – WUT; Michał Ramotowski (standing) – ISE PW; Aneta Michalkiewicz (standing) – SPIE Student Chapter Coordinator; prof. Allan Boardman – Univ. of Salford, SPIE&OSA Fellow; prof. Ryszard S.Romaniuk – WUT, SPIE Fellow; Krisinda Plenkovich – SPIE Director of Education and Community Services, SPIE Headquarters, Bellingham, WA, USA [spie.org]; Tina Kidger – Kidger Optics Associates [www.kidger.com]; dr Emery L.Moore – SPIE President 1990 [elmonics.com]; prof Tomasz R.Woliński – President of the Photonics Society of Poland, SPIE Fellow; Faculty of Physics WUT, Tomasz Pławski – Jefferson Lab., USA.

KEiT, Polish Academy of Sciences PAN [keit.pan.pl]. The Symposium is held twice a year: during the last week of May in WILGA and during the next to the last weekend of January in Warsaw. This year Symposium is the eleventh meeting in WILGA Resort owned by Warsaw University of Technology. The first Symposium of this series was organized at the Faculty of Electronics and Information Technologies of WUT eleven years ago in January 1998. The second was held in WILGA in May 1998. The WILGA Symposia were organized under the wings of IEEE Poland Section, IEEE Region 8 Student Activities and SPIE Poland Chapter (transferred to Photonics Society of Poland in 2008). For several years, the WILGA Symposia have been international.

During these eleven years of WILGA Symposium continuity, the number of participants, mainly young researchers, reached over 3500. There were published 12 volumes of Proceedings of SPIE in the USA. These volumes contain around 1000 research and technical papers. In parallel, there were published together a few hundred papers in the national and international journals, including the ones indexed by the ISI in Philadelphia. The more than a decade technical achievement of WILGA Symposium is probably one of the biggest in comparison to similar international meetings of young researchers in this country. The WILGA Symposium is filling a few roles: it is a very current digest of the young science, it is absolutely free debating and comparison platform for young researchers, it is a good pattern for those starting their research and/or academic career, it is a place where the form and contents of more advanced young

researchers is friendly, politely but accurately polished, it is equally a place of meeting for the tutors and mentors of young researchers, Ph.D. and M.Sc. students, etc.

The organizers of WILGA Symposium are M.Sc. and Ph.D. students of Warsaw University of Technology who realize their theses with the PERG/ELHEP Research Group in the Institute of Electronic Systems as well as students associated in SPIE Student Branch of WUT, OSA, IEEE and in particular IEEE-LEOS. A chair of WILGA 2008 Organization Committee was Mr Dominik Rybka, a Ph.D. student of ISE PW and simultaneously an employee of the Sołtan Institute for Nuclear Problems in Świerk (IPJ) [www.ipj.gov.pl].

The WILGA 2008 Symposium gathered more than 150 participants out of a number of technical universities from around this country. More than 100 research and technical papers were presented. The participants were mainly M.Sc. and Ph.D. students, arriving to WILGA alone or with their tutors and mentors. In particular, WILGA is a kind of Ph.D. work digest realized by young researchers in the areas of web engineering, photonics, apparatus for high energy physics experiments. WILGA 2008 gathered, among others, representatives of the following technical universities: Warsaw, Białystok, Lublin, Gdańsk, Poznań, Łódź, Lublin.

The topical sessions of WILGA 2008 Symposium concerned mainly the following subjects: computer simulations in electronics and electrical engineering, construction of photonics and electronics apparatus for high energy physics experiments, optical fiber optoelectronics, European program WARMER – water resources protection in Europe, coherent and non-coherent optical tomography, design and construction of optimal learning systems, design of free electron laser machine, European programs – CARE, EuCARD, European XFEL, ILC, photonic optical fibers filled with liquid crystals, optoelectronic sensors, web engineering, and in particular development of wiki standard, etc.

Symposium proceedings will be published traditionally as a volume of Proc. SPIE. Some of the papers will be published in Electronics and Telecommunications Quarterly by PAS and in Elektronika monthly journal by SEP. A group of selected papers is usually published in international journals indexed by ISI.

Certain changes in Symposium organization and publication of proceedings are forced by the changes in the research ministry regulations concerning the list of categorization points for particular publications and journals. For example, the SPIE Proceedings used to have 4 points on the previous list while now they have only 2 points. This is in spite of the fact that Proc. SPIE are very broadly indexed, much broader in comparison to other similar publications. One can estimate that Proc.SPIE are around several % of the serious world publications in the field of photonics. Till today, there are around 8000 volumes of Proc. SPIE published and under preparations. Each volume has around 60 papers which gives together the biggest world publications database in photonics of around half a million papers. The national community of photonics, represented by the Photonics Society of Poland will apply to the ministry to reconsider the evaluation of Proc. SPIE for more categorization points. More than 200 Proc. SPIE volumes have been published as a result of the initiatives of SPIE Poland Chapter, since 1986.

Symposium was opened complementarily by the person writing these words, because WILGA is a Symposium organized by students for students. Faculty members present during the Symposium are only guests and do only a topical supervision of students activities and review

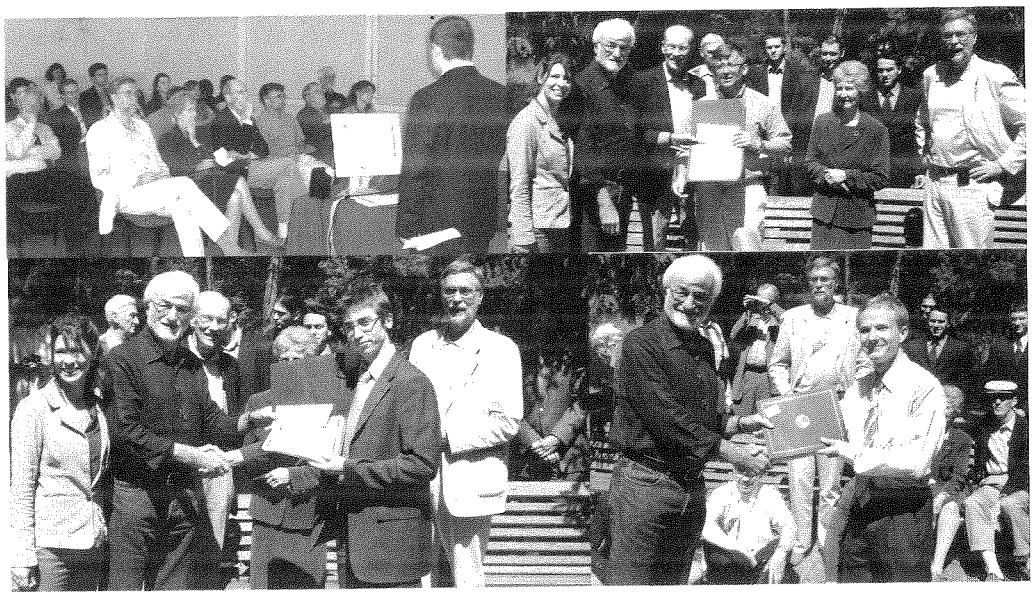

Sunday competitive session during WILGA 21008 Symposium with participation of SPIE Headquarters representatives. Professor Brian Culshaw from the Strathclyde University in Glasgow presents the SPIE awards for the best presenting students.

students papers. The opening presentation for WILGA Symposium usually concerns a summary of activities during the last academic year and plans for the next academic year of the young Research Group PERG/ELHEP ISE WUT. The Group consists of a few tens of young researchers active in web engineering and advanced applications of photonics and electronics systems.

A tradition of WILGA Symposium is that one of the keynote presentations is devoted to art, literature or humanities. Professor Tadeusz Morawski from the Institute of Radioelectronics WUT presented his research advances and literary work on palindromes. The presentation was triggered by the fifth book on palindromes written by this author. Finishing his very interesting presentation prof. T.Morawski, who is the most famous Polish palindromist and one of the authors who wrote the biggest numbers of solid palindromes in the world, was dedicating and signing a couple of copies of his books presented to the public.

A special session was organized on Sunday 1 June. The session was combined with a visit of the official delegation from SPIE headquarters – The International Society for Optical Engineering. The visit in Wilga was a part of SPIE participation in the Inaugural Symposium of the Photonics Society of Poland after its transformation from SPIE – Poland Chapter. The Symposium was held on 30-31 May at the Faculty of Physics, WUT, and the part of this Inaugural Symposium was this special students session in Wilga held on 1 June. The main part of the PSP Inauguration Symposium was held on Saturday 31 May and gathered more than 100 persons, representatives of research, technical, academic, business, governmental and other communities related to the field of photonics from the whole country. A number of the WILGA Symposium participants took part in the PSP Inauguration Symposium and vice versa.

presentatives.
st presenting

a summary
the young
esearchers
tems.
devoted to
electronics
tation was
interesting
one of the
cating and

ned with a
for Optical
Symposium
napter. The
s Inaugural
of the PSP
00 persons,
ommunities
Symposium

During the Sunday session of WILGA Symposium there was organized a competition for the best student paper presentation. The competition was sponsored by SPIE. The results were as follows: Aleksandra Czapla, Wydział Fizyki PW, Long period fiber gratings with liquid crystals; Andrzej Cichocki, PERG/ELHEP ISE PW, Astronomous power supply controller for MXGS; Krzysztof Iwaszczuk, Wydział Fizyki PW, Plane wave method for photonic liquid crystal fibers modelling. Sincere congratulations for the winners.

After the best student paper award ceremony a business meeting between representatives of SPIE and PSP was organized. There were debated a number of items concerning cooperation, like: functioning of SPIE Student Chapters, signing a Memorandum of Understanding between SPIE and PSP, organization of common meetings, common publications, building a new rapid internet publication under the title Photonics Letters [www.photonics.pl/PL].

The next XXIV Symposium WILGA 2009 is planned, as usual traditionally during the last week of May or on 25-31.05.2009. The January edition of WILGA 2009 Symposium is planned on 23-25 January 2009 at the Faculty of Electronics and Information Technology, WUT. The information about the WILGA Symposium is available at the following web page: http://wilga.ise.pw.edu.pl. All contacts with WILGA organizers are available through the email address: photonics@ise.pw.edu.pl. The WILGA Symposium organizers heartily invite young researchers and their tutors/mentors, working in the area of Internet engineering and advanced applications of photonics and electronics systems.

wid
on

of t
mat
freq
sec
The
The
stru

Key

Chir
high resi
location
based on
$y_n=y(nT_s)$
formed b
other cor
lobe leve

ELECTRONICS AND TELECOMMUNICATIONS QUARTERLY, 2008, 54, no 2, pp. 113–125

Recognition improvement of short chirp signals

WŁODZIMIERZ POGRIBNY, TADEUSZ LESZCZYŃSKI

University of Technology and Life Sciences
Institute of Telecommunications
ul. Kaliskiego 7, 85-796 Bydgoszcz, Poland
pohry@utp.edu.pl, leszcz@utp.edu.pl

Received 2008.02.20
Authorized 2008.05.24

Broadband signals with the use of linear frequency modulation LMF (so-called chirp signals) are widely used in localization. Recognition of the chirp signals depends mainly on their compression based on the matched filtration.

This work presents two simple solutions of the essential improvement of the recognition resolution of the short chirp signals, which product BT does not exceed 100. The first of them is connected with matching chirp and impulse response (IR) parameters to a specific window so that the form of the filter frequency response (FR) would be the nearest to the form of the window amplitude spectrum. The second one is based on removing the negative convolutions of the matched filtration in the time domain. The authors have found that the best result is achieved when both methods are used simultaneously. These ways were checked out for different windows and chirps with bigger BT too. Apart from that, the structure of matched filter (MF) with the use of above-mentioned methods is proposed.

Keywords: location systems, short chirp signal, matched filtration

1. INTRODUCTION

Chirp signals enable significant compression and at the same time are characterized by a high resistance to interferences. Therefore, they find applications in many fields, especially in location systems [1, 4]. The recognition of these signals is connected with their compression based on matched filtration whose convolutions $\{y_n\}_{n=0}^{2N-2}$ form the main and side lobes, where $y_n=y(nT_s)$, T_s is the sampling period, N is the number of the chirp samples. The main lobe is formed by the matched filtration of the chirp and comprises a few central convolutions, whilst other convolutions form the side lobes. The ratio SNR_{out} of the main lobe to the maximal side lobe level, expressed in dB, defines the degree of chirp compression and strongly influences

chirp recognition. Simultaneously, the main lobe width defines the resolution of the method. It is given by

$$\mathrm{SNR}_{\mathrm{out}} = 20\log\frac{y_c}{y_i},$$

where y_c – value of the main lobe is expressed by central convolution, y_i – maximal value of the convolution picked up from all convolutions except those forming the main lobe.

Therefore, it is necessary to decrease the width of the main lobe to only one sample (an ideal case) which is formed by the central convolution.

The chirp signals with large products of the signal band B and its duration T that is BT>>100 have been sufficiently examined so far. An increase of BT leads in most cases to compression improvement, but as it is shown in this work, significant compression can be obtained even if the BT is within 1.5 – 3 range only by fulfilling certain conditions.

The detection of signals with high BT does not cause difficulties on the condition that their compression depends on the boundary effects to a small degree only, especially when smoothing windows are used. The behavior of such signals is predictable, and while using digital matched filtration (including the use of 'fast convolutions' too) high compression can be obtained [2, 3]. The situation is entirely different when short chirp signals with BT<100 are processed. For these signals, apart from the lower compression, the influence of the boundary effect is greater, but the use of smoothing windows in this case is not always advisable as it decreases the signal power.

The authors have found out that for short chirp signals with small BT it is optimal to use the digital matched filtration on the basis of convolutions in the time domain, and not 'fast convolutions' in the frequency domain on the basis of DFT and IDFT, because of:

1) Higher rate of matched filtration in the time domain based on transversal filters when each convolution is obtained during one sampling period T_s. Such a filtration requires N parallel operations (where N is a number of signal samples) for obtaining all convolutions as opposed to the use of the fast convolutions which need N $\log_2$N operations;

2) Better accuracy of calculations because the filtration in the time domain does not need as many transformations as the filtration based on the fast convolutions in the frequency domain.

In [3], it is shown that matched filtration based on fast convolutions can ensure a high $\mathrm{SNR}_{\mathrm{out}}$ even for low BT when a sample number N_F, essentially bigger than N and BT, is provided. At that B is a bilateral signal band and a non-linear change of chirp frequency is performed. Then the main lobe width of the compressed chirp is narrow in reference to N_F. However, this method has some disadvantages.

Firstly, the main lobe always consists of a few samples because IFFT in this case is based only on the amplitude spectrum $\{|X(k)|\}$, where $X(k)$ is k-th term of the spectrum and

$$|X(k)| = \left[(\mathrm{Re}\,X(k))^2 + (\mathrm{Im}\,X(k))^2\right]^{1/2}.$$

It leads to using the amplitude spectrum envelope, which always forms the main lobe in the basis of a few samples, this approach worsens the resolution which is shown in figure 1(a). This situation is similar to an analog case, the example of which is shown in figure 1(b).

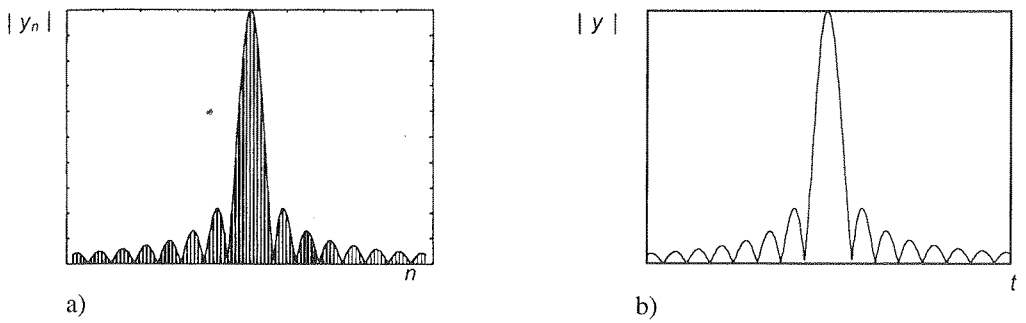

Fig. 1. Here are: (a) magnitude $\{|y_n|\}$ – result of a chirp signal digital matched filtration in frequency domain with the use of "fast convolutions"; (b) magnitude $|y(t)|$ – result of one analog matched filtration in the time domain with the use of delay line and surface wave

Secondly, that approach is realized by $N_F \log_2 N_F$ operations. This number limits essentially the recognition speed as well as the usage of that method in fast-acting location systems.

The study results show that the compression of short chirp signals depends mostly on additional processing of the obtained convolution results as well as on the initial phase and the sampling rate [5.6]. As it is pointed out, such effects have not been sufficiently examined.

Therefore, the authors of this work propose a new approach to a considerable improvement of the recognition resolution in the time domain of chirp signals with BT<100 on the basis of both:

1) matching of short chirp signal and corresponding impulse response (IR) parameters to a specific window, so that the form of the amplitude spectrum of the IR would be the nearest to the window spectrum, and 2) using nonlinear operations on matched filtration results. It is shown that the compression of the chirp signals with very small BT by using the proposed methods is as good as in the case of the higher BT. These ways are shown separately in subsections 3.1 and 3.2.

In the experiments, chirp signal durations ranging from 0,1 μs to 2.5 μs at linear frequency change from 0 MHz to 15 MHz were mainly used. In these cases, the product BT was rounded up and the equation N=2BT took place when one–sided band B was used. For comparison, the compression of chirp signals with BT up to 3000 has been studied too. Apart from rectangular window, the smoothing windows like Hamming's, Blackman's, Hanning's and triangular were used.

2. MATCHING FILTRATION ALGORITHM

An analog chirp-signal with constant amplitude A and linear frequency modulation is given by

$$x(t) = A \cos\left[2\pi\left(at + f_1\right) t + \varphi_0\right] \tag{1}$$

where $a=\Delta f/2\tau_i$, $\Delta f=f_2-f_1$ – deviation of the frequency, f_1 – initial frequency, f_2 – final frequency, τ_i – duration of the chirp signal, φ_0 – initial phase.

For realization of the digital matched filtration the signal (1) was presented in a form of time series $\{x_n\}$ with a sampling rate $f_s=1/T_s \geq 2f_2$, when the number of samples is equal N, where N=ENT($\tau_i f_s$), ENT – whole part of a number.

Each sample of the chirp-signal (1) is given as follows:

$$x_r = x(rT_s) = A\cos\left[2\pi\left(\frac{\Delta f}{2N}r + f_1\right)rT_s + \varphi_0\right], \tag{2}$$

where $\tau_i = NT_s$, $r = \overline{0,\ N-1}$.

Figure 2 shows the example of short chirp signal $x(t)$ and its samples $\{x_n\}$ obtained according to (2).

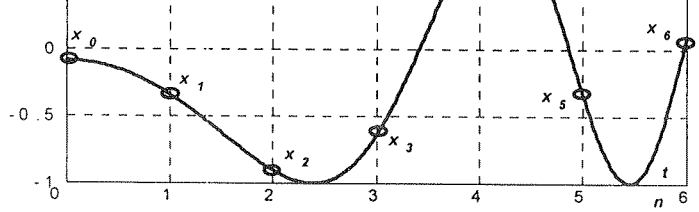

Fig. 2. Short chirp signal with parameters: A=1, Δf =15 MHz, τ_i = 0.2 μs, φ_0 =95°, BT = 3, f_s=30 MHz. The samples $\{x_n\}$ used for corresponding convolutions computing are shown

The IR of the matching filter without a smoothing window is a mirror reflection of an input signal (2):

$$h_n = x_{N-n}, \quad \text{where } n = \overline{1,\ N}. \tag{3}$$

In order to decrease the influence of Gibbs' oscillations, smoothing windows $\{w_n\}$ are applied in the time domain by using multiplication of corresponding weight factors of impulse response and window samples: $\{h_n w_n\}$ [7]. Then the algorithm of digital matched filtration is based on the convolution in the time domain and can be shown as follows:

$$y_n = \sum_{m=0}^{N-1} x_{n-m} h_m w_m, \tag{4}$$

or in matrix form which is more suitable for a specialized processor:

$$y_n = \mathbf{X}\cdot\mathbf{H}_w, \tag{5}$$

where

$$\mathbf{X}=[x_n \ldots x_{n-N+1}], \qquad \mathrm{H_w}=\begin{bmatrix} h_0 w_0 \\ \vdots \\ \vdots \\ h_{N-1} w_{N-1} \end{bmatrix}$$

Here y_n – n-th convolution result; $\{x_n\}$ – input signal samples; $\{h_n\}$ – weight factors of impulse response, N – number of weight factors and input signal samples, $\{w_n\}$ – smoothing window samples. For a rectangular window, there is assigned $\forall n$, $w_n = 1$. In this case, the complete number of convolutions is 2N-1. The matched filtration of chirp signal results in the values of a few central convolutions forming the main lobe whilst other convolutions make side lobes. In such MF, according to algorithm (5), the total number of multiplications for obtaining one convolution is N. However, if MF consists of N parallel channels with multipliers, one convolution is realized in time of one multiplication interval, which does not exceed T_s.

3. WAYS OF INCREASING THE SHORT CHIRP SIGNALS COMPRESSION

3.1. MATCHING OF THE CHIRP SIGNAL PARAMETERS

In order to improve the short chirp signal compression we propose to match the parameters (2) and (3) of these signals and IRs of filters to the windows.

Firstly, let us consider the case of smoothing windows usage. Usually, these windows are characterized by a ratio $\mathrm{SNR_w}$ of the main lobe to the maximal side lobe as well as the main lobe width.

$$\mathrm{SNR_w} = 20\log\frac{y_c}{y_s}$$

where y_c – value of the central convolution, y_s – maximal side lobe level of the convolution appointed from among convolutions excluding the convolutions forming the main lobe.

At this, bigger $\mathrm{SNR_w}$ and wider main lobe takes place. For example, the popular Hamming's window allows to obtain the $\mathrm{SNR_w}$ about 43 dB when the main lobe width is equal to a few sampling periods T_s. Its amplitude spectrum $\{|W(k)|\}$ has a Gaussian form [8].

The explanation of our approach is that we choose the chirp and IR parameters to obtain the windowed IR $\{h_m w_m\}$ with positive part of the envelope being the nearest to the window form and the form of its amplitude spectrum $\{|H_w(k)|\}$ being nearest to the $\{|W(k)|\}$, whilst the chirp amplitude spectrum $\{|X(k)|\}$ is rectangular. Then the filtration result in the frequency domain takes shape $\{|Y(k)|\}$, where $Y(k)= X(k)\cdot H_w(k)$, which is maximal similar to the $\{|H_w(k)|\}$, whilst in the time domain we have a signal $\{|y_n|\}$ the form of which is near to the $\{w_n\}$. It means that in this case a compression degree expressed by $\mathrm{SNR_{out}}$ of the signal $\{|y_n|\}$ is essentially defined by the smoothing window $\mathrm{SNR_w}$. Therefore, the choice of the specific window depends on the compression and resolution requirements, as well as the parameters of the chirp.

Secondly, it is known that the rectangular window usage leads to the smaller SNR_{out} than the smoothing one, but at the same time it ensures a narrower main lobe of the signal $\{y_n\}$. Therefore, this window usage is expedient for the recognition resolution improvement. In case of the rectangular window usage, we try to match the chirp and IR parameters to the window to obtain amplitude spectrum $\{|H(k)|\}$ form nearest to the rectangular form. It is connected with one from other peculiarities of the Fourier's transform, that an amplitude spectrum rectangular form in frequency domain corresponds to a signal of a type $\sin x / x$ in the time domain. In this case, the narrowness of the main lobe of the function $\sin x / x$ and its ratio to side lobes depends on rectangularity degree. Therefore, we propose to assign the IR $\{h_n\}_{n=0}^{N-1}$ parameters in such a way that its amplitude spectrum $\{|H(k)|\}_{k=-(N/2-1)}^{N/2-1}$ form would be maximally rectangular. So we estimate the rectangularity degree on the basis of a variance value:

$$D_H=\frac{1}{N}\sum_{k=-(N/2-1)}^{N/2-1}\left(|H(k)|-\overline{|H|}\right)^2 \quad \text{where} \quad \overline{|H|}=\frac{1}{N}\sum_{k=-(N/2-1)}^{N/2-1}|H(k)| \tag{6}$$

In the presented work, the matched filtration of short chirp signals was carried out using both classical Hamming's smoothing window and a rectangular window. For each of these cases, the influence of the initial phase and sampling rate on the short chirp signal compression and the amplitude spectrum rectangularity of its IR was examined. The detailed results were presented for chirp signals with durations 0.2 μs and 2.5 μs and linear momentary frequency change in the range from 0 MHz to 15 MHz (BT=3 and 37.5). The sampling rate f_s was changed from 29.8 MHz to 30.2 MHz and the initial phase of the signal was done in the range from 0° to 180°. Examinations were performed using simulation methods by means of specially created program.

At first, we studied computer simulation results of algorithm (4) with the use of Hamming's window and without any nonlinear operations. As a point of reference there were assigned the unmatched parameters φ_0=30° and f_s = 30 MHz of the chirp and IR to the window, when τ_i = 2.5 μs and BT=37.5. All values of the convolutions $\{|y_n|\}$ were taken into consideration. At that, SNR_{out} does not exceed 29.39 dB when the main lobe consists of no more than 7 samples.

However, if we match the IR parameters to the window, we obtain a better result, as it is illustrated in Figure 3. For the same parameters τ_i = 2.5 μs and BT = 37.5 as above, in Figure 3(a) the FR is shown, which is the amplitude spectrum of the IR matched to the Hamming's window when φ_0=106° and f_s=30.2 MHz, and in Figure 3(b) – the result of chirp signal matched filtration at these parameters and without nonlinear operations. Then SNR_{out} = 40.09 dB on the level of 7 samples per the main lobe.

It is advisable to note that in both above-mentioned cases the SNR_{out} does not exceed 7.9 dB on the level of 1 sample per the main lobe.

Next, it is important to study the influence of the rectangular window and matching of the short chirp and IR parameters to the window on the matched filtration result. In Figures 4 and 5 some effects of that usage are shown.

At first, some non-optimal parameters of IR $\{h_n\}_{n=0}^{N-1}$ as f_s=30 MHz and φ_0 = 30° for filtration of the chirp with BT = 37.5 were chosen. Figure 4(a) shows the form of the spectrum $\{|H(k)|\}_{k=0}^{N/2-1}$

outlying from rectangle and in Figure 4(b) result $\{y_n\}$ of the corresponding chirp compression on the basis of the filtration using this IR. Then the main lobe is formed of 1 sample beginning with the level of SNR_{out} = 22.77 dB.

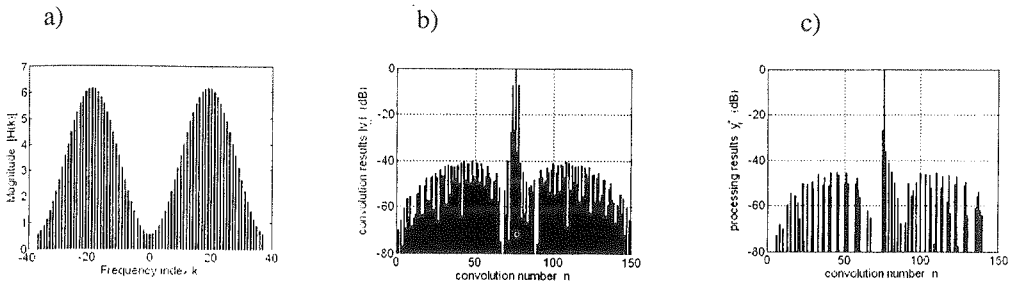

Fig.3. (a) amplitude spectrum of the matched IR to the Hamming's window, when φ_0=106°, f_s=30.2 MHz at τ_i=2.5 μs and BT=37.5 ; (b) result of the chirp signal matched filtration with the use of this IR and without any nonlinear operations; c) result of the matched filtration by using of the nonlinear operations and with the use of the matched IR to the Hamming window, when φ_0=100°, f_s=30.2 MHz, τ_i= 2.5 μs and BT=37.5

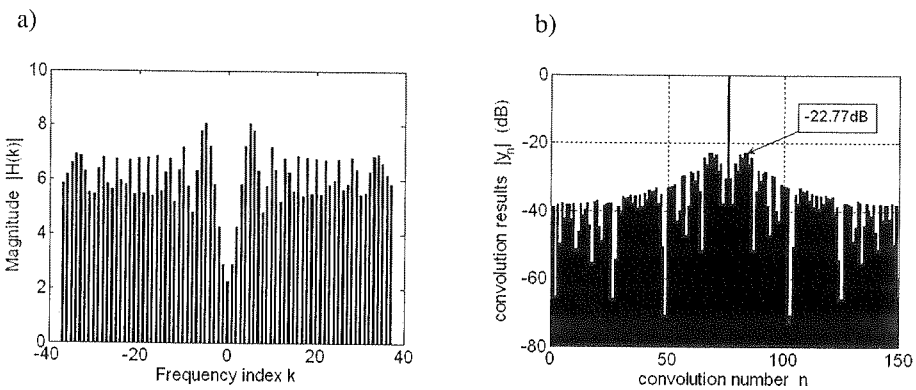

Fig.4. (a) amplitude spectrum of unmatched IR to the rectangular window when D_H=1.0765; (b) result of the chirp compression with usage of this IR and without any nonlinear operations

Secondly, the appropriate choice of the IR parameters enables matching IR to the window and improving the filtration result. In Figure 5(a), it is shown the amplitude spectrum of the maximally matched IR to the rectangular window when the initial phase is φ_0 = 108°, f_s=30.2 MHz and the minimized variance is D_H= 0.0711. In this case, the main lobe consists of 1 sample beginning with level of SNR_{out} = 33.92 dB.

The relation between D_H and φ_0 given in Figure 6(a) for the mentioned chirp in Figure 5 shows that minimum of D_H takes place by φ_0 = 108° just when the maximal compression is used.

The similar effect is obtained for very short chirp signals (BT=3) whose form and parameters are shown in Figure 2 and the caption. Figure 6(b) shows the dependence D_H on φ_0 for this chirp. Here the minimum of D_H corresponds to the maximum of SNR_{out}.

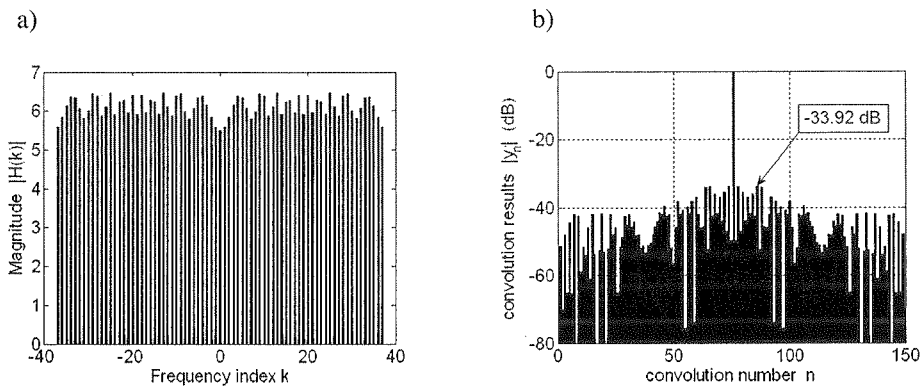

Fig.5. (a) amplitude spectrum of the matched IR to the rectangular window when $BT = 37.5$ and minimized $D_H = 0.0711$; (b) the result of the chirp signal matched filtration with the use of this IR and without any nonlinear operations

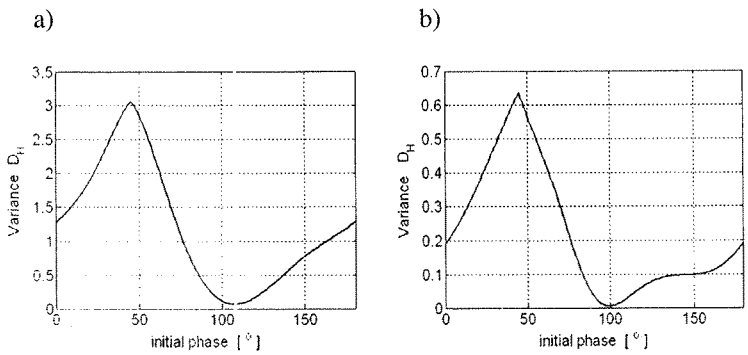

Fig.6. Relations between spectrum variance and initial phase for chirps with next parameters. (a) frequency range from 0 MHz to 15 MHz, τ_i = 2,5 μs, f_s=30,2 MHz, BT=37,5; (b) frequency range from 0 MHz to 15 MHz, τ_i = 0,2 μs, f_s=30 MHz, BT=3

In Figure 7, amplitude spectrum of the IR maximally matched to the rectangular window, when the FR minimized variance is $D_H = 0.0131$, as well as the filtration result for this chirp are presented. In this case $SNR_{out} = 20.26$ dB is obtained.

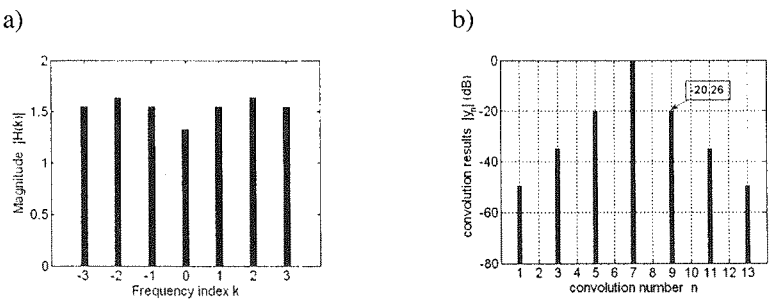

Fig.7. (a) amplitude spectrum of a maximally matched IR to the rectangular window when BT=3 and minimized variance is D_H= 0.0131; (b) result of the chirp signal compression with the use of rectangular window and without any nonlinear operations. Here chirp parameters are as described in figure 2

From the obtained simulation results, it can be concluded that the initial signal phase has an essential influence on SNR_{out} as well as the sampling rate. The influence of the phase on SNR_{out} is the largest for the sampling rate, differing from Nyquist's (30 MHz) frequency about $\pm$ 0.6666 %.

3.2. THE USE OF NONLINEAR OPERATIONS FOR MATCHED FILTRATION RESULTS

When a matched filtration result is obtained directly on the basis of the algorithm (5), a part of convolutions $\{y_n\}$ has negative values. Traditionally, those values are converted and, afterwards, together with positive convolutions form the set $\{|y_n|\}$, which is the envelope basis. At that, some former negative convolutions have big enough values and in part are situated near the main lobe. Accordingly, some of them become a part of the main lobe expanding it, which in consequence worsens the resolution and SNR_{out}. Therefore, we propose to reject the negative convolutions in order to increase SNR_{out} and to decrease the main lobe width to one sample, which is a limit case in relation to the resolution. Nonlinear operations for the elimination of the negative convolutions are realized on the basis of the following algorithm:

$$\forall y, \operatorname{sgn} y, \exists y^{+} \left((\operatorname{sgn} y_n = 1) \quad (y_n^{+} = y_n) \vee (\operatorname{sgn} y_n = -1) \quad (y_n^{+} = 0) \right) \tag{7}$$

where $y_n = \operatorname{sgn} y_n \cdot |y_n|$, $\operatorname{sgn} y_n \in \{1, -1\}$ – sequence sign, y_n^{+}- n-th processing result.

The explanation of additional processing of the matched filtration outcome in the time domain can be given with the use of the Figure 8. It is shown that after rejecting the negative convolutions from the set $\{y_n\}$ the set $\{|y_n|\}$ is transformed in to $\{y_n^{+}\}$.

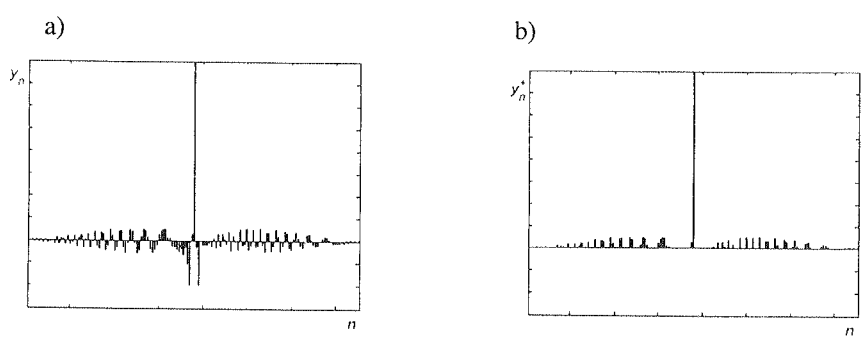

Fig. 8. Explanation of additional processing of the matched filtration outcome in time domain: (a) all convolutions $\{y_n\}$, (b) positive convolutions $\{y_n^{+}\}$ only. Here a liner scale is used

Now we show, using Figure 3(c), the compression result with the algorithm (6) usage when the chirp and windowed IR have the same parameters as in Figure 3(a) and 3(b) apart from φ_0=100. In this case, SNR_{out} is 45.04 dB on the level of 7 samples per the main lobe, i.e. better by about 5 dB than the result without the nonlinear operations adduced in Figure 3(b).

The best results of the compression were achieved while the matched filtration of short chirp signal with rectangular window was used and negative convolutions were rejected. Apart from it, when the sampling rate is unequal to the Nyquist's frequency about ± 0.6666 % (± 0.2 MHz) the SNR_{out} obtains one global maximum even when the main lobe consists of 1 sample only. At that, SNR_{out} depends significantly on the initial phase change.

We can note that the dependence of SNR_{out} on the initial phase differs for different windows by using or not using the nonlinear operations. Figure 9(a) and 9(b) show these dependences for the chirp with next parameters: $f_1 = 0, f_2$=15 MHz, $\tau_i = 2.5$ μs, BT = 37.5, f_s = 30.2 MHz. At that, those windows as rectangular, Hamming's, triangular, Blackman's, Hanning's were studied. Simultaneously, we considered the main lobe width equals to 1, 3, 5 and more samples.

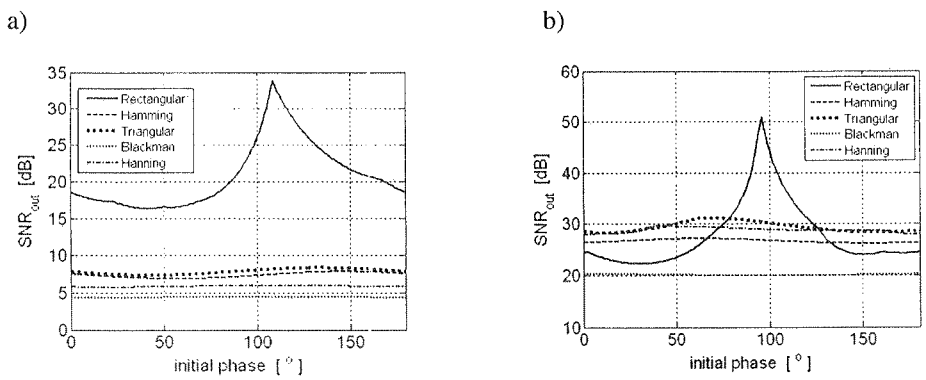

Fig.9. Dependence SNR_{out} on the initial phase for different windows when the chirp parameters are: $f_1 = 0, f_2$=15 MHz, τ_i = 2,5 μs, BT = 37.5, f_s = 30.2 MHz: (a) without non linear operations; (b) with using non linear operations. In both cases the main lobe consists of 1 sample

Analyzing the obtained rezults we can consider that by the use of different smoothing windows usage and taking into account only one sample in main lobe, SNR_{out} is practically independent on the initial phase as well as by using or not using the nonlinear operations. SNR_{out} behaves analogically when the main lobe consists of 3 samples and nonlinear operations are not used. The influence of the initial phase on SNR_{out} becomes significant when the main lobe consists of 3 and more samples by using nonlinear operations as well as 5 samples and the lack of those operations.

However, by using a rectangular window, dependence SNR_{out} on the initial phase is more detectable for each above mentioned case as Figures 10(a) and 10(b) illustrate.

Simulation results show that the character of SNR_{out} changes at the main lobe width d = 3, 5.7 and more samples are similar to the case when it is equal to 1 sample as Figures 10(a) and 10(b) demonstrate different BT. Therefore, it is expedient to concentrate on using the rectangular window in the matched filtration in time domain. This assumption can be confirmed with the use of Tables 1 and 2. They show the dependence of SNR_{out} on BT and using or not the nonlinear operations when matched filtration is based on both optimal f_s and φ_0. At that, Table1 includes the results of the Hamming window using.

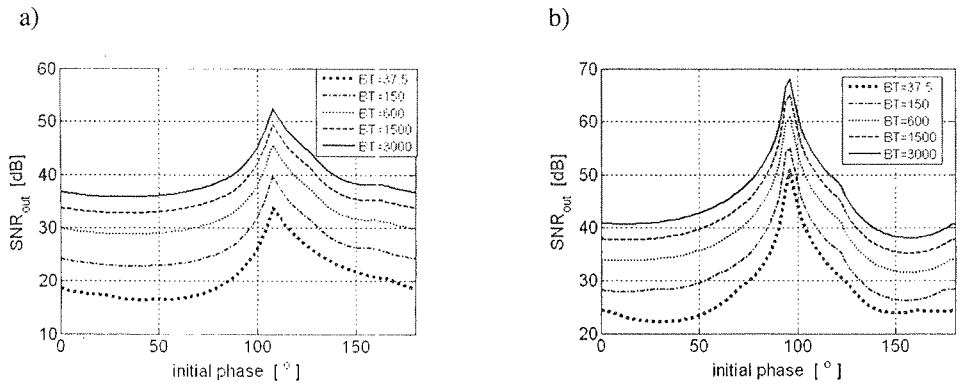

Fig. 10. Dependence SNR_{out} on the initial phase for rectangular window and different BT when f_1 =0, f_2=15 MHz, f_s = 30.2 MHz: (a) without non linear operations; (b) with using nonlinear operations. In all cases the main lobe consists of 1 sample only.

Table 1

Dependence of SNR_{out} on BT by the Hamming window usage and using or not using the nonlinear operations

#	BT	SNR_{out} (dB) Hamming window and: all convolutions / nonlinear operations				
		d=1	d=3	d=5	d=7	d=9
1	37.5	7.80/27.09	7.80/40.98	28.64/40.98	40.09/45.04	40.09/45.04
2	150	7.69/42.76	7.69/47.17	41.27/47.17	50.41/53.71	50.41/53.71
3	600	7.55/54.43	7.55/58.97	52.98/58.97	61.22/65.43	61.63/65.43
4	1500	7.49/62.40	7.49/66.88	60.87/66.88	65.70/73.33	65.84/73.33
5	3000	7.47/68.43	7.47/72.88	66.87/72.88	68.90/79.33	68.90/79.33

Table 1 shows that SNR_{out} depends always on the main lobe width d by using the smoothing window. Table 2 comprises the compression results by using the rectangular window and shows independence SNR_{out} on d in this case. In both cases, a usage of nonlinear operations improves essentially SNR_{out}.

Table 2

Dependence of SNR_{out} on BT by the rectangular window usage and using or not using the nonlinear operations

#	BT	SNR_{out} (dB) Rectangular window and: all convolutions / nonlinear operations				
		d=1	d=3	d=5	d=7	d=9
1	37.5	33.92/50.87	33.92/50.87	33.92/50.87	33.92/50.87	35.11/50.87
2	150	39.76/55.05	39.76/55.05	39.76/55.05	39.76/55.05	39.76/55.05
3	600	45.52/61.06	45.52/61.06	45.52/61.06	45.52/61.06	45.52/61.06
4	1500	49.41/65.16	49.41/65.16	49.41/65.16	49.41/65.16	49.41/65.16
5	3000	52.39/68.15	52.39/68.15	52.39/68.15	52.39/68.15	52.39/68.15

The simulations show that using the appropriately matched sampling rate, the initial phase, the rectangular window, and the non-linear operations in digital matching filtration in the time domain allows to achieve nonlinear effects, which are conducive to significant improvement of the short chirp signal (BT<100) recognition. In Figure 11(a) and 11(b) examples of the chirp signals processing with above mentioned parameters and the spectra identical those shown showed in Figures 5(a) and 7(a) are shown. The chirp with BT = 37.5 consists of N=75 samples and convolutions number is 2N-1=149, whilst one with BT = 3 has N=7 and 2N-1=13 respectively. In both cases, the width of the main lobe equals 1 sampling period. Although in the last case, the main lobe amplitude is only 2.305 when A=1, such big SNR_{out} appears place because after nonlinear operations the side lobes are about $1.45 \cdot 10^{-16}$.

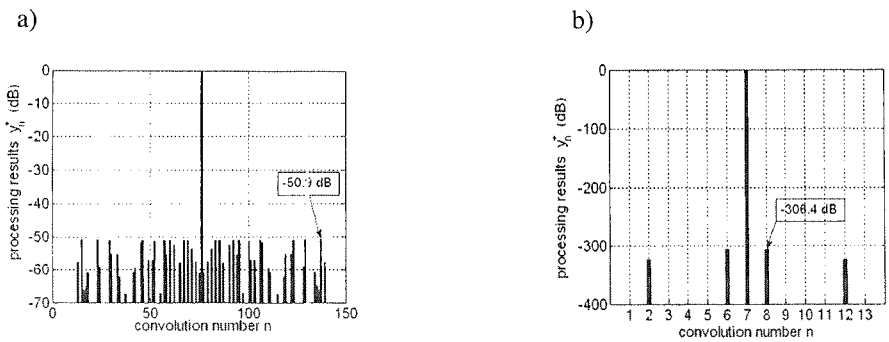

Fig.11. Results of the short chirp signals matched filtration by using of the nonlinear operations and with the use of the matched IR to the rectangular window when the chirp and IR parameters are: (a) $f_1 = 0, f_2 = 15$ MHz, $\tau_i = 2.5\ \mu$s, $\varphi_0 = 96°$, BT = 37.5, $f_s = 30.2$ MHz; (b) $f_1 = 0, f_2 = 15$ MHz, $\tau_i = 0.2\ \mu$s, $\varphi_0 = 95°$, BT = 3, $f_s = 30$ MHz

4. THE WORKED-OUT MATCHED FILTER STRUCTURE

Block schema of digital transversal matched filter working in the time domain, which processes c-bit PCM samples $\{x_n\}$ and contains N parallel channels and the nonlinear operation block is shown in Figure 12. The regularity of the structure of such a filter results in simplicity of its realisation. Input signal is given into PCM encoder (A/D). Then it runs through delaying elements DL and is multiplied by the proper filter weight factors $\{h_i\}$ in MPL blocks. The results of these operations are summed up in Σ block, which in consequence forms output signal $\{y_n\}$. Its sign controls the block SW that picks only positive convolutions $\{y_n^+\}$. The use of uniform blocks, realising basic operations in the filter, enables its easy implementation in different multiprocessor structures.

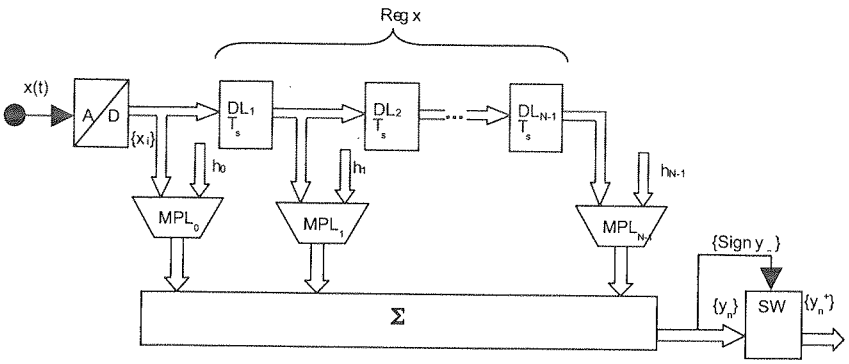

Fig.12. Structure of the worked-out matched filter. A/D – PCM encoder, DL – unit delay (register), MPL – multiplier, Σ – adder-accumulator, SW – switch for cutting out of the negative convolutions

5. CONCLUSION

In this work it is shown that for recognition of short chirp signals with BT<100 on the basis of the digital matched filtration in the time domain the best results were obtained when a rectangular window, well-matched parameters of the chirp and IR, and only positive convolutions are used. It is shown that when the sampling rate of the chirp signal is slightly different from f_N, we can obtain its optimal initial phase for achieving significant SNR_{out} and besides the main lobe width equals 1 sampling period only. The compression system (receiver) structure is also proposed, which consists of the matched filter with the nonlinear operations block realizing the proposed algorithm. Those N-channels matched filters working in the time domain are faster (about $\log_2 N$ times) than the filters on fast convolutions in the frequency domain, and have a better resolution. Apart from this, these simple filters have regular structure and are more viable for implementation in programmable circuits, e.g. FPGA devices.

6. REFERENCES

1. J. Tsui: *Digital Techniques for Wideband Receivers*, Artech House, Boston–London, 1995.
2. B. L. Lewis: *Aspects of Radar Signal Processing*, Artech House, Boston–London, 1986.
3. M. Tortoli, F. Baldanzi, C. Guidi, Atzeni: *Digital Design Improves Radar Pulse Compression*, Microwaves & RF, pp. 135-140, May 1997.
4. S. G. Schock, L. R. LeBlanc: *Chirp sonar: new technology for subbottom profiling*, Sea Technol., 31, pp. 35-43, 1990.
5. W. Pogribny, I. Rozhankivsky, T. Marciniak: *Compression of Location Signals Based on Chirp-Signals and Noise-Like Codes*, Acta Acustica united with Acustica, vol. 88, no. 5, pp. 678-681, 2002.
6. W. Pogribny, I. Rozhankivski, T. Leszczynski, E. Sedek: *Methods of Increase of Short Chirp Signals Compression*, in Proc. of the IEEE EUROCON 2007 International Conference on 'Computer as a Tool', Warsaw, pp. 930-935, 2007
7. R. G. Lyons: *Understanding Digital Signal Processing*, Addison Wesley Longman, Inc., 1997.
8. S. W. Smith: *Digital Signal Processing: A Practical Guide for Engineers and Scientists*, Elsevier Inc., Burlington, 2003.

C

sup
rad
elli
sup
tiu
it i
cur
of t

Key

Evol
elements.
is the uti
supercon
vital featu
amount o
as far as
such a cir
can be ba
mal metal

ELECTRONICS AND TELECOMMUNICATIONS QUARTERLY, 2008, 54, no 2, pp. 127–133

Optimization of the optical pulse energy for switches based on thin films of high-T_c superconductors

JAN WAŚKIEWICZ

Faculty of Electrical Engineering
Bialystok Technical University
ul. Wiejska 45 d, 15-351 Bialystok
jwaskiew@pb.bialystok.pl

Received 2008.06.03
Authorized 2008.06.30

This work proposes a method for lowering the energy of an optical impulse required to switch superconducting key elements, based on driving such components with the use of current and optical radiation impulses with varied lengths. The investigation was conducted with the aid of numerical modelling of the superconducting switching element response for a structure composed of a thin $YBa_2Cu_3O_{7-x}$ superconducting film deposited on a sapphire substrate (Al_2O_3) with a buffer layer composed of strontium titanate ($SrTiO_3$). It was proven that thanks to the driving with control impulses of varied lengths, it is possible to switch such elements with 1.6 – 3.5 times lower energy of the optical impulse and the current slightly higher than the critical current, as compared to the switching mechanism using impulses of the same length.

Keywords: high-T_c superconductors, optical switches, current-optical pulses, control characteristics

1. INTRODUCTION

Evolution of digital technology requires development of increasingly fast signal switching elements. One of the most promising and perspective means of achieving this particular goal is the utilization of superconducting materials. Digital input/output circuits based on high-T_c superconductors (HTS) can achieve switching frequencies at the order of 1 THz [1]. One of the vital features of superconducting switches – apart from the high switching speed – is the low amount of energy emitted by such electronic components. It is estimated that it can be lowered as far as 10^{-19} J/bit [1]. This particular energy has a direct impact on the operation reliability of such a circuit. One of the possible operation principles for superconducting switching elements can be based on transition of the given material from the superconducting (S) state into the normal metal state (N), caused by electric current, magnetic field, optical radiation or microwave

impulses [2,3]. The switching energies of the electronic elements under development are higher when compared to the aforementioned value, since such components feature a number of energy loss mechanisms, which are not accounted for in the balance estimations. One of the ways to boost efficiency of the HTS-film switching process is the application of simultaneous current and optical impulses [4].

This work proposes therefore a method for lowering the energy of an optical impulse required to switch a HTS element, based on driving such components with the use of current and optical radiation impulses with varied lengths.

2. THE METHOD

The superconducting switching elements are typically manufactured in the form of thin-film structures with a superconducting layer forming a micro-bridge. The experimental research commonly utilizes high-T_c superconducting materials (HTS), with $YBa_2Cu_3O_{7-x}$ as an example of a typical material. In order to obtain the highest possible quality HTS-layers, the substrate and the superconducting material are typically separated by a buffer (intermediate) layer with a crystallographic structure compliant the HTS-material in question.

In this work, it is hereby proposed to utilize the mathematical-physical modelling method for conductivity switching processes in thin HTS-films to obtain the characteristics for HTS-keys driven by current and optical impulses. The geometric model [5,6] comprises five parallel and unlimited layers (Fig. 1): a superconducting material 1, a buffer layer 3, a substrate 5 and a couple layers 2,4 modelling the contact regions. The superconducting layer is subject to an optical radiation impulse with the energy density E_F, and it is additionally polarized with the electrical current I. The external surface of the substrate is cooled with liquid nitrogen to the final temperature of T_o=78K. The analysis of the process of destruction and recreation of superconductivity phenomenon in such structures conducted in [5], indicated that with the film thickness h_f>10nm and the time scale $\tau > 0.1$ns the switching between the superconducting (S) and normal (N) states is mainly controlled by the bolometric mechanism. Heating of the superconducting layer occurs due to emission of the Joule's heat and absorption of the incident optical radiation. The energy generated in the layer is then transferred to the thermostat via thermal conductivity mechanism. Heat abstraction results in recreation of the superconductivity. As a result of all the aforementioned processes, a resistive response of the key $R(\tau)$ is thus observed.

The modelling of the HTS-key response was conducted for a structure composed of a thin $YBa_2Cu_3O_{7-x}$ superconductor film deposited on a sapphire substrate (Al_2O_3) with a buffer layer composed of strontium titanate ($SrTiO_3$). The thicknesses of the individual layers were defined as follows: superconductor $h_f = 0.2\mu$m, buffer $h_b = 1\mu$m and substrate h_s= 0.5mm. Table 1 presents the parameters of the examined structure, assumed for the calculations. The resistivity of the HTS-film in the phase transition region N-S is approximated using a two-dimensional, non-linear function $\rho(T,j)$ of temperature and current density [6] using initial $T_{c,b}$ and final $T_{c,e}$ temperatures of the superconductor phase transition, critical current density j_c and the specific resistivity

ρ in the N state. The assumed values of critical temperatures $T_{c,b}$ and $T_{c,e}$ correspond to the width of the superconductivity transition of ΔT_c=1K (defined at the level of 10 and 90% of the $\rho(T_{c,b})$ value), which indicates a good quality of the deposited film. The thermal conductivity of the $YBa_2Cu_3O_{7-x}$ film (λ_f) and the thermal boundary resistance $R_{T,k}$ between the HTS-film and buffer layer were taken from [7].

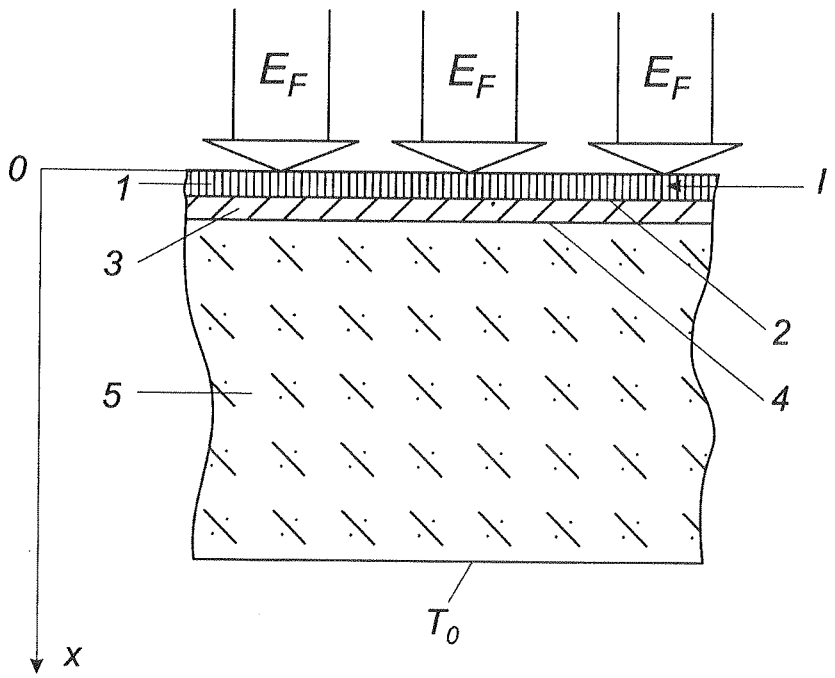

Fig. 1. The physical-geometric model of an HTS-element (1 – HTS film; 3 – buffer layer; 5 – substrate; 2 and 4 – areas of thermal contacts; E_F – optical radiation; I – current; T_o – temperature of the thermostat).

3. CONTROL CHARACTERISTICS FOR HTS-KEYS

The HTS-switches operate in the optimum mode only when the superconductor reaches the N state corresponding to the initial phase of the N-S-transition and does not suffer from overheating. Therefore in this paper it is proposed to control the HTS switching element with the aid of an optical and current impulse with varied lengths: τ_F and τ_I. The energy of the optical impulse E_F is selected in such way that the film temperature at time τ_F reaches $T_{c,b}$ i.e. the key switches on completely. The current impulse (longer than the optical one) is used to sustain the key response signal at the level close to $R(T_{c,b})$. The current amplitude I is selected in such way that the HTS-film temperature at time τ_I also reaches $T_{c,b}$ which corresponds to the compensation condition for the thermal power guided to the thermostat via the Joule's heat generated.

Table 1

Parameters of HTS-structure as taken for calculations in the superconducting film

Parameter	Symbol	Value	Unit	Parameter	Symbol	Value	Unit
$YBa_2Cu_3O_{7-x}$ – film							
Thickness	h_f	0,2	μm	Reflection coefficient	R_v	0,1	
Width	w_f	20	μm	Linear absorption coefficient	κ	10	μm^{-1}
Length	l_f	2	mm	Thermal conductivity	λ_f	2	W/m · K
Temperature of N-S initiation	$T_{c,b}$	90	K	Heat capacity	c_f	150	J/kg · K
Temperature of N-S completion	$T_{c,e}$	86,7	K	Specific density	ρ_f	6350	kg/m^3
Resistivity at $T_{c,b}$	$\rho(T_{c,b})$	0,1	mΩ cm	Thermal boundary resistance: film –	$R_{T,k}$	$5 \cdot 10^{-8}$	m^2K/W
Critical current density at 78K	$j_c(78)$	10^6	A/cm^2	buffer layer and buffer layer – substrate			
$SrTiO_3$-buffer layer				Al_2O_3-substrate			
Thermal conductivity	λ	5	W/m · K	Thermal conductivity	λ	900	W/m · K
Heat capacity	c	200	J/kg · K	Heat capacity	c	100	J/kg · K
Specific density	ρ	5000	kg/m^3	Specific density	ρ	4000	kg/m^3

The modelling of the operation of HTS switching elements was conducted for rectangular current and optical radiation impulses which were started at the same time. The impulse length τ_I varied between 1μs and 5μs, while $\tau_F=(0.1\text{-}1)\tau_I$, which was defined in such a way to compare the obtained results with [8], where the control characteristics for the analogous HTS-structures driven with current and optical radiation impulses of the same length τ_{imp} were presented. The said paper indicated that the most significant reduction in the response switching time τ_{sw} due to introduction of the buffer $SrTiO_3$ layer in the HTS-structure based on Al_2O_3 substrate was observed for the $\tau_{imp}= 5\mu s$ and $h_b=1\mu m$.

Figure 2 depicts the obtained relations between the optical impulse energy E_F (Fig. 2.a) and current amplitude I (Fig. 2.b) and the duration of the optical impulse τ_F in the proposed control mode for various lengths of the current impulse τ_I. Along with the decrease in the τ_F in relation to τ_I, there is also a significant decrease in the value of E_F energy. The amount of radiant energy required for turning the HTS-switch on under $\tau_F = \tau_I$ is between 3.5 (for $\tau_I = 5\mu s$) and 1.6 (for $\tau_I = 1\mu s$) times larger when compared to the system parameters for an optical impulse 10 times shorter than the current impulse. In such system, the current keeping the key switched on varies by approximately 2% and is only slightly higher than the critical current at T_o ($I_c(78K) = 40mA$). The decrease in the E_F energy results from a decrease in the amount of heat guided to the substrate of the HTS-structure and then to the thermostat when the key is switched on for shorter τ_F. A vital role in the process of maintaining the heat in the superconducting layer is played by the buffer $SrTiO_3$ layer [9].

A decrease in the E_F energy coupled with the decrease in τ_I with the constant optical impulse duration τ_F (Fig. 2.a) is caused by the reduced amount of heat accumulated in the HTS-structure during the process of switching the key on. This in turns results from the differences in the shape of heating curves for the HTS-film (Fig. 3.a). The process of switching the key on (Fig. 3.a

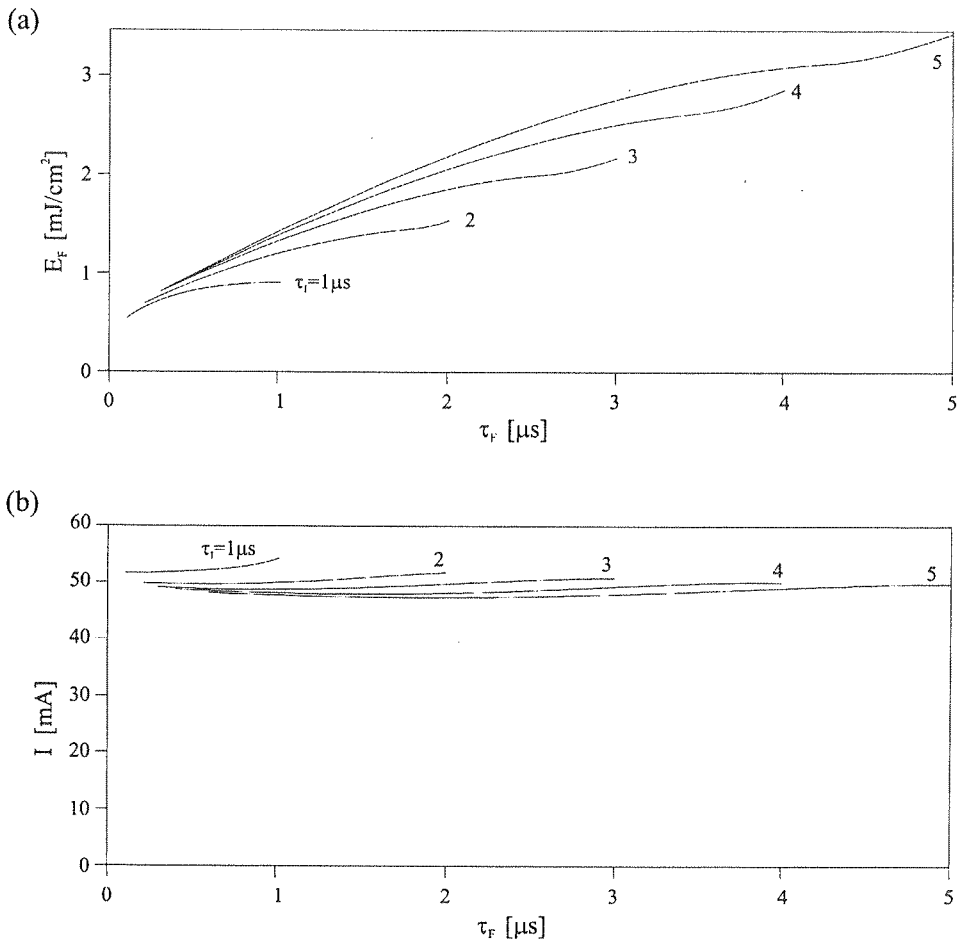

Fig. 2. A relation between the optical impulse energy E_F (a) and current amplitude I (b) and the duration of the optical impulse τ_F in the proposed control mode for various lengths of the current impulse τ_I

and 3.b) has two distinctive phases: the first one – until the inflexion of heating curves at approximately 1μs – when the increase in the key resistivity occurs mainly due to the heating of the structure with the optical impulse, and the second one – where the HTS-film is switched into the N state. During the second phase the film is heated predominantly by the electrical current due to emission of the Joule's heat. The increase in the temperature and resistance is highly non-linear in this phase which may result eventually in a thermal instability of the examined structure. This particular phenomenon is caused by the strong non-linear relation $\varrho(T)$ in the region of the S-N-transition. The coexistence of the aforementioned two heating mechanisms within the HTS-film determines the course of the heating curve. To maintain the key in the on state in the case of longer current impulses, the required current amplitude I is lower (curve 5 in Fig. 2.b). Therefore, during the process of switching the given key on, the required E_F energy is higher.

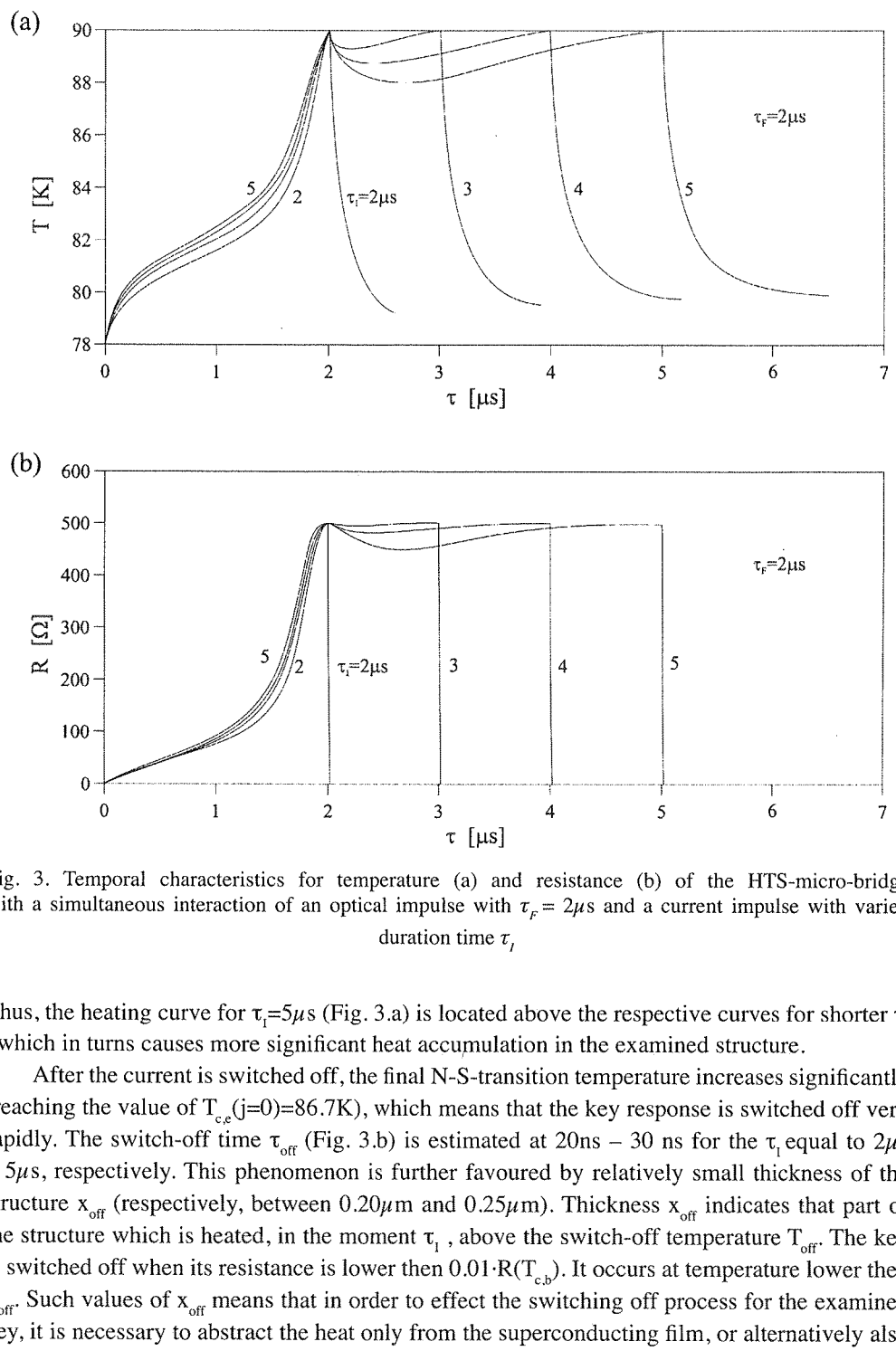

Fig. 3. Temporal characteristics for temperature (a) and resistance (b) of the HTS-micro-bridge with a simultaneous interaction of an optical impulse with $\tau_F = 2\mu s$ and a current impulse with varied duration time τ_I

Thus, the heating curve for τ_I=5μs (Fig. 3.a) is located above the respective curves for shorter τ_I , which in turns causes more significant heat accumulation in the examined structure.

After the current is switched off, the final N-S-transition temperature increases significantly (reaching the value of $T_{c,e}(j=0)$=86.7K), which means that the key response is switched off very rapidly. The switch-off time τ_{off} (Fig. 3.b) is estimated at 20ns – 30 ns for the τ_I equal to 2μs – 5μs, respectively. This phenomenon is further favoured by relatively small thickness of the structure x_{off} (respectively, between 0.20μm and 0.25μm). Thickness x_{off} indicates that part of the structure which is heated, in the moment τ_I , above the switch-off temperature T_{off}. The key is switched off when its resistance is lower then $0.01 \cdot R(T_{c,b})$. It occurs at temperature lower then T_{off}. Such values of x_{off} means that in order to effect the switching off process for the examined key, it is necessary to abstract the heat only from the superconducting film, or alternatively also

from the ultra thin region of the buffer layer adjacent to the micro-bridge. Due to the very short τ_{off} time, the response switching time τ_{sw} is virtually equal to the switching on time τ_{on}, which in turns is uniformly defined by the control mode and must be equal to the length of the radiation impulse τ_F.

4. CONCLUSIONS

Thanks to the driving with control impulses of varied lengths, it is possible to switch high-T_c superconducting elements with 1.6 – 3.5 times lower energy of the optical impulse and the current slightly higher than the critical current, as compared to the switching mechanism employing impulses with the same length. The proposed the control mechanism also allows to reduce maximally the response switching time.

5. ACKNOWLEDGEMENTS

The paper was supported by The Polish Scientific Research Committee in project no. PB-W/WE/9/06.

6. REFERENCES

1. P. Bunyk, K. Likharev, D. Zinoviev: *RSFQ technology: physics and devices*, International Journal of High Speed Electronics, vol. 11, no 1, pp. 257-305, 2001.
2. G. Sabouret, C. Williams, R. Sobolewski: *Resistive switching dynamics in current-biased $YBa_2Cu_3O_{7-x}$ microbridges excited by nanosecond electrical pulses*, Phys. Rev. B, vol. 66, no 13, pp. 132501-1-4, 2002.
3. C. Williams, Y. Xu, R. Adam, M. Darula, O. Harnack, J. Scherbel, M. Siegel, F. A. Hegmann, R. Sobolewski: *Ultrafast YBCO photodetector based on the kinetic-inductive process*, IEEE Transactions on Applied Superconductivity, vol.11, no 1, pt. 1, pp. 578-81, 2001.
4. J. Waskiewicz: *Control mode optimization for superconductor switches driven by current-optical pulses*, Proc. SPIE, vol. 5948, pp. 21.1-7, 2005.
5. A.V. Mezenov, Y. Vas'kevich: *Model of current and optical conductivity switching in $YBa_2Cu_3O_{7-x}$ films*, Technical Physics, vol. 44, no 10, pp. 1198-202, 1999.
6. A.V. Mezenov, A.V. Yankevich, J. Waskiewicz: *Modeling the electrical response of thin films of high-temperature superconductors to laser and current pulses*, Journal of Optical Technology, vol. 66, no 8, pp. 749-754, 1999.
7. A.V. Mezenov, J. Waskiewicz: *Modelling of electrical response of superconducting films to current and optical pulses*, Proc. XV Symp. Electromagnetic Phenomena in nonlinear circuits (Liége), pp. 245-248, 1998.
8. J. Waskiewicz: *Optimal control characteristics of superconductor switching elements driven by current and laser pulses*, Proc. SPIE, vol. 6599, pp. 05.1-5, 2007.
9. J. Waskiewicz: *Reasons of switch-off time decrease in superconductor switches with a buffer layer*, Physica C, vol. 372-376, no 2, pp. 630-633, 2002.

a ser

effic
analy
Mark

an in
an or

Keyw

The fi
was to dete
In this
objective i
service sys
To sol
systems an

Artykuł finan
praktycznych

ELECTRONICS AND TELECOMMUNICATIONS QUARTERLY, 2008, 54, no 2, pp. 135–147

Strategies evaluation on the attempts to gain access to a service system (the second problem of an impatient customer)

ROMAN SZOSTEK

Rzeszów University of Technology
Department of Quantitative Methods in Economics
ul. Wincentego Pola 2, 35-959 Rzeszów
rszostek@prz.rzeszow.pl

Received 2008.02.01
Authorized 2008.06.02

The paper introduces the solution of the optimization problem consisting in choosing a more efficient strategy while accessing a service system. To solve the problem a method of queuing systems analysis by included Markov chains [1][4] was used. The examined system is described by non-Markovian model.

The presented issue was called the second problem of an impatient customer. The first problem of an impatient customer was discussed in paper [5]. Author's comprehensive study formulates and solves an original task of the second problem of an impatient customer.

Keywords: optimization, objective (cost) function, system parameters, probabilistic methods, Markov process, non-Markovian process, included Markov chain

1. INTRODUCTION

The first problem of an impatient customer was introduced and solved in paper [5]. The task was to determine the optimal time between the successive attempts to access a service system.

In this paper the second problem of an impatient customer was formulated and solved. The objective is to select a more efficient of the two different strategies on the attempt to access a service system.

To solve the above mentioned problems it is necessary to introduce the models of the examined systems and an objective function. The models are nondeterministic and non-Markovian.

Artykuł finansowany ze środków Sieci Naukowej Aearonautica Integra z pozycji promocja wyników i zastosowań praktycznych badań naukowych prowadzonych w ramach Sieci.

2. PROBLEM FORMULATION

The given configuration of four satellites is visualized in Fig. 1. Satellite A's task is to send a data set to satellites D_1 or D_2. As the direct connection between those satellites is not possible, the data transmission has to be made by satellite C, which charges a fee for the time during which its resources are used. Satellite C is always idle and ready to cooperate, while satellites A and C are idle and busy interchangeably. While one of them is busy doing other tasks, it cannot receive data from satellite A. Satellites D_1 and D_2 operate independently and it does not matter to which of them satellite A sends data. At a given time instant satellite A can try to send data to only one of the satellites D_1 or D_2.

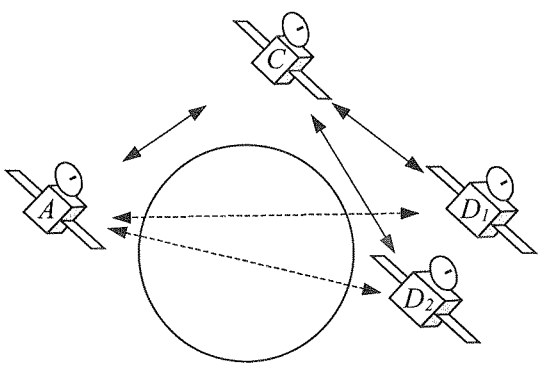

Fig. 1. Problem illustration

Satellite A's task is, therefore, to gain access to the resources of satellites D_1 or D_2. However, it has no information about the state of the other satellites, until it makes an attempt to send data. If the attempt fails (because the satellite to which an attempt to transmit data was made is busy), then after time T satellite A makes another attempt to send data to either satellite. The following attempts are made in the same time intervals T, until one of the satellites is ready to receive data.

Every attempt to send data by satellite C, even if it is unsuccessful, results in costs amounting to c_1. It is assumed that the waiting time of satellite A to obtain connection also generates a unit cost of c_2. Thus, the costs function of obtaining connection by satellite A has the following form:

$$F(T) = c_1 N_{sr}(T) + c_2 T_{sr}(T) \tag{1}$$

where: $N_{sr}(T)$ – the mean number of attempts made to obtain connection by satellite A,
$T_{sr}(T)$ – the mean time of obtaining connection by satellite A,
$c_1 \in \boldsymbol{R}_+ \cup \{0\}$ – cost of one attempt to obtain connection,
$c_2 \in \boldsymbol{R}_+ \cup \{0\}$ – cost of (connection) waiting time unit.

The M/M/1/-/1 system is assumed to be the model describing the state of satellite D_i. The time when the satellite is idle and when it is busy is, therefore, subjected to exponential distribution. It is not possible to queue to none of satellites D_i resources. The graph of satellites states is shown in Fig. 2. In state W satellite is idle, while in state Z satellite is busy.

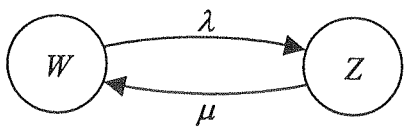

Fig. 2. Graph of states for the M/M/1/-/1 system

In order to obtain connection satellite A can proceed different strategies, two of which are compared in this paper.

The first strategy consists in selecting one of the satellites D_1 or D_2 and making attempts to connect to this satellite only in time intervals T.

In the second strategy the attempts to connect are made with both satellites D_1 and D_2 interchangeably. Time interval between the attempts is T as well. In this strategy both the first and the second satellite are checked in time intervals $2T$.

In the following sections it will be proved which of the two proposed strategies is more efficient, that is, for which strategy the cost function (1) has the smaller value.

3. ANALYSIS OF THE FIRST STRATEGY

The attempts to obtain connection by satellite A can be regarded as an additional determined stream of arrivals to satellite D_1 resources. The system given in Fig. 2 together with an additional determined stream will be called the extended system. In Fig. 3 graph of the extended system states is shown. The extended system is non-Markovian.

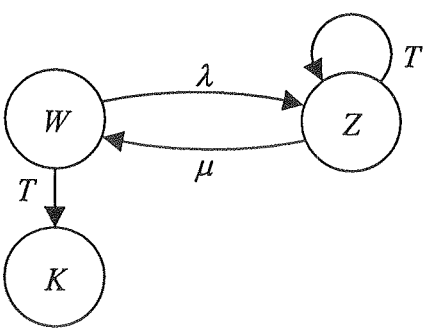

Fig. 3. Graph of states for M/M/1/-/1 system extended by determined stream of arrivals representing an additional customer

The additional (absorbing) node K represents the situation in which satellite A obtains connection. Transition to state K is possible only from state W (idle system). The additional transition from state Z to Z represents the situation when the attempt to obtain connection by satellite A has failed.

The extended system has a nonexponential service node and can be analysed by included Markov chains.

3.1. TRANSITION PROCESSES FOR SATELLITE D_i

This paragraph demonstrates the transition processes in the system shown in Fig. 2. Their knowledge is necessary for further strategy analysis.

Assume the following symbols:

A_i – event that satellite A obtained connection in ith attempt ($i = 0, 1, 2, ...$),

B_i – event that satellite A did not obtain connection in ith attempt ($i = 0, 1, 2, ...$).

The following attempts are made in time intervals T. The attempt i ($i = 0,1,2,...$) is made at time iT.

At a time instant of zero-test satellite D_i is in stationary state. Thus, we obtain:

$$\begin{cases} \lambda p(A_0) = \mu p(B_0) \\ p(A_0) + p(B_0) = 1 \end{cases} \tag{2}$$

That is:

$$\begin{cases} p(A_0) = \dfrac{\mu}{\lambda + \mu} \\ p(B_0) = \dfrac{\lambda}{\lambda + \mu} \end{cases} \tag{3}$$

If the first attempt to obtain connection has failed, then after time T satellite A tries again. Assuming that the system given in Fig. 2 is the Markov system (memoryless) then we obtain:

$$\begin{cases} p_z(T) := p(B_{i+1} / B_i) = p(B_1 / B_0), & i = 0,1,2,... \\ p_w(T) := p(A_{i+1} / B_i) = p(A_1 / B_0), & i = 0,1,2,... \end{cases} \tag{4}$$

The following symbols are introduced:

$p_w(T)$ – probability that the satellite D_i is idle at a time instant T, assuming that at a time instant T=0 it was busy, that is $p_w(0)$=0,

$p_z(T)$ – probability that the satellite D_i is busy at a time instant T, assuming that at a time instant T=0 it was busy, that is $p_w(0)$=1.

For the calculation of the above values it is necessary to solve the system of differential equations which describes the transition processes in the system from Fig. 2.

$$\begin{cases} \dot{p}_z(T) = +\lambda p_w(T) - \mu p_z(T) \\ \dot{p}_w(T) = -\lambda p_w(T) + \mu p_z(T) \end{cases} \tag{5}$$

The solution of the system of equations (5) has the following form:

$$\begin{cases} p_z(T) = p(B_{i+1} / B_i) = \dfrac{\lambda}{\lambda+\mu} + \dfrac{\mu}{\lambda+\mu} e^{-(\lambda+\mu)T} \\ p_w(T) = p(A_{i+1} / B_i) = \dfrac{\mu}{\lambda+\mu} - \dfrac{\mu}{\lambda+\mu} e^{-(\lambda+\mu)T} \end{cases} \tag{6}$$

where: $i = 0,1,2,...$

The graphs of $p_z(T)$ and $p_w(T)$ functions are shown in Fig. 4.

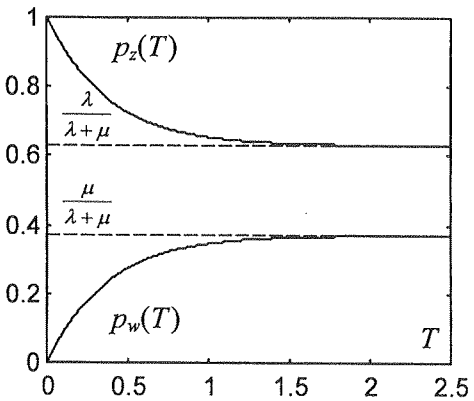

Fig. 4. Graphs of functions $p_z(T)$ and $p_w(T)$

3.2. CONTRUCTION OF THE INCLUDED MARKOW CHAIN

The included Markov chain for the system given in Fig. 3 has two states. That is so because the system at a time instant just after the attempt to gain access to a service system can be in state K (satellite A obtained connection) or in state Z (satellite A did not obtain connection). In Fig. 5 graph of states of included Markov chain is shown.

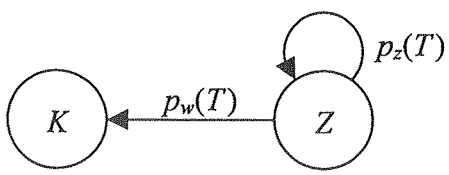

Fig. 5. Graph of states of included Markov chain

Assume the following symbols (i=0,1,2,... is the attempt number):
$q_K(i)$ – the probability that the Markov chain is in state K,
$q_Z(i)$ – the probability that the Markov chain is in state Z.

The equations describing the included Markov chain have the following form:

$$[q_K(i+1), q_Z(i+1)] = [q_K(i), q_Z(i)] \begin{bmatrix} 1 & 0 \\ p_w(T) & p_z(T) \end{bmatrix} \tag{7}$$

Where: $i = 0,1,2,...$

The following initial conditions are also fulfilled (on the basis of (3))

$$[q_K(0), q_Z(0)] = [\frac{\mu}{\lambda+\mu}, \frac{\lambda}{\lambda+\mu}] \tag{8}$$

The equations (7) and (8) define Markov chain describing transition processes in the examined extended system.

Let us determine the probability $\hat{p}_i$ that satellite A obtaines connection exactly in ith attempt (i=0,1,2,...). It can be done in two ways:

First method (direct)

$$\begin{cases} \hat{p}_0 = p(A_0) \\ \hat{p}_i = p(A_i \wedge B_{i-1} \wedge ... \wedge B_0) = \\ \quad = p(A_i / B_{i-1}) p(B_{i-1} \wedge ... \wedge B_0) = ... = \\ \quad = p(A_i / B_{i-1}) p(B_{i-1} / B_{i-2}) ... p(B_1 / B_0) p(B_0), \qquad i = 1,2,3,... \end{cases} \tag{9}$$

Second method (we use (7))

$$\begin{cases} \hat{p}_0 = q_K(0) \\ \hat{p}_i = q_K(i) - q_K(i-1), \qquad i = 1,2,3,... \end{cases} \tag{10}$$

In both the first and the second case we obtain:

$$\begin{cases} \hat{p}_0 = \dfrac{\mu}{\lambda+\mu} \\ \hat{p}_i = \dfrac{\lambda}{\lambda+\mu} p_z^{i-1}(T) p_w(T), \qquad i = 1,2,3,... \end{cases} \tag{11}$$

The values of $\hat{p}_i$ describe the distribution of waiting time of satellite A for the connection to satellite D_i. The following relation occurs:

$$\sum_{i=0}^{\infty} \hat{p}_i = 1 \tag{12}$$

3.3. THE EXTENDED SYSTEM PARAMETERS

The mean number of attempts to obtain connection is:

$$N_{sr}(T) = 1\hat{p}_0 + 2\hat{p}_1 + 3\hat{p}_2 + \ldots = 1 + \sum_{i=1}^{\infty} i\hat{p}_i \tag{13}$$

The mean waiting time to obtain connection is given by:

$$T_{sr}(T) = 0T\hat{p}_0 + 1T\hat{p}_1 + 2T\hat{p}_2 + \ldots = T\sum_{1}^{\infty} i\hat{p}_i \tag{14}$$

After taking into account (6) and (11) we obtain desired parameters:

$$N_{sr}(T) = 1 + \frac{\lambda}{\lambda+\mu}\frac{1}{p_w(T)} = 1 + \frac{\lambda}{\mu(1-e^{-(\lambda+\mu)T})} \tag{15}$$

$$T_{sr}(T) = T\frac{\lambda}{\lambda+\mu}\frac{1}{p_w(T)} = \frac{\lambda T}{\mu(1-e^{-(\lambda+\mu)T})} \tag{16}$$

In Fig. 6 graph of function $N_{sr}(T)$ is visualized.

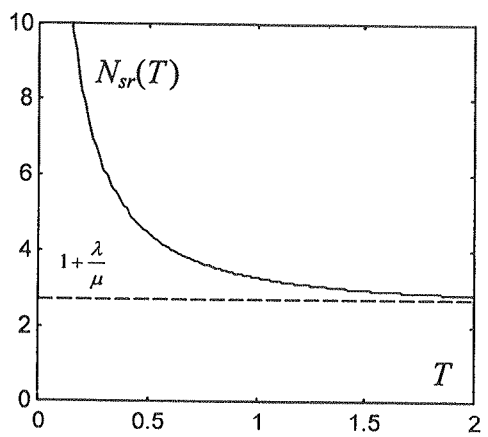

Fig. 6. Graph of function $N_{sr}(T)$

Graph of function $T_{sr}(T)$ is shown in Fig. 7.

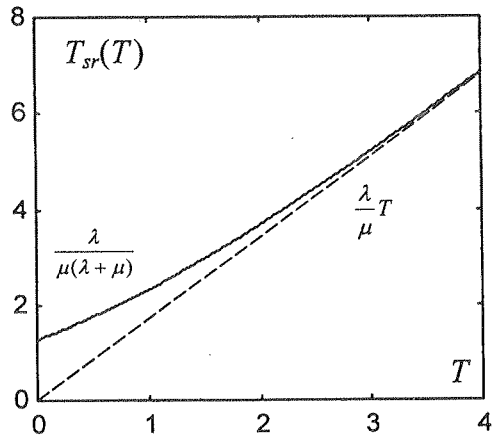

Fig. 7. Graph of function $T_{sr}(T)$

4. ANALYSIS OF THE SECOND STRATEGY

For the second strategy the extended system consists of two M/M/1/-/1 systems and determined stream of arrivals representing the additional satellite A attempting to obtain connection.

4.1. TRANSITION PROCESSES IN THE SERVICE SYSTEMS

Attempts to obtain connections are made to satellites D_1 and D_2 interchangeably. By the numbers 0, 2, 4, ... we denote the attempts to connect to satellite D_1, while by the numbers 1, 3, 5, ... the attempts to connect to satellite D_2. Assume the following symbols:

A_{2i}^1 – the event that a connection to satellite D_1 in the attempt $2i$ is obtained
B_{2i}^1 – the event that a connection to satellite D_1 in the attempt $2i$ in not obtained
A_{2i+1}^2 – the event that a connection to satellite D_2 in the attempt $(2i+1)$ is obtained
B_{2i+1}^2 – the event that a connection to satellite D_2 in the attempt $(2i+1)$ is not obtained
where: $i = 0,1,2,...$

During the zero-test and the first attempt the satellites D_1 and D_2 are in a steady state. Thus, (similarly to case (3)) we have:

$$\begin{cases} p(A_0^1) = p(A_1^2) = \dfrac{\mu}{\lambda+\mu} \\ p(B_0^1) = p(B_1^2) = \dfrac{\lambda}{\lambda+\mu} \end{cases} \tag{17}$$

As we assumed that satellite D_1 and D_2 are operating in the same way, the following conditional probabilities are identical for both systems. These probabilities were calculated in section 3.1 (see Eq. 6). For satellite D_1 we have:

$$\begin{cases} p_z(2T) := p(B^1_{i+2} / B^1_i) = p(B^1_2 / B^1_0) = \dfrac{\lambda}{\lambda+\mu} + \dfrac{\mu}{\lambda+\mu} e^{-(\lambda+\mu)2T} \\ p_w(2T) := p(A^1_{i+2} / B^1_i) = p(A^1_2 / B^1_0) = \dfrac{\mu}{\lambda+\mu} - \dfrac{\mu}{\lambda+\mu} e^{-(\lambda+\mu)2T} \end{cases} \tag{18}$$

where: i=0, 2, 4, ...

and for satellite D_2:

$$\begin{cases} p_z(2T) := p(B^2_{i+2} / B^2_i) = p(B^2_3 / B^2_1) = \dfrac{\lambda}{\lambda+\mu} + \dfrac{\mu}{\lambda+\mu} e^{-(\lambda+\mu)2T} \\ p_w(2T) := p(A^2_{i+2} / B^2_i) = p(A^2_3 / B^2_1) = \dfrac{\mu}{\lambda+\mu} - \dfrac{\mu}{\lambda+\mu} e^{-(\lambda+\mu)2T} \end{cases} \tag{19}$$

where: i=1, 3, 5, ...

4.2. CONSTRUCTION OF THE INCLUDED MARKOV CHAIN

The included Markov chain for the considered system has two states and it is heterogeneous. After the attempt to obtain connection the system can be in state K (satellite A gained access to a service system) or in state Z (satellite A did not gain access to a service system).

In this case the equations describing the included Markov chain have the following form:

$$\begin{cases} [q_K(1), q_Z(1)] = [q_K(0), q_Z(0)] \begin{bmatrix} 1 & 0 \\ \dfrac{\mu}{\lambda+\mu} & \dfrac{\lambda}{\lambda+\mu} \end{bmatrix} \\ [q_K(i+1), q_Z(i+1)] = [q_K(i), q_Z(i)] \begin{bmatrix} 1 & 0 \\ p_w(2T) & p_z(2T) \end{bmatrix}, \quad i = 1,2,3,... \end{cases} \tag{20}$$

The following initial conditions are also fulfilled (on the basis of (17)):

$$[q_K(0), q_Z(0)] = [\frac{\mu}{\lambda+\mu}, \frac{\lambda}{\lambda+\mu}] \tag{21}$$

The equations (20) and (21) describe the transition processes in the examined extended system.

We calculate the probabilities $\widetilde{p}_i$ that satellite A obtains connection exactly in the ith attempt (i=0,1,2,...). Analogously to the first strategy it can be done in two ways:

Fist method (direct):

$$\begin{cases} \widetilde{p}_0 = p(A_0^1) \\ \widetilde{p}_1 = p(A_1^2 \wedge B_0^1) \\ \widetilde{p}_{2i} = p(A_{2i}^1 \wedge B_{2i-1}^2 \wedge \ldots \wedge B_2^1 \wedge B_1^2 \wedge B_0^1) = \\ \quad = p([A_{2i}^1 \wedge B_{2i-2}^1 \wedge \ldots \wedge B_2^1 \wedge B_0^1] \wedge [B_{2i-1}^2 \wedge B_{2i-3}^2 \wedge \ldots \wedge B_3^2 \wedge B_1^2]) = \\ \quad = p(A_{2i}^1 / B_{2i-2}^1) p(B_{2i-2}^1 / B_{2i-4}^1) \ldots p(B_2^1 / B_0^1) p(B_0^1) \cdot \\ \quad \cdot p(B_{2i-1}^2 / B_{2i-3}^2) p(B_{2i-3}^2 / B_{2i-5}^2) \ldots p(B_3^2 / B_1^2) p(B_1^2), \qquad i = 1,2,3,\ldots \\ \widetilde{p}_{2i+1} = p(A_{2i+1}^2 \wedge B_{2i}^1 \wedge \ldots \wedge B_2^1 \wedge B_1^2 \wedge B_0^1) = \\ \quad = p([B_{2i}^1 \wedge B_{2i-2}^1 \wedge \ldots \wedge B_2^1 \wedge B_0^1] \wedge [A_{2i+1}^2 \wedge B_{2i-1}^2 \wedge \ldots \wedge B_3^2 \wedge B_1^2]) = \\ \quad = p(B_{2i}^1 / B_{2i-2}^1) p(B_{2i-2}^1 / B_{2i-4}^1) \ldots p(B_2^1 / B_0^1) p(B_0^1) \cdot \\ \quad \cdot p(A_{2i+1}^2 / B_{2i-1}^2) p(B_{2i-1}^2 / B_{2i-3}^2) \ldots p(B_3^2 / B_1^2) p(B_1^2), \qquad i = 1,2,3,\ldots \end{cases} \tag{22}$$

Second method (we use (20)):

$$\begin{cases} \widetilde{p}_0 = q_K(0) \\ \widetilde{p}_i = q_K(i) - q_K(i-1) \qquad i = 1,2,3,\ldots \end{cases} \tag{23}$$

Thus, in both cases, after taking into account (17), (18) and (19) we obtain:

$$\begin{cases} \widetilde{p}_0 = \dfrac{\mu}{\lambda + \mu} \\ \widetilde{p}_1 = \dfrac{\lambda}{\lambda + \mu} \dfrac{\mu}{\lambda + \mu} \\ \widetilde{p}_i = \left(\dfrac{\lambda}{\lambda + \mu} \right)^2 p_z^{i-2}(2T) p_w(2T), \qquad i = 2,3,4,\ldots \end{cases} \tag{24}$$

The values of $\widetilde{p}_i$ describe the distribution of waiting time for a service. The following relation occurs:

$$\sum_{i=0}^{\infty} \widetilde{p}_i = 1 \tag{25}$$

4.3. THE EXTENDED SYSTEM PARAMETERS

The mean number of attempts made till the time instant in which a connection is obtained:

$$\widetilde{N}_{sr}(T) = 1\widetilde{p}_0 + 2\widetilde{p}_1 + 3\widetilde{p}_2 + \ldots = 1 + \sum_{i=1}^{\infty} i\widetilde{p}_i \tag{26}$$

The mean waiting time for obtaining connection is:

$$\widetilde{T}_{sr}(T) = 0T\widetilde{p}_0 + 1T\widetilde{p}_1 + 2T\widetilde{p}_2 + \ldots = T\sum_{1}^{\infty} i\widetilde{p}_i \tag{27}$$

After taking into account (18), (19) and (24) we obtain desired parameters:

$$\widetilde{N}_{sr}(T) = 1 + \frac{\lambda}{\lambda+\mu}\,\frac{p_w(2T) + \dfrac{\lambda}{\lambda+\mu}}{p_w(2T)} = 1 + \frac{\lambda\left(1 - \dfrac{\mu}{\lambda+\mu}e^{-(\lambda+\mu)2T}\right)}{\mu(1-e^{-(\lambda+\mu)2T})} \tag{28}$$

$$\widetilde{T}_{sr}(T) = T\,\frac{\lambda}{\lambda+\mu}\,\frac{p_w(2T) + \dfrac{\lambda}{\lambda+\mu}}{p_w(2T)} = \frac{\lambda\left(1 - \dfrac{\mu}{\lambda+\mu}e^{-(\lambda+\mu)2T}\right)T}{\mu(1-e^{-(\lambda+\mu)2T})} \tag{29}$$

5. STRATEGIES COMPARISON

For the first strategy the cost function $F(T)$ given in the expression (1), after taking into account (15) and (16), has the following form:

$$F(T) = \frac{\lambda}{\mu}\cdot\frac{c_2T + c_1}{1-e^{-(\lambda+\mu)T}} + c_1 \tag{30}$$

The graph of function $F_C(T)$ is shown in Fig. 8 (when $c_1, c_2 > 0$).

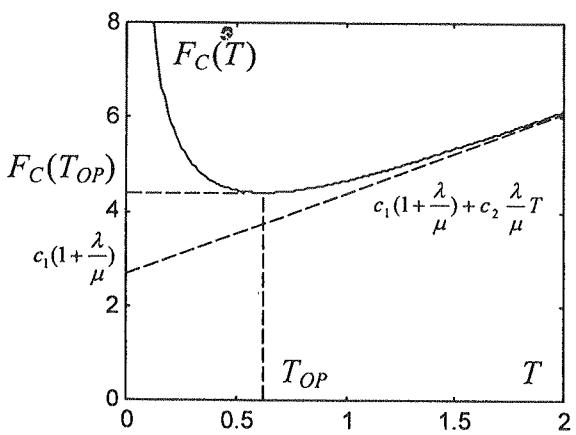

Fig. 8. Graph of the objective function $F_C(T)$

For the second strategy after taking into account (28) and (29) we obtain:

$$\widetilde{F}(T) = \frac{\lambda}{\mu}\cdot\frac{\left(1 - \dfrac{\mu}{\lambda+\mu}e^{-(\lambda+\mu)2T}\right)}{1-e^{-(\lambda+\mu)2T}}(c_2T + c_1) + c_1 \tag{31}$$

In order to compare both strategies we calculate the value of the following expression:

$$\frac{\widetilde{F}(T)-c_1}{F(T)-c_1}=\frac{\widetilde{N}_{sr}(T)-1}{N_{sr}(T)-1}=\frac{\widetilde{T}_{sr}(T)}{T_{sr}(T)}=\frac{1-\dfrac{\mu}{\lambda+\mu}e^{-(\lambda+\mu)2T}}{1+e^{-(\lambda+\mu)T}}<1 \tag{32}$$

The graph of relation (32) in time function T is depicted in Fig. 9.

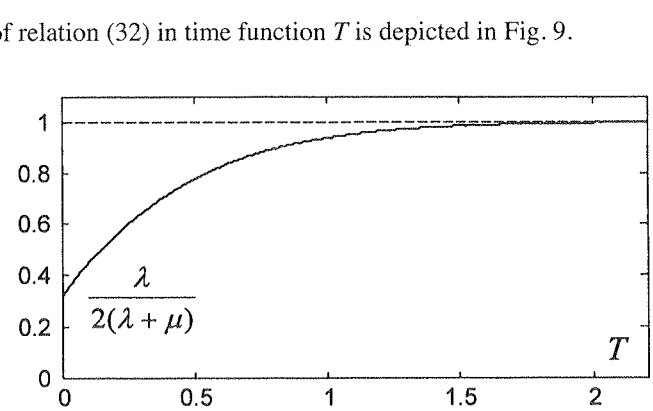

Fig. 9. Graph of function of Eq.(32)

The mean costs for the first strategy are higher than those for the second strategy $\widetilde{F}(T)$. Thus, in terms of assumed criteria, the second strategy seems to be more efficient.

The advantages resulting from choosing the second strategy are the higher the smaller the expression (32) value is (time interval T between the successive attempts is considerably small).

6. CONCLUSION

Presented in the paper the method of solving the considered problem can be easily applied in cases of more complex models of service systems as well. The only condition of its implementation is the possibility of transition processes determination in service systems (satellite D_i). For more complex systems these transition processes can be calculated by numerical methods. As the assumed models of service systems were Markovian it was possible to solve the problem by analytical methods.

Investigated in the paper the extended systems are non-Markovian. Their analysis was made using included Markov chains. For the solution of the stated problem it was necessary to analyse transition processes in these systems.

7. REFERENCES

1. G. T. Artamonow, O. M. Briechow: *Analiticzeskije wierojatnostnyje modieli funkcionirowanija EWM.* Moskwa, Wyd. Energija, 1978.

2. T. Czachórski: *Modele kolejkowe systemów komputerowych*. Gliwice, Politechnika Śląska, skrypty uczelniane nr 1844, 1994.
3. B. Filipowicz: *Modelowanie i optymalizacja systemów kolejkowych cz. I. Systemy markowskie*. Kraków, Wyd. T. Rudkowski, 1995.
4. B. Filipowicz: *Modelowanie i optymalizacja systemów kolejkowych cz. II. Systemy niemarkowskie*. Kraków, Wyd. FHU Poldex, 2000.
5. R. Szostek: *Systemy kolejkowe z niewykładniczym węzłem obsługi*. Kraków, Wydawnictwa AGH, Elektrotechnika i Elektronika, 2000, Tom 19/1, ss. 1-8.
6. F. Zitek: *Stracony czas. Elementy teorii obsługi masowej*. Poznań, PWN, 1977.

ELECTRONICS AND TELECOMMUNICATIONS QUARTERLY, 2008, 54, no 2, pp. 149–166

Two algorithms for obtaining fixed polarity arithmetic expansion representation of quaternary functions

CECILIA C. LOZANO[1], BOGDAN J. FALKOWSKI[1], TADEUSZ ŁUBA[2]

[1] Nanyang Technological University
School of Electrical and Electronic Engineering
Singapore
e-mail: <cicilia, efalkowski>@ntu.edu.sg
[2] Warsaw University of Technology
Institute of Telecommunications
Poland
e-mail: luba@tele.pw.edu.pl

Received 2008.04.09
Authorized 2008.06.05

Multiple-valued logic has attracted research interests as one way to improve and overcome the limitations encountered in circuits employing two-valued (binary) logic. In particular, much attention has been paid to the three-valued (ternary) and four-valued (quaternary) logic which form the smallest multiple-valued fields. In this article two algorithms for efficient calculation of quaternary fixed polarity arithmetic expansions (QFPAEs) representation of quaternary functions are presented. The first algorithm operates on disjoint cubes array representation of the input function and is suitable for obtaining selected spectral coefficients. The second algorithm starts from QFPAE in polarity zero and is advantageous for deriving either all QFPAE spectra or QFPAE coefficient vector in nonzero polarities. Both algorithms are simple and have high possibilities of parallel implementation. In order to show the advantage of the proposed algorithm, the computational costs for the second algorithm have been derived and compared with the fast transform method. The comparison shows that the algorithm has lower computational cost for generating the complete polarity matrix.

Keywords: fixed polarity arithmetic expansions, quaternary functions, spectral techniques, disjoint cubes, recursive algorithm

1. INTRODUCTION

In recent years, there have been major advances in integrated circuit technology that have made feasible the implementation of complex systems [4]. They include the ever-increasing use of multiple-valued logic combined with spectral methods to overcome the main two problems of

current VLSI technology: interconnections and chip pin-out problems [4]. Multiple-valued logic can represent the problem much more concisely than it could be in binary logic and appears as an adequate tool for coping with problems of higher size of complexity [1], [2], [5], [6], [11], [13], [17]–[20]. Multiple-valued approach increases the information density over the interconnections and thus their efficiency.

Spectral expansions are alternative representations of logic functions/signals in which the information is redistributed and presented differently in terms of spectral coefficients. The use of spectral representations often allows certain operations or analysis to be performed more efficiently on the data. Such representations have found applications in many areas, including design for testability, testing and verification, Boolean matching, quantum computing, and detection of symmetry and decomposability [2], [3], [5], [14], [16], [19]. In line with the interest in multiple-valued logic, various spectral expansions have been proposed for multiple-valued functions [2], [5], [12], [19].

Quaternary (four-valued) logic is one case of multiple-valued logic which is often encountered in many proposed multiple-valued applications. One reason for this is the ease of the conversion between the binary and quaternary signals or variables. Examples of applications employing four-valued logic include pipelined image processing [13], design of systolic architecture [1], and multi-level memories [6]. In this article two algorithms to generate the quaternary fixed polarity arithmetic expansions (QFPAEs) representation of quaternary functions are proposed. QFPAE is a spectral expansion for quaternary function that can be thought of as the arithmetic counterpart of fixed polarity Reed-Muller (FPRM) expansions over GF(4) discussed in [12]. The two expansions have similar forms. However, QFPAE employs modulo 4 and normal decimal arithmetic operations whereas in the FPRM over GF(4) all the addition, multiplication, and power operations are executed over GF(4)

For both FPRM over GF(4) and QFPAE, a quaternary function may have 4^n possible forms where the one with the least number of product terms (nonzero spectral coefficients) is said to be the optimal expansion. In some applications, it may be desirable to identify the optimal expansion as such expansion has simpler hardware implementation, requires less storage, and can be computed faster. Generally, all 4^n expansions need to be generated to obtain the optimal expansion.

The two algorithms presented here in this article developed based on different properties of QFPAE transforms. The first algorithm directly uses the relations between the truth vector elements and the spectral coefficients of a particular QFPAE expansion while the second algorithm utilizes the relations that exist between different QFPAE expansions to recursively derive the required polarity matrix elements. They also take as input different representations of the input function. The first algorithm takes disjoint cubes array representation of the input function while the second algorithm starts from the QFPAE in polarity zero [10]. For the first algorithm, if the input is given in either truth vector or non-disjoint cubes array, the input need to be first preprocessed to obtain the equivalent disjoint cubes array representation. The algorithm presented in [8] can be used for this purpose.

This article is organized as follows. Basic symbols and theories related to the QFPAE are first presented in Section 2, followed by description of the two algorithms in Sections 3 and 4.

Conclusion is given in Section 5. Based on the given computational steps for the two algorithms, it can be observed that the computational time and cost of the first algorithm is heavily dependent on the size of the ON disjoint cubes array of the input function whereas for the second algorithm they are mostly influenced by the size of the input variables and therefore are more predictable. Computational cost formulae for the second algorithm in terms of the number of required arithmetic operations have been derived and presented here. The result shows that the algorithm is more efficient than the fast transform method for finding the complete polarity matrix, and hence, the optimal QFPAE for the input functions. It is interesting to note that the generation of complete QFPAE polarity matrix by the algorithm from the truth vector requires smaller number of arithmetic operations than the numbers of additions and multiplications performed by the algorithms in [7], [9], [12], [15] for FPRM transform over GF(4). Due to the fact that for some quaternary functions the QFPAEs can provide simpler representation than FPRM in terms of nonzero spectral coefficient numbers and the importance of arithmetic transform in testing and fault detection, the new algorithms can find applications in computer-aided circuit and network design.

2. BASIC THEORY AND DEFINITIONS

QFPAE is a polynomial representation of a quaternary function where the basic functions consist of all possible products of the modulo 4 powers of the input variables' literals. The phrase 'fixed polarity' in the QFPAE indicates that in the expansion each input variable must always appear in the same form or literal. Since each quaternary variable can be represented by four possible literals, it follows that an n-variable quaternary function has 4^n possible QFPAEs.

In order to differentiate the 4^n possible QFPAEs of a particular n-variable function, each QFPAE is assigned with a unique polarity number ω. Let the four possible literals of a quaternary input variable x_l be denoted by x_l, $\dot{x}_l$, $\ddot{x}_l$, and $\dddot{x}_l$, where $\dot{x}_l = x_l \oplus 1$, $\ddot{x}_l = x_l \oplus 2$, $\dddot{x}_l = x_l \oplus 3$, and $\oplus$ denotes modulo 4 addition. Then the polarity number ω of a QFPAE is taken as the decimal number representation of $<j_1, j_2, \cdots, j_n>$, i.e., $<\omega>_{10} = <j_1, j_2, \cdots, j_n>_4$, where j_l is set to the value of 0, 1, 2 or 3 if the corresponding variable x_l always appears as x_l, $\dot{x}_l$, $\ddot{x}_l$ or $\dddot{x}_l$ in the expansion, respectively.

The QFPAE for an n-variable quaternary function $f(\vec{x})$ in polarity ω is given by the following general expression:

$$f(\vec{x}) = \sum_{i=0}^{4^n-1} c_i^{\omega} \left[\prod_{l=1}^{n} \hat{x}_l^{k_l} \right] = \sum_{i=0}^{4^n-1} c_i^{\omega} \pi_i^{\omega} , \tag{1}$$

where $\vec{x} = [x_1, x_2, \cdots, x_n]$, c_i^{ω} is the i-th spectral coefficient of $f(\vec{x})$ in polarity ω, $\hat{x}_l \in \{x_l, \dot{x}_l, \ddot{x}_l, \dddot{x}_l\}$ is the literal of the l-th variable, i is the decimal number representation of quaternary number $<k_1, k_2, \cdots, k_n>$, ($<i>_{10} = <k_1, k_2, \cdots, k_n>_4$), and $\hat{x}_l^{k_l} \in \{0, 1, 2, 3\}$ is the k_l-th modulo 4 power of $\hat{x}_l$. In the expansion all the additions and multiplications are performed in standard arithmetic algebra.

From the given general expression, it can be seen that each of the 4^n product terms in a QFPAE is a product of a spectral coefficient with the corresponding basis function π_i^{ω}. Since the basis functions and their ordering are fixed for QFPAEs with the same number of input variables n and polarity number ω, a QFPAE can be completely represented by a vector containing all of its spectral coefficients. Such vector for QFPAE in polarity ω is called the spectral coefficient vector, denoted by C^{ω}. It is defined as

$$C^{\omega} = [c_0^{\omega}, c_1^{\omega}, ..., c_{4^n-1}^{\omega}] \tag{2}$$

where c_i^{ω} denote the i-th spectral coefficient inside the QFPAE in polarity ω ($0 \le \omega \le 4^n - 1$).

The collection of all QFPAE spectral coefficient vectors for a particular n-variable quaternary function $f(\vec{x})$ form the polarity matrix of $f(\vec{x})$, denoted by P[$f(\vec{x})$]. It is defined as a $4^n \times 4^n$ matrix where the m-th row of the matrix ($0 \le m \le 4^n - 1$) corresponds to C^m. That is,

$$P[f(\vec{x})] = \left[C^0, C^1, ..., C^{4^n-1}\right]^T \tag{3}$$

where T denotes matrix transpose operator. Obviously, the polarity matrix contains all QFPAE spectral coefficients of $f(\vec{x})$ such that if we denote the element that is located at row g and column h of P[$f(\vec{x})$] by P_{gh} ($0 \le g, h \le 4^n - 1$) then $P_{gh} = c_h^g$. Due to the chosen ordering of the polarity matrix, we can state that the optimal QFPAE polarity number(s) for $f(\vec{x})$ is simply the index number(s) of the P[$f(\vec{x})$] row(s) with the maximum number of zeros it its columns.

The following relations exist between the truth vector and QFPAE spectral coefficient vector of an n-variable quaternary function $f(\vec{x})$. Let $\vec{F} = \left[F_0, F_1, ..., F_{4^n-1}\right]^T$ be the truth vector of $f(\vec{x})$, where $\vec{x} = [x_1, x_2, \cdots, x_n]$, $F_0 = f(0,0,\cdots,0)$, $F_1 = f(0,0,\cdots,1)$, and $F_{4^n-1} = f(3,3,\cdots,3)$. Then C^{ω} for $f(\vec{x})$ can be obtained from $\vec{F}$ by

$$C^{\omega} = \frac{1}{2^n} \cdot S_n^{<\omega>} \cdot \vec{F} = \frac{1}{2^n} \cdot \left(\otimes \prod_{l=1}^{n} S_1^{<j_l>} \right) \cdot \vec{F}, \tag{4}$$

where $\otimes$ denotes Kronecker product [3], [5], [11] and $<\omega>_{10} = <j_1, j_2, \cdots, j_n>_4$.

Conversely, $\vec{F}$ can be obtained back from C^{ω} by

$$F = T_n^{<\omega>} \cdot C^{\omega} = \left(\otimes \prod_{l=1}^{n} T_1^{<j_l>} \right) \cdot C^{\omega}. \tag{5}$$

The transform matrices $S_n^{<\omega>}$ and $T_n^{<\omega>}$ are said to be the forward and inverse QFPAE matrices, respectively. Table 1 shows their basic transform matrices $T_1^{<j_l>}$ and $S_1^{<j_l>}$ for all possible polarities of j_1.

The recursive algorithm presented in Section 4 of this article is developed based on an equation that relates the spectral coefficient vector in polarity zero C^0 with any spectral coefficient vectors C^{ω}. The equation can be derived from (4) and (5) as follows (recall that $<\omega>_{10} = <j_1, j_2, \cdots, j_n>_4$):

$$
\begin{aligned}
C^{\omega} &= \frac{1}{2^n}\cdot S_n^{<\omega>}\cdot \vec{F} = \frac{1}{2^n}\cdot S_n^{<\omega>}\cdot T_n^0\cdot C^0 \\
&= \frac{1}{2^n}\cdot\left(\otimes\prod_{l=1}^{n} S_1^{<j_l>}\right)\cdot\left(\otimes\prod_{l=1}^{n} T_1^{<0>}\right)\cdot C^0 \\
&= \left(\otimes\prod_{l=1}^{n}\left(\frac{1}{2}\cdot S_1^{<j_l>}\cdot T_1^{<0>}\right)\right)\cdot C^0 \\
&= \left(\otimes\prod_{l=1}^{n} Z_1^{<j_l>}\right)\cdot C^0 = Z_n^{<\omega>}\cdot C^0.
\end{aligned}
\tag{6}
$$

The four basic transform matrices $Z_1^{<j_l>}$ are listed in the rightmost column of Table 1.

Example 1. Let $f(\vec{x})$ be a two-variable quaternary function with the truth vector $\vec{F}=[2,1,0,3,1,2,1,2,2,3,0,1,1,0,1,0]^T$. Then, by (4) C^7 for $f(\vec{x})$ can be calculated by

$$C^7 = \frac{1}{4}\cdot S_2^{<7>}\cdot\vec{F} = \frac{1}{4}\cdot(S_1^{<1>}\otimes S_1^{<3>})\cdot\vec{F}.$$

$$
= \frac{1}{4}\begin{bmatrix}
0&0&0&0&0&0&0&0&0&0&0&0&4&0&0\\
0&0&0&0&0&0&0&0&0&0&0&0&-2&0&2\\
0&0&0&0&0&0&0&0&0&0&0&-2&-4&6&0\\
0&0&0&0&0&0&0&0&0&0&0&2&2&-2&-2\\
0&0&0&0&0&2&0&0&0&0&0&0&-2&0&0\\
0&0&0&0&0&-1&0&1&0&0&0&0&1&0&-1\\
0&0&0&0&-1&-2&3&0&0&0&0&1&2&-3&0\\
0&0&0&0&1&1&-1&-1&0&0&0&0&-1&-1&1&1\\
0&6&0&0&0&0&0&0&0&-2&0&0&0&-4&0&0\\
0&-3&0&3&0&0&0&0&0&1&0&-1&0&2&0&-2\\
-3&-6&9&0&0&0&0&0&1&2&-3&0&2&4&-6&0\\
3&3&-3&-3&0&0&0&0&-1&-1&1&1&-2&-2&2&2\\
0&-2&0&0&0&-2&0&0&0&2&0&0&0&2&0&0\\
0&1&0&-1&0&1&0&-1&0&-1&0&1&0&-1&0&1\\
1&2&-3&0&1&2&-3&0&-1&-2&3&0&-1&-2&3&0\\
-1&-1&1&1&-1&-1&1&1&1&1&-1&-1&1&1&-1&-1
\end{bmatrix}\cdot\begin{bmatrix}2\\1\\0\\3\\1\\2\\1\\2\\2\\3\\0\\1\\1\\0\\1\\0\end{bmatrix} = \begin{bmatrix}0\\0\\1\\0\\1\\0\\-1\\0\\0\\2\\-2\\-1\\0\\-1\\0\\1\end{bmatrix}.
$$

Thus, the QFPAE for $f(\vec{x})$ in polarity seven is

$$f(\vec{x}) = \ddot{x}_2^{\,2} + \dot{x}_1 - \dot{x}_1\ddot{x}_2^{\,2} + 2\dot{x}_1^{\,2}\ddot{x}_2 - 2\dot{x}_1^{\,2}\ddot{x}_2^{\,2} - \dot{x}_1^{\,2}\ddot{x}_2^{\,3} - \dot{x}_1^{\,3}\ddot{x}_2 + \dot{x}_1^{\,3}\ddot{x}_2^{\,3}.$$

Table 1

Basic transform matrices for QFPAE

j_l	$T_1^{<j_l>}$	$S_1^{<j_l>}$	$Z_1^{<j_l>}$
0	$\begin{bmatrix}1&0&0&0\\1&1&1&1\\1&2&0&0\\1&3&1&3\end{bmatrix}$	$\begin{bmatrix}2&0&0&0\\-1&0&1&0\\-2&3&0&-1\\1&-1&-1&1\end{bmatrix}$	$\begin{bmatrix}1&0&0&0\\0&1&0&0\\0&0&1&0\\0&0&0&1\end{bmatrix}$
1	$\begin{bmatrix}1&1&1&1\\1&2&0&0\\1&3&1&3\\1&0&0&0\end{bmatrix}$	$\begin{bmatrix}0&0&0&2\\0&1&0&-1\\3&0&-1&-2\\-1&-1&1&1\end{bmatrix}$	$\begin{bmatrix}1&3&1&3\\0&-1&0&-1\\0&-4&-1&-3\\0&2&0&1\end{bmatrix}$

Table 1 (cd)

Basic transform matrices for QFPAE

2	$\begin{bmatrix} 1 & 2 & 0 & 0 \\ 1 & 3 & 1 & 3 \\ 1 & 0 & 0 & 0 \\ 1 & 1 & 1 & 1 \end{bmatrix}$	$\begin{bmatrix} 0 & 0 & 2 & 0 \\ 1 & 0 & -1 & 0 \\ 0 & -1 & -2 & 3 \\ -1 & 1 & 1 & -1 \end{bmatrix}$	$\begin{bmatrix} 1 & 2 & 0 & 0 \\ 0 & -1 & 0 & 0 \\ 0 & 2 & 1 & 4 \\ 0 & 0 & 0 & -1 \end{bmatrix}$
3	$\begin{bmatrix} 1 & 3 & 1 & 3 \\ 1 & 0 & 0 & 0 \\ 1 & 1 & 1 & 1 \\ 1 & 2 & 0 & 0 \end{bmatrix}$	$\begin{bmatrix} 0 & 2 & 0 & 0 \\ 0 & -1 & 0 & 1 \\ -1 & -2 & 3 & 0 \\ 1 & 1 & -1 & -1 \end{bmatrix}$	$\begin{bmatrix} 1 & 1 & 1 & 1 \\ 0 & 1 & 0 & 1 \\ 0 & 2 & -1 & -1 \\ 0 & -2 & 0 & -1 \end{bmatrix}$

3. ALGORITHM TO CALCULATE QFPAE SPECTRAL COEFFICIENTS FROM DISJOINT CUBES ARRAY REPRESENTATION

In this Section, an algorithm that directly calculates QFPAE spectral coefficients from disjoint cubes array representations of the input function is presented. The algorithm calculates each spectral coefficient independently from other spectral coefficients, allowing parallel computation of the different spectral coefficients. Since it performs the same operations on each of the ON cubes, the performance of the algorithm depends largely on the number of disjoint ON cubes of the input function as well as the number of spectral coefficients to be calculated. Thus, this algorithm works well for cases where the number of the disjoint ON cubes of the input function is relatively small and/or only few spectral coefficients need to be calculated. On the other hand, due to the independent and uniform manner in which the algorithm carries out the calculation, the algorithm requires very small memory space. In the worst case, at any one time only the intermediate value of the spectral coefficient being calculated and the ON cube currently being operated on need to be stored in memory. This allows the algorithm to be used to calculate the QFPAE spectra of large functions on which other algorithms are not feasible due to lack of memory space. In the following, some definitions necessary for the algorithm are first presented followed by the description of the algorithm.

3.1. BASIC DEFINITIONS

The literal of a quaternary variable in a cube is denoted by $X_i^{S_i}$, where $S_i \subseteq \{0,1,2,3\}$ is said to be the true set of literal X_i and $X_i^{S_i} = \begin{cases} 1 \text{ if } X_i \in S_i \\ 0 \text{ if } X_i \notin S_i \end{cases}$. A quaternary cube is a product of literals $X_1^{S_1} X_2^{S_2} \ldots X_i^{S_i}$, where $i \leq n$. A cube covers one or more minterms, which are defined as the product of n literals $X_1^{S_1} X_2^{S_2} \ldots X_n^{S_n}$ in which every set S_i has only one element.

Based on the value of the function output, the cubes of a completely specified function are divided into ON cube and OFF cube. A cube is said to be an ON cube if the function output for the cube is not equal to zero. Otherwise, it is an OFF cube.

An array of cubes is disjoint if none of the cubes share common minterms with another cube in the array. Otherwise the array is said to be nondisjoint (overlapped).

A cube can be represented by its positional notation such that each literal is represented by r (number of input values) binary digits, with the $(i + 1)$-th digit set to 1 when i is a member of the true set of the literal and 0 otherwise.

The missing literal ('–') in a quaternary cube corresponds to the literal $X_i^{\{0,1,2,3\}}$ as well as the positional notation '1111'.

Example 2. Let $X_1^{\{1,2\}} X_2^{\{0,1,3\}} X_3^{\{3\}}$ be a quaternary cube with three input variables. Then the minterms covered by the cube are $X_1^{\{1\}}, X_2^{\{0\}}, X_3^{\{3\}}, X_1^{\{2\}}, X_2^{\{0\}}, X_3^{\{3\}}, X_1^{\{1\}} X_2^{\{1\}} X_3^{\{3\}}, X_1^{\{2\}} X_2^{\{1\}} X_3^{\{3\}}$, $X_1^{\{1\}} X_2^{\{3\}} X_3^{\{3\}}$, and $X_1^{\{2\}} X_2^{\{3\}} X_3^{\{3\}}$ or 103, 203, 113, 213, 133, and 233, respectively. In positional notation, the cube is represented by 0110–1101–0001.

3.2. STEPS OF THE ALGORITHM

The algorithm presented in this Section takes an array of ON disjoint cubes representation of the quaternary input function as its input, where the cubes can be represented as integer coded cube or by its positional notation. For each spectral coefficient to be calculated, the algorithm operates on each ON disjoint cubes one by one to obtain the contribution of the cube to the value of the spectral coefficient. The contributions of all the ON cubes are then summed up in standard arithmetic algebra to obtain the value for the spectral coefficient.

Let z be the number of ON disjoint cubes inside the quaternary input function and h_q^i be the contribution of the q-th ON disjoint cube to the value of the i-th spectral coefficient c_i^{ω}. Then, we can write that

$$c_i^{\omega} = \sum_{q=1}^{z} h_q^i . \tag{7}$$

The steps executed inside the algorithm to obtain h_q^i are listed below. Two operators are used inside the algorithm: ω-adjustment and π-adjustment operators. The ω-adjustment operator is an operator that takes a polarity digit and a quaternary cube literal as its inputs whereas the π-adjustment operator is defined as an operation between a spectral coefficient index digit and a quaternary cube literal. For both operators, the cube input can be represented in the form of either integer coded cube or positional notation. Tables 2 and 3 show the ω-adjustment operation when the cube is an integer coded cube and in positional notation, respectively whereas the π-adjustment operation for the two different cases are given in Tables 4 and 5.

Algorithm to calculate the contribution of each ON disjoint cube to the value of QFPAE spectral coefficients

Let the q-th ON disjoint cube of an n-variable quaternary function be given by $q = q_1 q_2 \ldots q_n$ and the spectral coefficient to be calculated be c_i^{ω}. Then the value of h_q^i as described above can be generated through the following steps:

Step 1: Generate the n-digit quaternary representation of the spectral coefficient index i, $< k_1, k_2, ..., k_n >$ and polarity number ω, $< j_1, j_2, \cdots, j_n >$.

Step 2: Perform bitwise operation on q and ω:

$$q' = q_{\omega\text{-}adj}\omega.$$

Step 3: Set $i' = i$. If the cube q' does not have missing literals, go to Step 4. Otherwise perform the following:

– If the cube is an integer coded cube:

For every digit of the cube q' ($1 \le l \le n$), if q'_l = '–' then set $q'_l = i'_l$ and $i'_l = 0$.

– If the cube is represented by its positional notation:

For every literal in the cube q'_l ($1 \le l \le n$), if $q'_l = 1111$ then set $q'_l = 1000, 0100, 0010$ or 0001 according to whether $i'_l = 0, 1, 2$ or 3, respectively. Subsequently set $i'_l = 0$.

Step 4: Perform bitwise operation on q' and i':

$$q'' = q'_{\pi\text{-}adj}i'.$$

Step 5: Set $M = \prod_{l=1}^{n} q''_l$.

Step 6: Determine the sign of h_q^i by the following:

– If the cube is an integer coded cube:

Perform bitwise modulo 3 addition, $temp = q' \oplus i'$. If the number of nonzero digit in $temp$ is even, $sign = 1$. Else, $sign = -1$.

– If the cube is represented by its positional notation:

Set $temp = 0$. For every nonzero digit in i', i'_l ($1 \le l \le n$): if (i'_l and the leftmost digit in the positional notation of the l-th input variable in $q' = 1$) or ($i'_l = 2$ and the second leftmost digit in the positional notation of the l-th input variable in $q' = 0$) or ($i'_l = 3$ and both the rightmost and leftmost digits in the positional notation of the l-th input variable in $q' = 0$) or ($i'_l = 3$ and both the middle digits in the positional notation of the l-th input variable in $q' = 1$) then set $temp = temp + 1$. If the final value of $temp$ is even, $sign = 1$. Else, $sign = -1$.

Step 7: Let $f(q)$ be the output value of the disjoint cube q. Then,

$$h_q^i = \frac{1}{2^n} \times sign \times M \times f(q).$$

4. ALGORITHM FOR RECURSIVE GENERATION OF QFPAE POLARITY MATRIX

The algorithm presented in Section 3 is well suited for calculation of selected spectral coefficients. However, for cases where the complete spectral coefficient vector or the complete polarity matrix need to be generated the algorithm may require long computational time and hence not feasible. To address this problem in this Section another algorithm is presented which is more suitable for generating either selected spectral coefficient vectors or the complete polarity matrix. The algorithm utilizes the relations that exist between the subvectors of QFPAE spectral

coefficient vectors in different polarities to first generate a recursive definition for the QFPAE polarity matrix. The recursive definition is then modified based on the arithmetic relations between the elements of the matrix so that the algorithm incurs smaller computational cost. This in turn translates into faster computational time.

Table 2

Cube ω-adjustment operation (quaternary integer coded cube)

ω-*adj*	Polarity digit			
Cube digit	0	1	2	3
0	0	1	2	3
1	1	2	3	0
2	2	3	0	1
3	3	0	1	2
-	-	-	-	-

Table 3

Cube ω-adjustment operation (quaternary positional notation)

ω-*adj*	Polarity digit			
Variable positional notation	0	1	2	3
0001	0001	1000	0100	0010
0010	0010	0001	1000	0100
0011	0011	1001	1100	0110
0100	0100	0010	0001	1000
0101	0101	1010	0101	1010
0110	0110	0011	1001	1100
0111	0111	1011	1101	1110
1000	1000	0100	0010	0001
1001	1001	1100	0110	0011
1010	1010	0101	1010	0101
1011	1011	1101	1110	0111
1100	1100	0110	0011	1001
1101	1101	1110	0111	1011
1110	1110	0111	1011	1101
1111	1111	1111	1111	1111

Table 4

Cube ω-adjustment operation (quaternary integer coded cube)

π-*adj*	Spectral coefficient index digit			
Cube digit	0	1	2	3
0	2	1	2	1
1	0	0	3	1
2	0	1	0	1
3	0	0	1	1

Table 5

Cube ω-adjustment operation (quaternary positional notation)

π-*adj*	Spectral coefficient index digit			
Variable positional notation	0	1	2	3
0001	0	0	1	1
0010	0	1	0	1
0011	0	1	1	0
0100	0	0	3	1
0101	0	0	2	0
0110	0	1	3	2
0111	0	1	2	1
1000	2	1	2	1
1001	2	1	3	2
1010	2	0	2	0
1011	2	0	3	1
1100	2	1	1	0
1101	2	1	0	1
1110	2	0	1	1

4.1. RECURSIVE DEFINITIONS FOR QFPAE POLARITY MATRIX

The development of the recursive definitions that are used by the recursive algorithm is given here. For the recursive definitions' generation, let the following recursive decomposition of spectral coefficient vector C^{ω} be first defined.

Each coefficient vector C^{ω} can be decomposed into four equal size subvectors such that

$$C^{\omega} = [c^{\omega}_{[n-1,0]}, c^{\omega}_{[n-1,1]}, c^{\omega}_{[n-1,2]}, c^{\omega}_{[n-1,3]}]. \tag{8}$$

Since there are 4^n elements in C^{ω}, each of the subvectors $c^{\omega}_{[n-1,q]}$ $(q \in \{0,1,2,3\})$ contains 4^{n-1} elements.

Let the decomposition above be recursive such that each subvector of C^{ω} can be further decomposed into four smaller subvectors of the same size:

$$c^{\omega}_{[p,q]} = [c^{\omega}_{[p-1,q0]}, c^{\omega}_{[p-1,q1]}, c^{\omega}_{[p-1,q2]}, c^{\omega}_{[p-1,q3]}], \tag{9}$$

where $1 \le p \le n$ and q is the $(n\text{-}p)$-digit quaternary number representation of any decimal number from 0 to $4^{n-p}-1$. Also, let $<q>_{10}$ be the decimal number representation of q in $c^{\omega}_{[p,q]}$. Then, it follows that the elements of the subvector $c^{\omega}_{[p,q]}$ correspond to the polarity matrix $\mathrm{P}[f(\vec{x})]$ elements with row index numbers ω and column index numbers j, where $\left(<q>_{10} \cdot 4^{p}\right) \le j < \left(<q>_{10} + 1\right) \cdot 4^{p}$.

Let the recursive definition for the polarity matrix be defined as follows:

$$T_p(t)=\begin{bmatrix} T_{p-1}(t_{00}) & T_{p-1}(t_{01}) & T_{p-1}(t_{02}) & T_{p-1}(t_{03}) \\ T_{p-1}(t_{10}) & T_{p-1}(t_{11}) & T_{p-1}(t_{12}) & T_{p-1}(t_{13}) \\ T_{p-1}(t_{20}) & T_{p-1}(t_{21}) & T_{p-1}(t_{22}) & T_{p-1}(t_{23}) \\ T_{p-1}(t_{30}) & T_{p-1}(t_{31}) & T_{p-1}(t_{32}) & T_{p-1}(t_{33}) \end{bmatrix} \tag{10}$$

where $T_p(t)$ denote a $4^p \times 4^p$ matrix with vector t as its first row.

Since $\mathrm{P}[f(\vec{x})]$ is a $4^n \times 4^n$ matrix and the first row of $\mathrm{P}[f(\vec{x})]$ is the spectral coefficient vector C^0, it is clear that based on (10) $\mathrm{P}[f(\vec{x})]=T_n(C^0)$. Furthermore, if we compare the recursive definition in (10) with the definition of the polarity matrix in Section 1 it can be deduced that when $t=c^{\omega}_{[p.q]}$, then the vectors $t_{t_1t_2}$ $(0 \le t_1, t_2 \le 3)$ inside $T_p(t)$ correspond to the vectors $c^{\omega+(t_1.4^{p-1})}_{[p-1,qt_2]}$.

Using the relations above, the recursive equation for QFPAE polarity matrix can now be derived. Let us start by examining the case when $n = 1$. When $n = 1$, we have

$$\begin{aligned} T_1(C^0) &= \begin{bmatrix} T_0(t_{00}) & T_0(t_{01}) & T_0(t_{02}) & T_0(t_{03}) \\ T_0(t_{10}) & T_0(t_{11}) & T_0(t_{12}) & T_0(t_{13}) \\ T_0(t_{20}) & T_0(t_{21}) & T_0(t_{22}) & T_0(t_{23}) \\ T_0(t_{30}) & T_0(t_{31}) & T_0(t_{32}) & T_0(t_{33}) \end{bmatrix} \\ &= \begin{bmatrix} T_0(c^0_{[0,0]}) & T_0(c^0_{[0,1]}) & T_0(c^0_{[0,2]}) & T_0(c^0_{[0,3]}) \\ T_0(c^1_{[0,0]}) & T_0(c^1_{[0,1]}) & T_0(c^1_{[0,2]}) & T_0(c^1_{[0,3]}) \\ T_0(c^2_{[0,0]}) & T_0(c^2_{[0,1]}) & T_0(c^2_{[0,2]}) & T_0(c^2_{[0,3]}) \\ T_0(c^3_{[0,0]}) & T_0(c^3_{[0,1]}) & T_0(c^3_{[0,2]}) & T_0(c^3_{[0,3]}) \end{bmatrix}. \end{aligned} \tag{11}$$

From the description of the decomposition in (8) and (9) it is clear that each subvector $c^{\omega}_{[p.q]}$ has 4^p elements. It follows that when $p = 0$ each subvector $c^{\omega}_{[p.q]}$ has only one element which is the spectral coefficient $c^{\omega}_{<q>_{10}}$. Since, according to the definition of $T_p(c^{\omega}_{[p.q]})$, the matrix $T_0(c^{\omega}_{[0,q]})$ has only one element $c^{\omega}_{[0,q]} = c^{\omega}_{<q>_{10}}$, by substituting $T_0(c^{\omega}_{[0,q]})$ with $c^{\omega}_{<q>_{10}}$ in (11) we have

$$T_1(C^0)=\begin{bmatrix} c^0_0 & c^0_1 & c^0_2 & c^0_3 \\ c^1_0 & c^1_1 & c^1_2 & c^1_3 \\ c^2_0 & c^2_1 & c^2_2 & c^2_3 \\ c^3_0 & c^3_1 & c^3_2 & c^3_3 \end{bmatrix} \tag{12}$$

which is the polarity matrix for $n = 0$. By applying the relation (6) between the first row and other rows of the polarity matrix, the derivation can be continued as follows:

$$T_1(C^0)=\begin{bmatrix} c^0_0 & c^0_1 & c^0_2 & c^0_3 \\ c^0_0+3c^0_1+c^0_2+3c^0_3 & -(c^0_1+c^0_3) & -(4c^0_1+c^0_2+3c^0_3) & 2c^0_1+c^0_3 \\ c^0_0+2c^0_1 & -c^0_1 & 2c^0_1+c^0_2+4c^0_3 & -c^0_3 \\ c^0_0+c^0_1+c^0_2+c^0_3 & c^0_1+c^0_3 & 2c^0_1-c^0_2-c^0_3 & -(2c^0_1+c^0_3) \end{bmatrix}$$

$$= \begin{bmatrix} T_0(t_{00}) & T_0(t_{01}) & T_0(t_{02}) & T_0(t_{03}) \\ T_0(t_{00}+3t_{01}+t_{02}+3t_{03}) & -T_0(t_{01}+t_{03}) & -T_0(4t_{01}+t_{02}+3t_{03}) & T_0(2t_{01}+t_{03}) \\ T_0(t_{00}+2t_{01}) & -T_0(t_{01}) & T_0(2t_{01}+t_{02}+4t_{03}) & -T_0(t_{03}) \\ T_0(t_{00}+t_{01}+t_{02}+t_{03}) & T_0(t_{01}+t_{03}) & T_0(2t_{01}-t_{02}-t_{03}) & -T_0(2t_{01}+t_{03}) \end{bmatrix}.$$

Due to the property of the Kronecker product used to build the QFPAE transform matrices as well as the way the spectral coefficient vectors are arranged in the polarity matrix, it turned out that the above recursive definition can be generalized for larger values for n such that for any n and any p, $1 \le p \le n$, the following recursive definition can be used to generate the complete polarity matrix:

$$T_p(t) = \begin{bmatrix} T_{p-1}(t_{00}) & T_{p-1}(t_{01}) & T_{p-1}(t_{02}) & T_{p-1}(t_{03}) \\ T_{p-1}(t_{00}+3t_{01}+t_{02}+3t_{03}) & -T_{p-1}(t_{01}+t_{03}) & -T_{p-1}(4t_{01}+t_{02}+3t_{03}) & T_{p-1}(2t_{01}+t_{03}) \\ T_{p-1}(t_{00}+2t_{01}) & -T_{p-1}(t_{01}) & T_{p-1}(2t_{01}+t_{02}+4t_{03}) & -T_{p-1}(t_{03}) \\ T_{p-1}(t_{00}+t_{01}+t_{02}+t_{03}) & T_{p-1}(t_{01}+t_{03}) & T_{p-1}(2t_{01}-t_{02}-t_{03}) & -T_{p-1}(2t_{01}+t_{03}) \end{bmatrix}$$

$$= \begin{bmatrix} T_{p-1}(t_{00}) & T_{p-1}(t_{01}) & T_{p-1}(t_{02}) & T_{p-1}(t_{03}) \\ T_{p-1}(t_{00})+3T_{p-1}(t_{01})+T_{p-1}(t_{02})+3T_{p-1}(t_{03}) & -T_{p-1}(t_{01})-T_{p-1}(t_{03}) & -4T_{p-1}(t_{01})-T_{p-1}(t_{02})-3T_{p-1}(t_{03}) & 2T_{p-1}(t_{01})+T_{p-1}(t_{03}) \\ T_{p-1}(t_{00})+2T_{p-1}(t_{01}) & -T_{p-1}(t_{01}) & 2T_{p-1}(t_{01})+T_{p-1}(t_{02})+4T_{p-1}(t_{03}) & -T_{p-1}(t_{03}) \\ T_{p-1}(t_{00})+T_{p-1}(t_{01})+T_{p-1}(t_{02})+T_{p-1}(t_{03}) & T_{p-1}(t_{01})+T_{p-1}(t_{03}) & 2T_{p-1}(t_{01})-T_{p-1}(t_{02})-T_{p-1}(t_{03}) & -2T_{p-1}(t_{01})-T_{p-1}(t_{03}) \end{bmatrix}. \quad (13)$$

The derivation of the polarity matrix based on (13) requires the first row elements of a particular submatrix $T_p(t)$ to be known before the rest of the matrix elements can be computed. When each of the submatrices T_{p-1} is calculated directly from the first row submatrices T_{p-1}, the computation of the submatrices T_{p-1} in the other rows of $T_p(t)$ will require 17 additions and 10 multiplications (exclusive of the negation operations), where each addition or multiplication is of the size of the T_{p-1} elements being operated on. However, observation of (13) shows that this computational cost can be greatly reduced if we take into account the arithmetic relations between them as follows:

$$T_p(t) = \begin{bmatrix} T_{p-1}(t_{00}) & T_{p-1}(t_{01}) & T_{p-1}(t_{02}) & T_{p-1}(t_{03}) \\ T_{p-1}(t_{30})+T_{p-1}(t_{03})+T_{p-1}(t_{13}) & -T_{p-1}(t_{01})-T_{p-1}(t_{03}) & T_{p-1}(t_{00})-T_{p-1}(t_{10})-T_{p-1}(t_{01}) & 2T_{p-1}(t_{01})+T_{p-1}(t_{03}) \\ T_{p-1}(t_{00})+2T_{p-1}(t_{01}) & -T_{p-1}(t_{01}) & T_{p-1}(t_{03})-2T_{p-1}(t_{01})-T_{p-1}(t_{12}) & -T_{p-1}(t_{03}) \\ T_{p-1}(t_{00})+T_{p-1}(t_{01})+T_{p-1}(t_{02})+T_{p-1}(t_{03}) & -T_{p-1}(t_{11}) & 2T_{p-1}(t_{01})-T_{p-1}(t_{02})-T_{p-1}(t_{03}) & -T_{p-1}(t_{13}) \end{bmatrix}. \quad (14)$$

Let three intermediate vectors $R1_{[p-1]}$, $R2_{[p-1]}$, and $R3_{[p-1]}$ of length 4^{p-1} be defined where $R1_{[p-1]} = T_{p-1}(t_{01}) + T_{p-1}(t_{03})$, $R2_{[p-1]} = T_{p-1}(t_{00}) + T_{p-1}(t_{02})$, and $R3_{[p-1]} = 2T_{p-1}(t_{01}) - T_{p-1}(t_{03})$, respectively. Then (14) can be further simplified into the following equation:

$$T_p\left(c^{(q}_{[p,q]}\right) = \begin{bmatrix} T_{p-1}(t_{00}) & T_{p-1}(t_{01}) \\ T_{p-1}(t_{30}) + T_{p-1}(t_{03}) + T_{p-1}(t_{13}) & -R1_{[p-1]} \\ T_{p-1}(t_{00}) + 2T_{p-1}(t_{01}) & -T_{p-1}(t_{01}) \\ R1_{[p-1]} + R2_{[p-1]} & -T_{p-1}(t_{11}) \end{bmatrix}$$

$$\begin{bmatrix} T_{p-1}(t_{02}) & T_{p-1}(t_{03}) \\ T_{p-1}(t_{00}) - T_{p-1}(t_{10}) - T_{p-1}(t_{01}) & 2T_{p-1}(t_{01}) + T_{p-1}(t_{03}) \\ -T_{p-1}(t_{12}) - R3_{[p-1]} & -T_{p-1}(t_{03}) \\ R3_{[p-1]} - T_{p-1}(t_{02}) & -T_{p-1}(t_{13}) \end{bmatrix}. \quad (15)$$

4.2. STEPS OF THE ALGORITHM

The QFPAE polarity matrix can be defined recursively using either (13) or (15). An algorithm that utilizes them for calculating the required polarity matrix elements is presented in this Section. The presented algorithm computes either complete or partial polarity matrix for the input function in a recursive manner based on the recursive definitions.

As mentioned above, the generation of the polarity matrix based on (13) and (15) require that the first row of the polarity matrix, i.e. C^0, is known as it is the starting point of the recursion. Therefore, if the input quaternary function is given in the form of the truth vector, the algorithm always starts by first calculating C^0 for the function by (4) before it continues with the generation of the required polarity matrix elements.

Depending on whether the target output is the complete polarity matrix or a particular spectral coefficient vector, the algorithm executes different computation steps. For complete polarity matrix, the algorithm performs the following steps:

Step 1: Let P$[f(\vec{x})]$ be $T_n(c^0_{[n,0]})$ with C^0 as the first row of the matrix. Set $p = n$.

Step 2: Divide $T_n(c^0_{[n,0]})$ into $4^{n-p} \times 4^{n-p}$ T_p matrices. For each of the T_p matrices, identify its T_p–$1(t_{t_1 t_2})$ submatrices ($0 \le t_1, t_2 \le 3$) according to (10).

Step 3: For each T_p matrices whose t_{00}, t_{01}, t_{02}, and t_{03} are known, calculate the unknown first row elements of its T_{p-1} matrices, i.e., $t_{t_1 t_2}$ ($0 \le t_1, t_2 \le 3$) except t_{11}, t_{21}, t_{23}, and t_{33} from t_{00}, t_{01}, t_{02}, and t_{03} according to the flow diagram shown in Fig. 1. In the figure, the dashed line – – – – indicates that the sign of the signal should be inverted. It should be noted that the flow diagram is developed based on (15) as it requires smaller number of arithmetic operations compared to (13) or (14).

Step 4: Decrement p by 1. If $p = 0$, go to Step 5. Otherwise go back to Step 2.

Step 5: Complete the polarity matrix by copying all the $T_p t_{31}$, $T_p t_{01}$, $T_p t_{03}$, and $T_p t_{13}$ matrices to the corresponding $T_p t_{11}$, $T_p t_{21}$, $T_p t_{23}$, and $T_p t_{33}$ matrices with the signs inverted, where p changes from 0 to n–1.

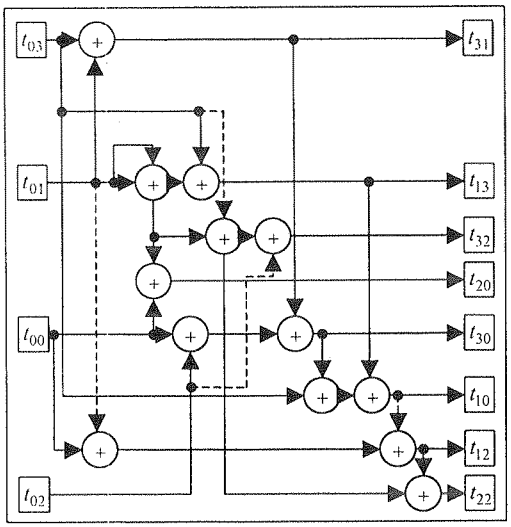

Fig. 1. Flow diagram for each recursion stage (complete polarity matrix generation)

Alternatively, the algorithm can also be used to generate the elements of a selected coefficient vector only. When this is the case, the algorithm calculates the required spectral coefficients based on the recursive definition given in (13) rather than (15) so that they can be obtained without first deriving the complete polarity matrix. The steps of the algorithm for generating coefficient vector in polarity ω (recall that $< \omega >_{10} = < j_1, j_2, \cdots, j_n >_4$) from C^0 are as follows:

Step 1: Let P[$f(\vec{x})$] be $T_n(c^0_{[n,0]})$ with C^0 as the first row of the matrix. Set $p = 1$.

Step 2: Divide $T_n(c^0_{[n,0]})$ into $4^{p-1} \times 4^{p-1}$ T_{n+1-p} matrices. For each of the T_{n+1-p} matrices whose first row elements are known, identify its T_{p-1} $(t_{t_1 t_2})$ submatrices ($0 \le t_1, t_2 \le 3$) according to (10).

Step 3: Let $r = j_p$. If $r = 0$, go to Step 4. Otherwise, for each of the T_{n+1-p} matrices whose first row elements are generated in the previous recursion stage, calculate its t_{r0}, t_{r1}, t_{r2} and t_{r3} using

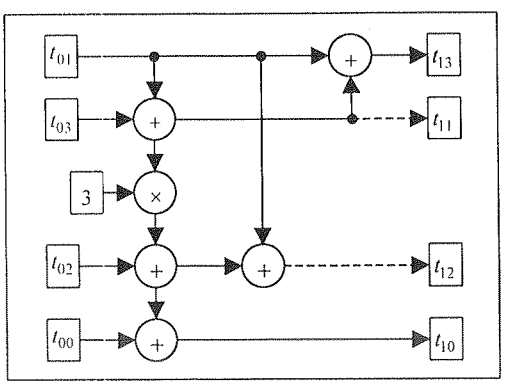

Fig. 2. Flow diagram in a recursion stage of coefficient vector generation when $r = 1$

the flow diagrams in Figs. 2, 3, and 4 when $r = 1, 2$, or 3, respectively. As in Fig. 1, the dashed line – – – – in the figures indicates that the sign of the signal should be inverted.

Step 4: Increment p by 1. If $p = n + 1$, the required coefficient vector has been obtained and the algorithm is finished. Otherwise go back to Step 2.

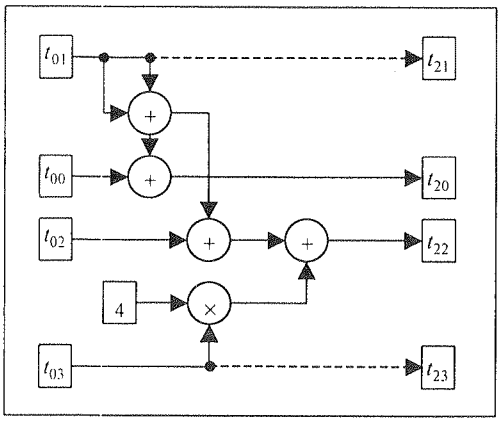

Fig. 3. Flow diagram in a recursion stage of coefficient vector generation when $r = 2$

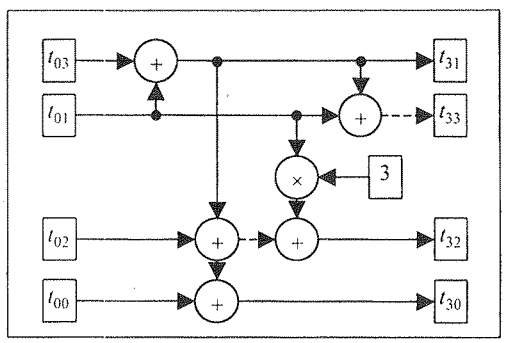

Fig. 4. Flow diagram in a recursion stage of coefficient vector generation when $r = 3$

4.3. COMPUTATIONAL COST OF THE ALGORITHM

Based on the steps of the algorithm given above, the computational cost of the algorithm in terms of the numbers of additions and multiplications that need to be performed can be determined.

For an n-variable quaternary function, the computational cost of generating the complete QFPAE polarity matrix from the coefficient vector in polarity zero using the algorithm is

$$13 \cdot (12^n - 4^n)/8 \text{ additions/subtractions.} \tag{16}$$

On the other hand, when the algorithm is used to generate the spectral coefficient vector in polarity ω of an n-variable quaternary function, its computational cost is

$$(5a + 4b) \cdot 4^{n-1} \text{ additions/subtractions}$$

and $$(a + b) \cdot 4^{n-1} \text{ multiplications,} \quad (17)$$

where a is the number of '1' and '3' digits in the quaternary number representation of ω and b is the number of '2' digits in the quaternary number representation of ω.

It should be noted that in the process of generating the coefficient vector in polarity ω for an n-variable quaternary function, the algorithm also derives $u-1$ ($0 \le u \le n-1$) other coefficient vectors for the function (excluding C^{ω}), where u is the total number of nonzero digits in the quaternary number representation of ω. More precisely, if a set Y be defined such that $Y = \{y_1, y_2, \ldots, y_u\} = \{y | j_y \neq 0\}$ then in the process of generating C^{ω} the algorithm also generates the spectral coefficient vectors with polarity numbers $<j_1 j_2 .. j_{y_1} 00...0>_{10}$ where the value of l varies from 1 to $u-1$. Consequently, when the algorithm is used to calculate two spectral coefficient vectors C^{ω_a} and C^{ω_b} where $< \omega >_{10} = < a_1, a_2, \cdots, a_n >_4$ and $< \omega >_{10} = < b_1, b_2, \cdots, b_n >_4$ then the computational cost of the algorithm is given by (computational cost of computing C^{ω_a} + computational cost of computing C^{ω_b} – computational cost of computing C^{ω_c}) where ; l = the largest i such that $a_g = b_g$ for all g, $1 \le g \le i$. Thus, when the quaternary number representations of ω_a and ω_b share the same first few digits the computational cost is smaller than the sum of computing C^{ω_a} and C^{ω_b} separately.

The computational cost of calculating a spectral coefficient vector of an n-variable quaternary function by fast transform of (4) is $6n \times 4^{n-1}$ additions/subtractions and $3n \times 4^{n-1}$ multiplications when it is assumed that the division by 2^n is performed by bit shifting operation. It follows that the cost of generating the complete polarity matrix from the truth vector by fast transform of (4) is $6n \times 4^{2n-1}$ additions/subtractions and $3n \times 4^{2n-1}$ multiplications. In order to show that the proposed recursive algorithm is more efficient than (4), the computational costs of deriving the complete polarity matrix from the truth vector by the recursive algorithm and by fast transform of (4) are derived and listed in Table 6 for $n \le 7$. Note that the cost of obtaining C^0 from truth vector by fast transform of (4) has been added to the cost of the recursive algorithm. It can be clearly seen from the table that the recursive algorithm has significantly smaller computational cost and thus is much faster.

Table 6

Computational costs of generating complete polarity matrix

n	Fast transform of (4)		Recursive algorithm	
	Add/Sub $6n \cdot 4^{2n-1}$	Mult $3n \cdot 4^{2n-1}$	Add/Sub $\left(13.\left(12^n - 4^n\right)/8\right) + 6n \cdot 4^{n-1}$	Mult $3n \cdot 4^{n-1}$
1	24	12	19	3
2	768	384	256	24
3	18432	9216	2992	144
4	393216	196608	34816	768
5	7864320	3932160	410368	3840
6	150994944	75497472	4882432	18432

5. CONCLUSION

Two algorithms for calculation of QFPAEs have been presented. The basic concepts and the computational steps for the algorithms have been described. The algorithms are targeted to address different problems. The first algorithm is aimed for calculation of selected spectral coefficients only, such as those arise in decomposition and fault detection algorithms, whereas the recursive algorithm is more advantageous to find the optimal QFPAE.

The theory presented in this article may be of interest not only to researchers working in the area of multiple-valued logic functions but also in other areas where mathematical models of multiple-valued expansions and functions are used. One such area is software modeling for machine learning and knowledge discovery that uses either purely digital (binary or multiple-valued) or analog models. The resulting QFPAEs can be used as the mathematical apparatus to analyze the stability of finite automata giving more flexibility that the known results for binary dynamic systems [11] as well as the bases of new quaternary word decision diagrams in a manner similar to the ones developed in [3], [16], [18], [19].

6. ACKNOWLEDGMENTS

This paper was supported by Agency for Science, Technology and Research in Singapore (Grant No. 0621200011) as well as Ministry of Science and Higher Education in Poland (Grant No. SINGAPUR/31/2006).

7. REFERENCES

1. N. Abu-Khader, P. Siy: *Multiple-Valued Logic Approach for a Systolic AB^2 Circuit in Galois Field*. 35th IEEE International Symposium on Multiple-Valued Logic, Calgary, Canada, 2005, pp. 88-93.
2. A. N. Al-Rabadi: *Reversible Logic Synthesis: From Fundamentals to Quantum Computing*. Springer-Verlag, New York, 2004.
3. J. T. Astola, R. S. Stankovic: *Fundamentals of Switching Theory and Logic Design: A Hands on Approach*. Springer, Dordrecht, 2006.
4. H. Chang, L. Cooke, M. Hunt, G. Martin, A. McNelly, L. Todd: *Surviving the SOC Revolution, a Guide to Platform-Based Design*. Kluwer Academic Publishers, Boston, 1999.
5. M. Davio, J. P. Deschamps, A. Thayse: *Discrete and Switching Functions*. McGraw-Hill, New York, 1978.
6. E. Dubrova: *Multiple-Valued Logic in VLSI: Challenges and Opportunities*. 17th IEEE Norchip Conference, Oslo, Norway, 1999, pp. 340-350.
7. B. J. Falkowski, S. Rahardja: *Efficient Computation of Quaternary Reed-Muller Expansions*. IEE Proc. on Computers and Digital Techniques, vol. 142, No. 5, September, 1995, pp. 345-352.
8. B. J. Falkowski, C. C. Lozano, S. Rahardja: *Generation of Disjoint Cubes for Multiple-Valued Functions*. 37th IEEE International Symposium on Circuits and Systems, Vancouver, Canada, 2004, pp. 133-136.
9. B. J. Falkowski, C. C. Lozano: *Quaternary Fixed Polarity Reed-Muller Expansion Computation Through Operations on Disjoint Cubes and Its Comparison with Other Methods*. Computers and Electrical Engineering, An International J., vol. 31, No. 2, March, 2005, pp. 112-131.
10. B. J. Falkowski, C. C. Lozano, T. Łuba: *Efficient Algorithm for Calculation of Quaternary Fixed Polarity Arithmetic Expansions*. 37th IEEE International Symposium on Multiple-Valued Logic, Oslo, Norway, 2007, CD publication.

11. G. P. Gavrilov, A. A. Sapozhenko: *Problems and Exercises on Course of Discrete Mathematics*. Science, Moscow, 1992, in Russian.
12. D. H. Green: *Reed-Muller Expansions with Fixed and Mixed Polarities over GF(4)*. IEE Proc. on Computers and Digital Techniques, vol. 137, No. 5, September, 1990, pp. 380-388.
13. M. Kameyama, T. Hanyu, T. Higuchi: *Design and Implementation of Quaternary NMOS Integrated Circuits for Pipelined Image Processing*. IEEE J. of Solid-State Circuits, vol. 22, No. 1, February, 1987, pp. 20-27.
14. M. G. Karpovsky, R. S. Stankovic, C. Moraga: *Spectral Techniques in Binary and Multiple-Valued Switching Theory: A Review of Results in The Decade 1991-2000*. 31st IEEE International Symposium on Multiple-Valued Logic, Warsaw, Poland, 2001, pp. 41-46.
15. S. Rahardja, B. J. Falkowski: *Efficient Algorithm to Calculated Reed-Muller Expansions over GF(4)*. IEE Proc. on Circuits, Devices, and Systems, vol. 148, No. 6, December, 2001, pp. 289-295.
16. T. Sasao, M. Fujita: *Representations of Discrete Functions*. Kluwer Academic Publishers, Boston, 1996.
17. T. Sasao: *Design Methods for Multiple-Valued Input Address Generators*. 36th IEEE International Symposium on Multiple-Valued Logic, Singapore, 2006, CD publication.
18. A. Srinivasan, T. Kam, S. H. Malik, R. K. Brayton: *Algorithms for Discrete Function Manipulation*. 8th IEEE International Conference on Computer-Aided Design, Santa Clara, CA, USA, 1990, pp. 92-95.
19. S. N. Yanushkevich, D. M. Miller, V. P. Shmerko, R. S. Stankovic: *Decision Diagram Techniques for Micro- and Nanoelectronic Design*. CRC Press, Boca Raton, 2006.
20. Y. Yuminaka, T. Morishita, T. Aoki, T. Higuchi: *Multiple-Valued Data Recovery Techniques for Band-Limited Channels in VLSI*. 32nd IEEE International Symposium on Multiple-Valued Logic, Boston, MA, USA, 2002, pp. 54-60.

ELECTRONICS AND TELECOMMUNICATIONS QUARTERLY, 2008, 54, no 2, pp. 167–177

Arithmetic and Boolean techniques for derivation of system reliability expressions

BOGDAN J. FALKOWSKI[1], CECILIA C. LOZANO[1], TADEUSZ ŁUBA[2]

[1] Nanyang Technological University
School of Electrical and Electronic Engineering
Singapore
e-mail: <cicilia, efalkowski>@ntu.edu.sg
[2] Warsaw University of Technology
Institute of Telecommunications
Poland
e-mail: luba@tele.pw.edu.pl

Received 2008.04.12
Authorized 2008.06.16

Reliability analysis of a system conducted in the Probabilistic (Arithmetic) domain is lengthy and error-prone. An alternative method is to consider the system reliability components to be Boolean variables rather than Probabilistic variables and to treat the whole problem as if it were Boolean. This method allows the use of powerful Boolean reduction theorems to contain the size of the problem. In order for the conversion of the reliability expression from Boolean domain back to the Probabilistic domain to be on a one-to-one basis, the Boolean expression should be fully disjoint. In this article basic properties and definitions of Probabilistic and Boolean domains are presented. Evaluation of reliability of a system directly from Arithmetic expansion is also discussed. Since the reliability expression may be directly obtained from disjoint cube representation, two methods to obtain disjoint cubes representation of the path set expression of the system are also shown.

Keywords: reliability analysis, Arithmetic transforms, Boolean techniques

1. INTRODUCTION

Arithmetic transforms and expansions are frequently used to derive the reliability expressions of a system [10]. The reliability expressions can also be directly obtained from the Boolean expressions representing the path set of the system derived from the reliability block diagram (RBD) provided that all the cubes of such a Boolean expression are disjoint [11]. In such a case, the disjoint Boolean expression can be directly converted into a corresponding Arithmetic expression representing the reliability of the system (R).

This article shows basic definitions and notations for both Boolean and Probabilistic domains. Arithmetic (Probabilistic) transform, spectrum and expansion are defined and illustrated with example. By using Arithmetic transforms in an optimal polarity for Boolean function, the number of terms in the Boolean polynomials can be minimized, which results in faster calculation of the value of such polynomial [4]–[7]. The importance of disjoint cube representation in reliability analysis is also explained. Finally, two different methods to calculate the disjoint cube representation of the path set expression of the system are introduced. The first method is based on the Arithmetic transform and the relationship between Boolean and Arithmetic identities. On the other hand, the second method directly operates on the cubes arrays representation of the input to produce the optimal disjoint cube representation for it. The methods presented in this paper are illustrated through several examples. The same system is used in all the examples and different techniques to obtain the final reliability expression are also discussed.

2. BOOLEAN AND PROBABILISTIC RELATIONSHIPS, BASIC DEFINITIONS AND NOTATIONS

A Probabilistic variable is denoted by upper case alphabetic symbols e.g., A, B and C. These symbols are used to identify both a component and its reliability or unreliability. For example, the reliability of a component A is written as A whereas its unreliability is written either as $(1 - A)$ or $\overline{A}$.

A literal $\tilde{x}$ is a variable of a Boolean function in either affirmation (x) or negation ($\bar{x}$) i.e., $\tilde{x} \in \{x, \bar{x}\}$.

A minterm of an n-variable Boolean function is an AND term of exactly n different literals. A Boolean function is completely specified if all its values belong to the set $\{0, 1\}$.

An OFF/FALSE or ON/TRUE minterm is one for which the value of the Boolean function is 0 or 1 respectively.

A cube is a product term describing one or more minterms. Similar to minterms, there are OFF and ON cubes.

Disjoint cubes are cubes that do not have common minterms whereas non-disjoint cubes are cubes that overlap i.e., they have common minterms.

A path set [1], [3], [9], [11], [12] is a Boolean expression which consists of the logical OR of all successful paths (minimal tie-sets) through the RBD.

The comparison of Boolean and Probabilistic algebras is shown in Table 1 while some important Boolean laws are given in Table 2.

Arithmetic transform converts the Boolean expression into a corresponding Probabilistic expression which defines the reliability of the system [2], [4]–[8], [10], [13], [14].

Let $A(n)$ be the Arithmetic transform matrix defined as

$$A(n) = \bigotimes_{i=1}^{n} A(1), \quad A(1) = \begin{bmatrix} 1 & 0 \\ -1 & 1 \end{bmatrix} \tag{1}$$

where $A(1)$ is the basic Arithmetic transform matrix. For an n-variable Boolean function $f(x_1, x_2, \ldots x_n)$ given by the truth vector $\vec{F}$, the Arithmetic spectrum is

$$\vec{A}_f = A(n) \cdot \vec{F} = [a_0, a_1, a_2, a_{1,2}, \ldots, a_{1,2,\ldots,n}]^T \tag{2}$$

where T is the transpose operator.
The inverse Arithmetic transform matrix $A^{-1}(n)$ is given by

$$A^{-1}(n) = \bigotimes_{i=1}^{n} A^{-1}(1), \; A^{-1}(1) = \begin{bmatrix} 1 & 0 \\ 1 & 1 \end{bmatrix} \tag{3}$$

Hence the truth vector $\vec{F}$ can be obtained as

$$F = A^{-1}(n) \cdot \vec{A}_f \tag{4}$$

From the Arithmetic spectrum ($\vec{A}_f$) and the basis functions of $A^{-1}(n)$, the Arithmetic expansion can be derived as follows

$$f = a_0 + a_1 X_1 + a_2 X_2 + a_{1,2} X_1 X_2 + \ldots + a_{1,2,\ldots,n} X_1 X_2 \ldots X_n \tag{5}$$

Any Boolean function may be converted to an Arithmetic expansion using Table 3.

Table 1

Comparison of Boolean and Probabilistic algebras

Feature	Boolean Domain	Probabilistic Domain
Map	Karnaugh Map (K-map)	Probabilistic Map (P-map)
Variable	Boolean	Probabilistic
Data manipulation	Boolean axioms and theorems	Probability axioms and theorems
Value	Discrete values of 0 & 1 corresponding to false & true	Continuous values ranging from 0 to 1 with the extremes corresponding to wholly unreliable and wholly reliable respectively
Operator	OR : $\vee$ AND : $\wedge$ INVERT : $\bar{}$ EXOR : $\oplus$	Plus : + Minus : – Multiply : * Divide : $\div$ Overline : $\bar{R} = 1 - R$

Table 2

Boolean laws

Idempotent	$x \vee x = x$
Inverse	$x \vee \bar{x} = 1$
Identity	$1 \wedge x = x$
Absorption	$x \vee xy = x$
Reduction	$x \vee \bar{x}y = x \vee y$
Reduction	$xy \vee x\bar{y} = x$
Reduction	$xy \vee \bar{x}y = y$

Table 3

Boolean and Arithmetic identities

$\bar{x} = \overline{X} = 1 - X$
$x \wedge y = XY$
$x \vee y = X + Y - XY$
$x \oplus y = X + Y - 2XY$

3. ARITHMETIC TRANSFORMS AND BOOLEAN TECHNIQUES

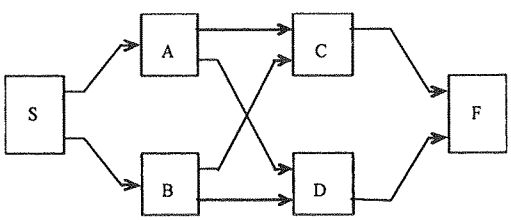

Note that S(Start) denotes the RBD source/input node and F(Finish) denotes the RBD sink/output node. Success is met if any of the following paths is working: AC, AD, BC or BD.

Fig.1. RBD of the system

The path set for the system in Fig. 1 is equal to

$$\text{Path set} = ac \vee ad \vee bc \vee bd \tag{6}$$

and is a Boolean expression with sum-of-product form. Each cube in the expression represents a possible path through the RBD. The collection of all minimal tie-sets covers all such paths. However, it is incorrect to conclude that the reliability of the system is simply the path set expression in which each lower-case Boolean variable is replaced by its corresponding Probabilistic variable i.e.,

$$R \neq AC + AD + BC + BD. \tag{7}$$

The reason is that these four original Boolean cubes are non-disjoint and any transfer to the Probabilistic domain (P-domain) must identify this overlap and account for it. On the other hand,

if the Boolean expression for the path set was already disjoint, then the transfer to the P-domain to derive the reliability function would be on a one-to-one basis. Therefore, it is very important to develop efficient methods to calculate disjoint cube representation for Boolean expressions.

This section describes two methods for generating disjoint cubes. The first method applies to small systems while the second method is more general and well-suited for computer implementation. The first method is directly derived from the Arithmetic expansions as shown in Example 1 while the second method takes disjoint cube representation of Boolean functions as shown in Examples 2 and 3.

The steps of the first method are as follows:

Step 1: Calculate the Arithmetic expansion of the path set.

Step 2: Manipulate the Arithmetic expansion using the relation of Boolean and Arithmetic identities given in Table 2 until a final Arithmetic expansion composed of mutually disjoint cubes is obtained.

Example 1. To illustrate the procedure, consider the RBD of the system shown in Fig. 1. From (6), we obtained the manipulation on Arithmetic expansion of the Boolean expression.
From the path set, the truth vector $\vec{F}$ is

$$\vec{F} = [0\,0\,0\,0\,0\,1\,1\,1\,0\,1\,1\,1\,0\,1\,1\,1]^{\mathrm{T}}$$

From (2), the Arithmetic spectrum is

$$\vec{A}_f = A(4) \times \vec{F} = [0\,0\,0\,0\,0\,1\,1\,-1\,0\,1\,1\,-1\,0\,-1\,-1\,1]^{\mathrm{T}}$$

From (5), we have

$$f = BD + BC - BCD + AD + AC - ACD - ABD - ABC + ABCD$$

Using the Boolean and Arithmetic identities from Table 3, the final Arithmetic expansion composed of mutually disjoint cubes may be obtained as follows

$$\begin{aligned} f &= BD+BC-BCD+AD+AC-ACD-ABD-ABC+ABCD \\ &= AC+AD-ACD+BC-ABC+BD-ABD+ABCD-BCD \\ &= AC+A\underline{D}(1-\underline{C})+BC(1-A)+(B-AB)(D-CD) \\ &= AC+A\underline{\bar{C}}D+\underline{A}BC+\underline{\bar{B}}(1-\underline{A})D(1-C) \\ &= AC+A\bar{C}D+\bar{A}BC+\bar{A}\bar{B}CD \end{aligned}$$

Since the above Arithmetic expansion is fully disjoint, it can be interpreted directly as the reliability of the system (R) i.e.,

$$R = AC+A\bar{C}D+\bar{A}BC+\bar{A}\bar{B}CD$$

The second algorithm generates an optimal disjoint cube representation of Boolean functions. In such a representation, each Boolean function is shown in the form of a set of arrays of disjoint cubes that completely covers this function. For practical functions, the number of disjoint cubes is much smaller than the number of minterms, so the memory span and computation time can be reduced significantly. As the input data, the Boolean functions are represented in the form of arrays of non-disjoint ON cubes. An ON array of an n-variable Boolean function f corresponds directly to a sum-of-product expression formed by all ON cubes of $f(x_1, x_2, \ldots, x_n)$.

The operation steps of the algorithm are listed below

Step 1: Represent the path set function in the form of an array of non-disjoint ON cubes.

Step 2: Sort the cubes by skip list according to their size.

Step 3: Compare each pair of cubes in the array. If the pair of cubes being compared are disjoint: continue to the next pair. Otherwise:
- Obtain the solution cube(s) of the operation Cube A disjoint sharp Cube B, where Cube A is the larger cube of the pair and Cube B is the smaller cube.
- Insert the solution cubes to the array and remove Cube B. If the solution cube is empty (i.e., Cube A completely covers/absorbs Cube B), simply remove Cube B.
- Continue to the next pair.

The algorithm should starts by comparing the largest cube with all others, starting from the smallest one. Then the next largest cube is taken and compared with all smaller cubes, and so on.

Step 4: Merge adjacent cubes of the same size on the K-map to obtain a smaller total number of disjoint cubes.

Skip List

i. Cubes of the same size are grouped together in a link list.
ii. An array of size n where n is the number of variables is used to store the addresses of the first cube in each group.
iii. Only the addresses of cubes are manipulated on. The length of the list storing the addresses changes dynamically as new cubes are generated or when present cubes are deleted.

Disjoint Sharp Operation ($\#_j$)

Let

Cube $A = a_1a_2a_3 \ldots a_n$
Cube $B = b_1b_2b_3 \ldots b_n$
Cube $C = c_1c_2c_3 \ldots c_n$

where $a_i, b_i, c_i \in \{0, 1, X\}$ for $i = 1, 2, \ldots, n$

The steps to perform Cube A $\#_j$ Cube B are listed below

Step 1. Set $k = 1$.

Step 2. If $b_k = X$ and $a_k \neq X$, goto Step 3.
Else if $k = n$, goto Step 8.
If $k \neq n$, then $k = k + 1$ and repeat Step 2.

Step 3. If $k = 1$, goto Step 4.
Else replace the $k-1$ leftmost literals in the solution cube (Cube C) by the result of the bitwise AND operation applied to corresponding literals in Cube A and Cube C.

$$c_1c_2\ldots c_{k-1} = a_1a_2\ldots a_{k-1} \bullet b_1b_2\ldots b_{k-1}$$

The bitwise AND operation is defined in Table 4.

Step 4. Replace the specific literal c_k by $\overline{a}_k$.

Step 5. Replace the $n-k$ rightmost literals in the solution cube (Cube C) with the corresponding literals in Cube B.

$$c_{k+1}c_{k+2}\ldots c_n = b_{k+1}b_{k+2}\ldots b_n$$

Table 4

Bitwise AND operation

•	0	1	X
0	0	0	0
1	0	1	1
X	0	1	x

Step 6. Insert the solution Cube C in the list.
Step 7. If $k \neq n$, increment k by 1 and repeat Step 2.
Else goto Step 8.
Step 8. Delete Cube B from the list.

To illustrate the Disjoint Sharp Operation, an example is shown below.

Example 2. The Karnaugh Map for the system in Fig. 1 is given in Fig 2. The steps to obtain Cube 1 $\#_j$ Cube 4 are listed below.

First, let Cube A = Cube 1 = 1X1X and Cube B = Cube 4 = X11X.

First Iteration

Step 1. Set $k = 1$.
Step 2. $k = 1$, $a_1 = 1$ and $b_1 = \mathrm{X}$.
Condition is met: $b_k = \mathrm{X}$ and $a_k \neq \mathrm{X}$.
Goto Step 3.
Step 3. Since $k = 1$, goto Step 4.
Step 4. $c_k = c_1 = \overline{a_1} = 0$
Step 5. $n - k = 4 - 1 = 3$
$c_2c_3c_4 = b_2b_3b_4 = 11\mathrm{X}$
Step 6. Cube $C = 011\mathrm{X}$. Insert Cube C into the list.
Step 7. $k = 1 \neq n = 4$
$\therefore\ k = k + 1 = 1 + 1 = 2$
Goto Step 2.

Second Iteration

Step 2. $k = 2$, $a_2 = \mathrm{X}$ and $b_2 = 1$.
Condition is not met.
$k = 2 \neq n = 4$, $\therefore k = k + 1 = 2 + 1 = 3$
Repeat Step 2.

Third Iteration

Step 2. $k = 3$, $a_3 = 1$ and $b_3 = 1$.
Condition is not met.
$k = 3 \neq n = 4$, $\therefore k = k + 1 = 3 + 1 = 4$.
Repeat Step 2.

Fourth Iteration

Step 2. $k = 4$, $a_4 = X$ and $b_4 = X$.

Condition is not met.

Since $k = n = 4$, goto Step 8.

Step 8. Delete Cube B from the list.

The stages of the execution of the algorithm to generate a disjoint cube representation are shown in Example 3.

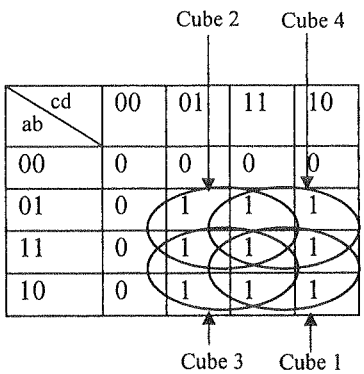

Fig. 2. K-map of the system in Fig. 1

Example 3.

Stage 1. Entry of the input array and sorting of the cubes according to their size. Since all the cubes are of the same size, sorting is not necessary.

cd / ab	00	01	11	10
00	0	0	0	0
01	0	1	1	1
11	0	1	1	1
10	0	1	1	1

[Cube1: 1X1X
Cube2: X1X1
Cube3: 1XX1
Cube4: X11X]

Stage 2. Cube 1 $\#_j$ Cube 4

ab \ cd	00	01	11	10
00	0	0	0	0
01	0	1	1	1
11	0	1	1	1
10	0	1	1	1

[Cube1: 1X1X
Cube2: X1X1
Cube3: 1XX1
Cube4: 011X]

Stage 3. Cube 1 $\#_j$ Cube 3

ab \ cd	00	01	11	10
01	0	1	1	1
11	0	1	1	1
10	0	1	1	1

[Cube1: 1X1X
Cube2: X1X1
Cube3: 1X01
Cube4: 011X]

Stage 4. Cube 1 $\#_j$ Cube 2

ab \ cd	00	01	11	10
00	0	0	0	0
01	0	1	1	1
11	0	1	1	1
10	0	1	1	1

[Cube1: 1X1X
Cube2: 011X
Cube3: 1X01
Cube4: 01X1
Cube5: 1101]

Stage 5. Cube 2 $\#_j$ Cube 4

ab \ cd	00	01	11	10
00	0	0	0	0
01	0	1	1	1
11	0	1	1	1
10	0	1	1	1

Cube1: 1X1X
Cube2: 011X
Cube3: 1X01
Cube4: 0101
Cube5: 1101

Stage 6. Cube 5 (1101) is absorbed by Cube 3 (1X01).
In this case, merging is not necessary. The final result is

ab \ cd	00	01	11	10
00	0	0	0	0
01	0	1	1	1
11	0	1	1	1
10	0	1	1	1

Cube1: 1X1X
Cube2: 011X
Cube3: 1X01
Cube4: 0101

Hence the path set of the system in Fig. 1 is

$$\text{pathset} = ac \vee acd \vee \bar{a}bc \vee \bar{a}\bar{b}cd$$

Since all the cubes are disjoint, the corresponding Arithmetic expansion which is also the reliability of the system (R) is

$$R = AC + A\bar{C}D + \bar{A}BC + \bar{A}\bar{B}CD$$

4. CONCLUSION

Reliability analysis is usually performed in Boolean domain. Arithmetic (Probabilistic) expression provides a new form of description from which the final reliability of the system may be obtained. Such an analysis and conversion is direct when the path set of the system is

represented by a set of disjoint cubes. If the path set is represented by an arbitrary set of cubes which overlap, it has to be converted to disjoint form. Two algorithms which perform such a conversion are described in this article. It should be noticed that the second algorithm is well suited for computer implementation and therefore applicable to the reliability analysis of large systems.

5. ACKNOWLEDGEMENTS

This paper was supported by Agency for Science, Technology and Research in Singapore (Grant No. 0621200011) as well as Ministry of Science and Higher Education in Poland (Grant No. SINGAPUR/31/2006).

5. REFERENCES

1. J. D. Andrews, T. R. Moss: *Reliability and Risk Assessment*. ASME Press, New York, 2002.
2. J. T. Astola, R. S. Stankovic: *Fundamentals of Switching Theory and Logic Design: A Hands on Approach*. Springer, Dordrecht, 2006.
3. R. E. Barlow: *Engineering Reliability. Society for Industrial and Applied Mathematics*, Philadelphia, 1998.
4. B. J. Falkowski, C. H. Chang: *Properties and Methods of Calculating Generalised Arithmetic and Adding Transforms*. IEE Proc. On Circuits Devices and Systems, vol. 144, No. 5, October, 1997, pp. 249-258.
5. B. J. Falkowski, C. H. Chang: *An Efficient Algorithm for the Calculation of Generalized Arithmetic Transforms from Disjoint Cubes of Boolean Functions*. VLSI Design, vol. 9, No. 2, April, 1999, pp. 135-146.
6. B. J. Falkowski: *A Note on the Polynomial Form of Boolean Functions and Related Topics*. IEEE Trans. on Computers, vol. 48, No. 8, August, 1999, pp. 860-864.
7. B. J. Falkowski: *Algorithms for Fast Arithmetic Transform*. 35th IEEE International. Symposium on Circuits and Systems, Phoenix, Arizona, USA, 2002, pp. 753-756.
8. R. P. Grimaldi: *Discrete and Combinatorial Mathematics: An Applied Introduction*. Longman, 1998.
9. H. Hecht: *Systems Reliability and Failure Prevention*. Artech House, Boston, 2004.
10. S. K. Kumar, M. A. Breuer: *Probabilistic Aspects of Boolean Switching Functions via a New Transform*. J. of the ACM, vol. 28, No. 3, July, 1981, pp. 502-520.
11. W. Kuo, M. J. Zuo: *Optimal Reliability Modeling: Principles and Applications*. John Wiley & Sons, Hoboken, 2003.
12. R. D. Leitch: *Reliability Analysis for Engineers*. Oxford University Press, Oxford, 1995.
13. T. Sasao, M. Fujita: *Representations of Discrete Functions*. Kluwer Academic Publishers, Boston, 1996.
14. S. N. Yanushkevich, D. M. Miller, V. P. Shmerko, R. S. Stankovic: *Decision Diagram Techniques for Micro- and Nanoelectronic Design*. CRC Press, Boca Raton, 2006.

(ba
inv
pro
cas

Key

Casca
utilized fo
The fu
coupler), d
configuratio
Cascad
that there a
types of cas
inversed or
Moreo
taps can be
In this a
is a band of
The cha
for transmiss

ELECTRONICS AND TELECOMMUNICATIONS QUARTERLY, 2008, 54, no 2, pp. 179–201

Analysis of the CaTV cascade taps

DARIUSZ KRZEMIENIECKI

Gdańskie Zakłady Teleelektroniczne TELKOM-TELMOR
80-425 Gdańsk ul. Mickiewicza 5/7
e-mail: dariusz.krzemieniecki@telmor.pl

Received 2008.03.12
Authorized 2008.05.30

This article presents cascade taps. Basic features of the cascade taps and influence of basic factors (ballast resistance, initial permeability, turns configuration) and transformer on crucial parameters were investigated in this article. Additionally, correction circuits for improvement of certain parameters were proposed. The research considers two-way, three-way and four-way cascade taps. Some examples of cascade taps applications were presented in this paper.

Keywords: unidirectional transformer, basic configuration, inversed configuration, cascade tap

1. INTRODUCTION

Cascade taps are common devices used as elements of CaTV system. They are mainly utilized for CaTV signal distribution to subscribers.

The fundamental element of each cascade tap is the unidirectional transformer (directional coupler), described in detail in following papers [1], [4], [8]. Fig. 1 illustrates its two main configurations: basic and inversed.

Cascade taps are compound of unidirectional transformer cascades. According to the fact that there are various configuration types of the unidirectional transformers, there are various types of cascade taps as well, which means, that taps can be constructed of transformers in basic, inversed or combined configurations.

Moreover, cascade taps can be utilized as some others devices parts. For example, cascade taps can be used by wall outlets and tapping multimedia wall outlets.

In this article working frequency band of 5-862 MHz (basic CaTV working frequency band) is a band of the highest interests.

The characteristic impedance of investigated cascade taps equals 75 Ω (standard impedance for transmission lines in CaTV system).

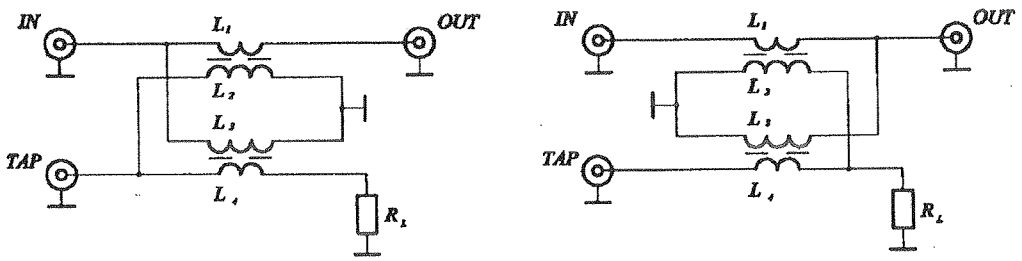

Fig 1. The unidirectional transformers in basic and inversed configuration

The following parameters will be taken into consideration: the main line attenuation IN-OUT, coupled line attenuation IN-TAP, IN reflectance, OUT reflectance, TAP reflectance, isolation between output and branch OUT-TAP, and TAP A-B isolation.

Similarly to unidirectional transformers, cascade taps are band devices. Fig. 2, 3 illustrates fundamental parameters of 10-dB cascade tap versus wide frequency band: IN-OUT and IN-TAP.

One-way cascade taps will not be presented in this paper. In fact, one-way tap is only the unidirectional transformer, which was widely described in the following articles [4], [8].

2. THE TWO-WAY CASCADE TAP

The two-way cascade tap is a cascade of two unidirectional transformers. Fig. 4 illustrates circuit consisting of basic configuration transformers, whilst Fig. 5 presents circuit consisted of transformers in inversed configuration. For theoretical analysis, the admittance matrix of the single unidirectional transformer will be used in the first place, then the admittance matrix of complete device will be calculated. This matrix for taps with transformer in basic configuration is illustrated by Table 1 (see also Fig. 4). Calculated matrixes are used for scattering matrixes calculations [4], [8]. Obviously, it is based on the node voltage method.

Fig. 6 illustrates exemplary theoretical characteristics of the two-way cascade tap with transformer in basic configuration, whilst Fig. 7 presents theoretical characteristics of the two-way cascade tap with transformers in inversed configuration. The 10-dB transformer with L_1, L_4 windings (1.5 windings) and L_2, L_3 windings (4.5 windings) were utilized (similarly to [4], [8], see also Fig. 1) by these devices.

Cascade taps with transformer in basic configuration have advantageous IN reflectance and worse: OUT reflectance, OUT-TAP and TAP A-B isolations.

Cascade taps with transformer in inversed configuration are characterized by worse IN reflectance and by better: OUT reflectance, OUT-TAP and TAP A-B isolations. It is noticeable that choice of appropriate configuration of the transformer determines cascade tap parameters. These features will be used for optimal configuration determination.

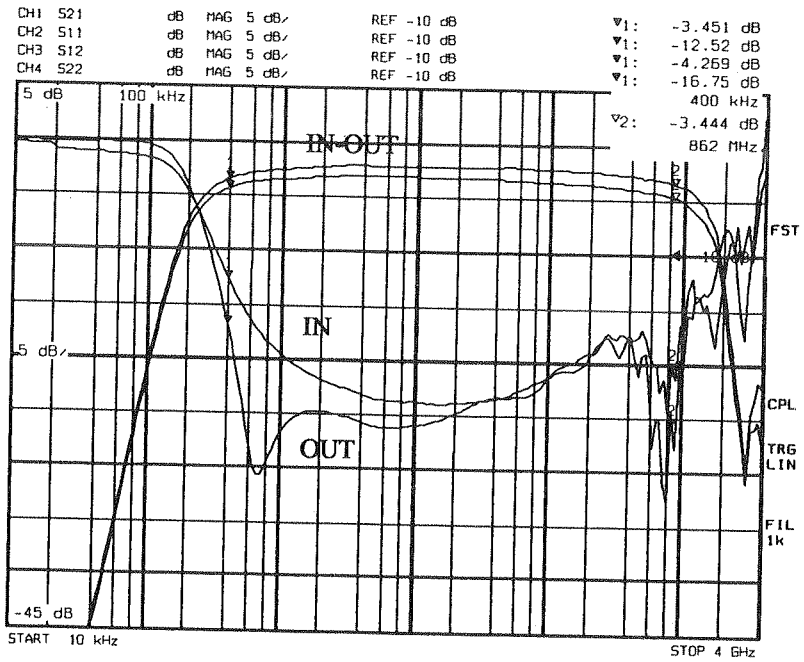

Fig. 2. The IN-OUT characteristic of the 10-dB dual cascade tap in wideband frequencies

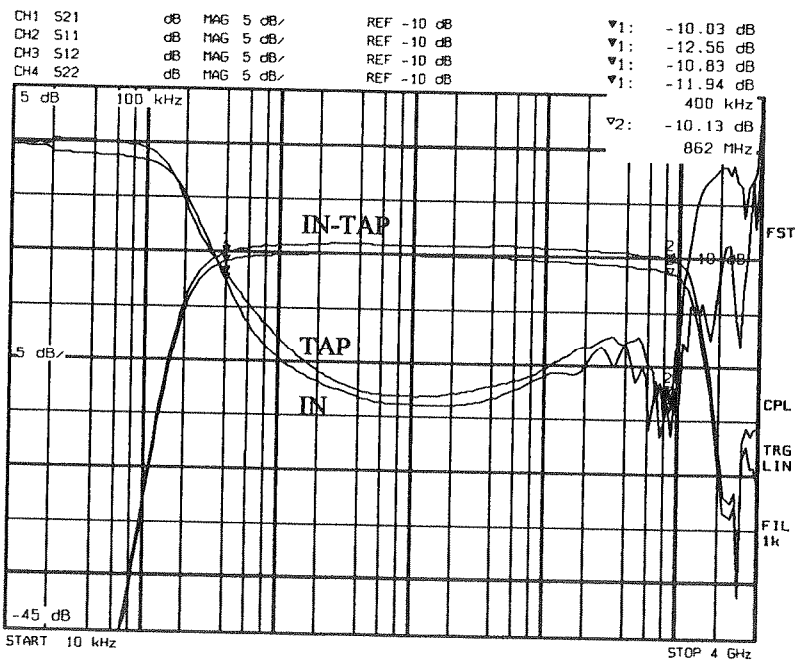

Fig. 3. The IN-TAP characteristic of the 10-dB dual cascade tap in wideband frequencies

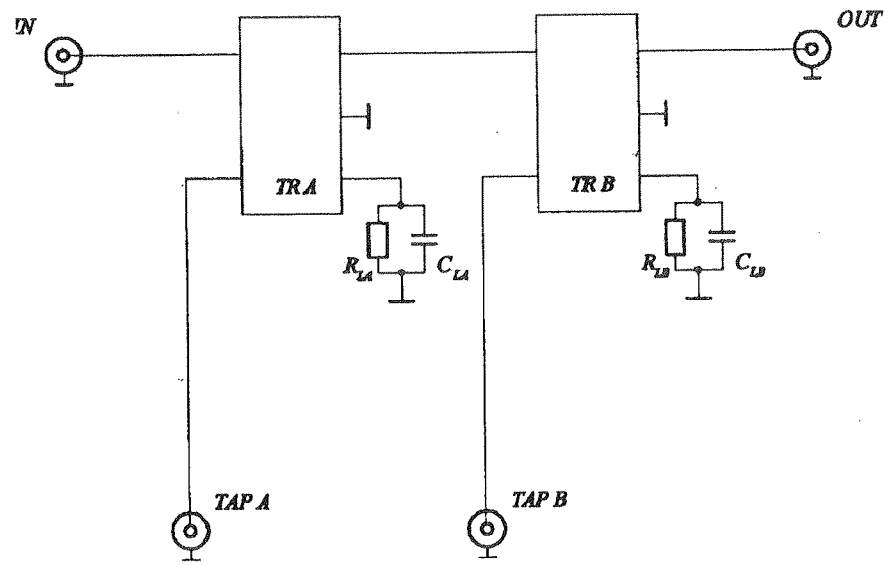

Fig. 4. The two-way tap with transformers in basic configuration

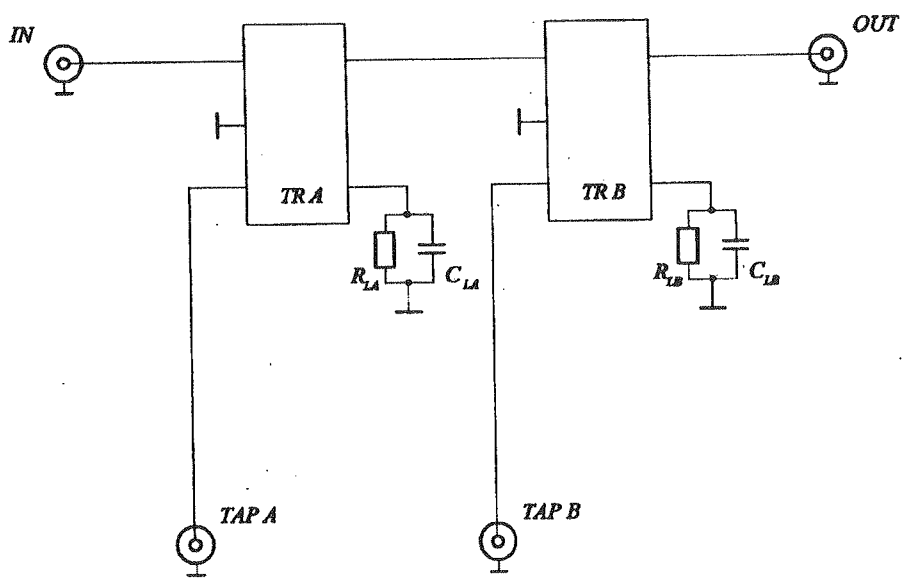

Fig. 5. The two-way tap with transformers in inversed configuration

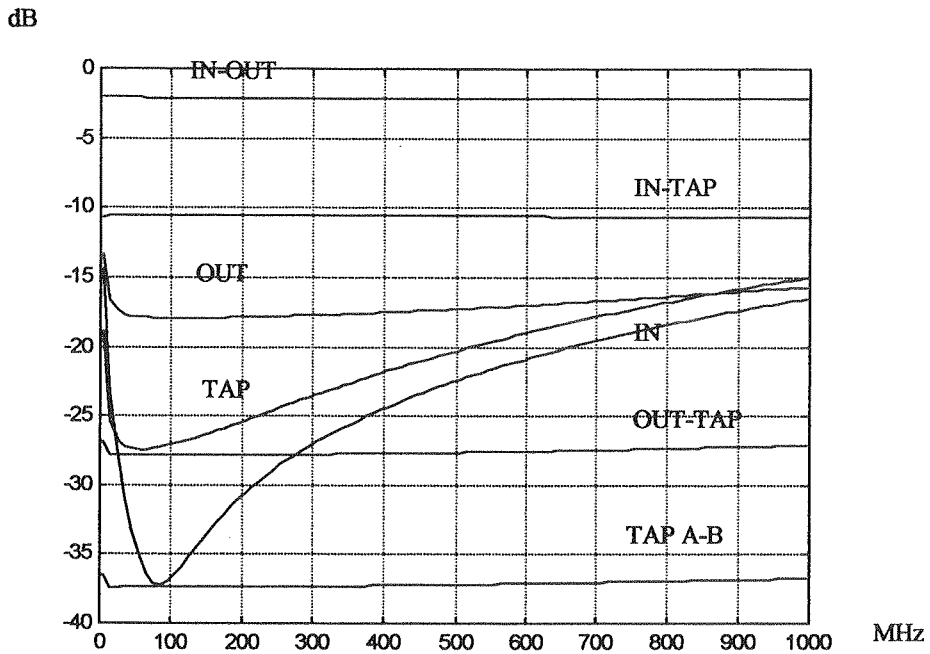

Fig. 6. The theoretical characteristic of the two-way tap with transformers in basic configurations

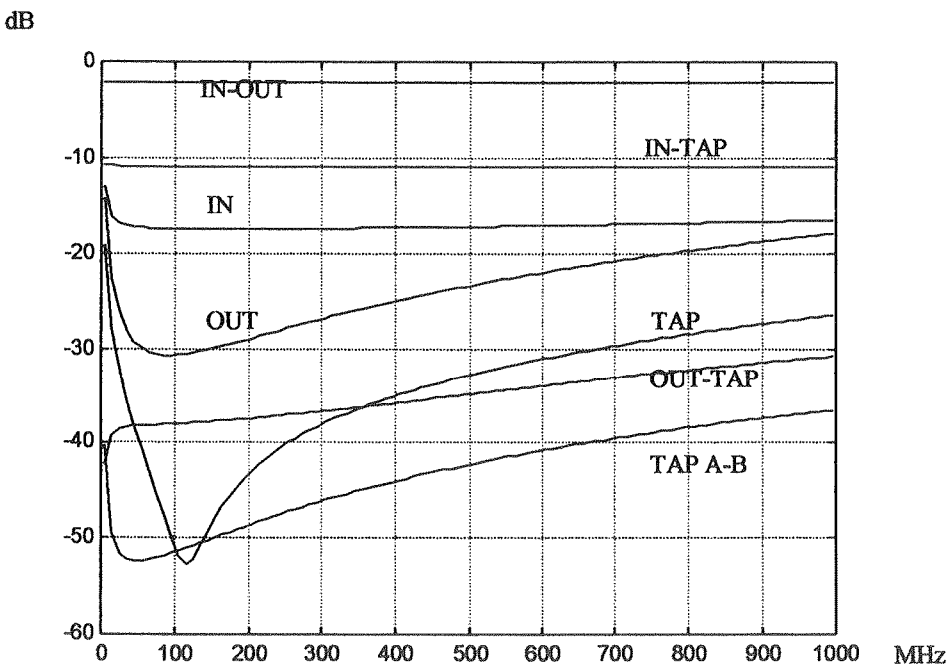

Fig. 7. The theoretical characteristic of the two-way tap with transformers in inversed configurations

Table 1

Admittance mattrix of the cascade tap i basic configuration

node	*IN*	-	*OUT*	*TAP A*	*TAP B*
IN	y_{11A}	y_{13A}	*0*	y_{12A}	*0*
-	y_{31A}	$y_{33A} + y_{11B}$	y_{13B}	y_{32A}	y_{12B}
OUT	*0*	y_{31B}	y_{33B}	*0*	y_{32B}
TAP A	y_{21A}	y_{23A}	*0*	y_{22A}	*0*
TAP B	*0*	y_{21B}	y_{23B}	*0*	y_{22B}

2.1. THE INFLUENCE OF THE BALLAST RESISTANCE

The influence of the ballast resistance is similar like as unidirectional transformer [4], [8]. Typical feature is that ballast resistor R_L has influence on TAP and OUT-TAP parameters of considered branch. The ballast resistor of the "A" transformer has influence on TAP and OUT-TAP parameters of the "A" transformer only, whilst it has no influence on TAP and OUT-TAP parameters of the "B" transformer. Regarding TAP A-B parameter there are some differences: the ballast resistor of the "A" transformer has influence on the TAP A-B parameter, whilst the ballast resistor of the "B" transformer has no influence on this parameter. The desired feature (similarly to unidirectional transformer) is to maintain the main line attenuation (IN-OUT), coupled line attenuation (IN-TAP) on the stable levels. That condition is guaranteed in fact: the ballast resistance has almost no influence on these parameters.

2.2. THE INFLUENCE OF THE INITIAL PERMEABILITY

The influence of the initial permeability on cascade taps for particular transformer configurations are presented by Fig. 8, 9. Obviously, the influence of the initial permeability at low frequencies (5 MHz at Fig. 8, 9) is evident. This influence decreases with increase in frequency and at 862 MHz there is practically no influence. Conclusions are analogue to already presented conclusions. For transformer in basic configuration the IN parameter is better, whilst the OUT, OUT-TAP and TAP A-B have worse characteristics, for transformer in inversed configuration opposite relation can be observed. Moreover, according to Fig. 8, 9 the most advantageous parameter characteristics for both configurations are obtained for initial permeability in the range of 3000-6000.

Similarly to the influence of the ballast resistance, the influence of the initial permeability on the IN-OUT and IN-TAP parameters is minimal, which is an advantageous feature.

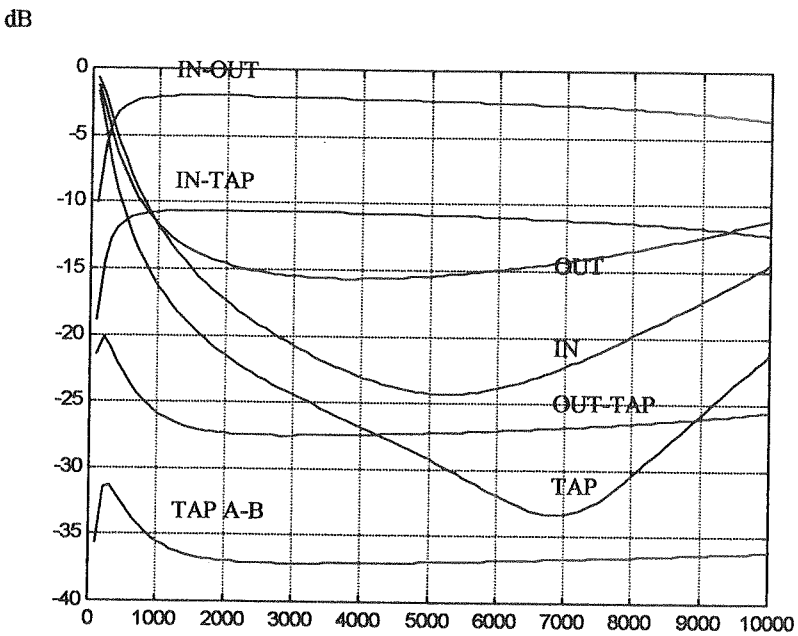

Fig. 8. The influence of the initial permeability for two-way tap with transformers in basic configurations, at frequency 5 MHz

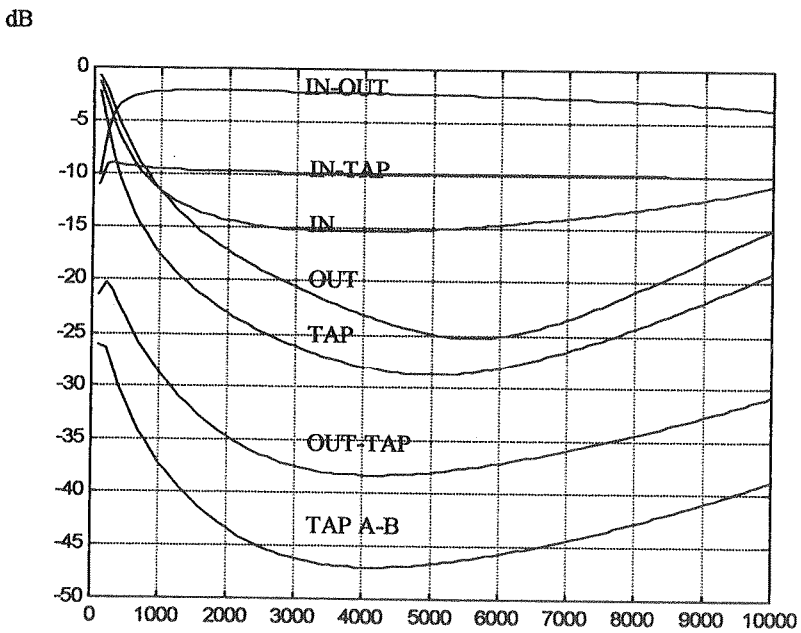

Fig. 9. The influence of the initial permeability for two-way tap with transformers in inversed configurations, at frequency 5 MHz

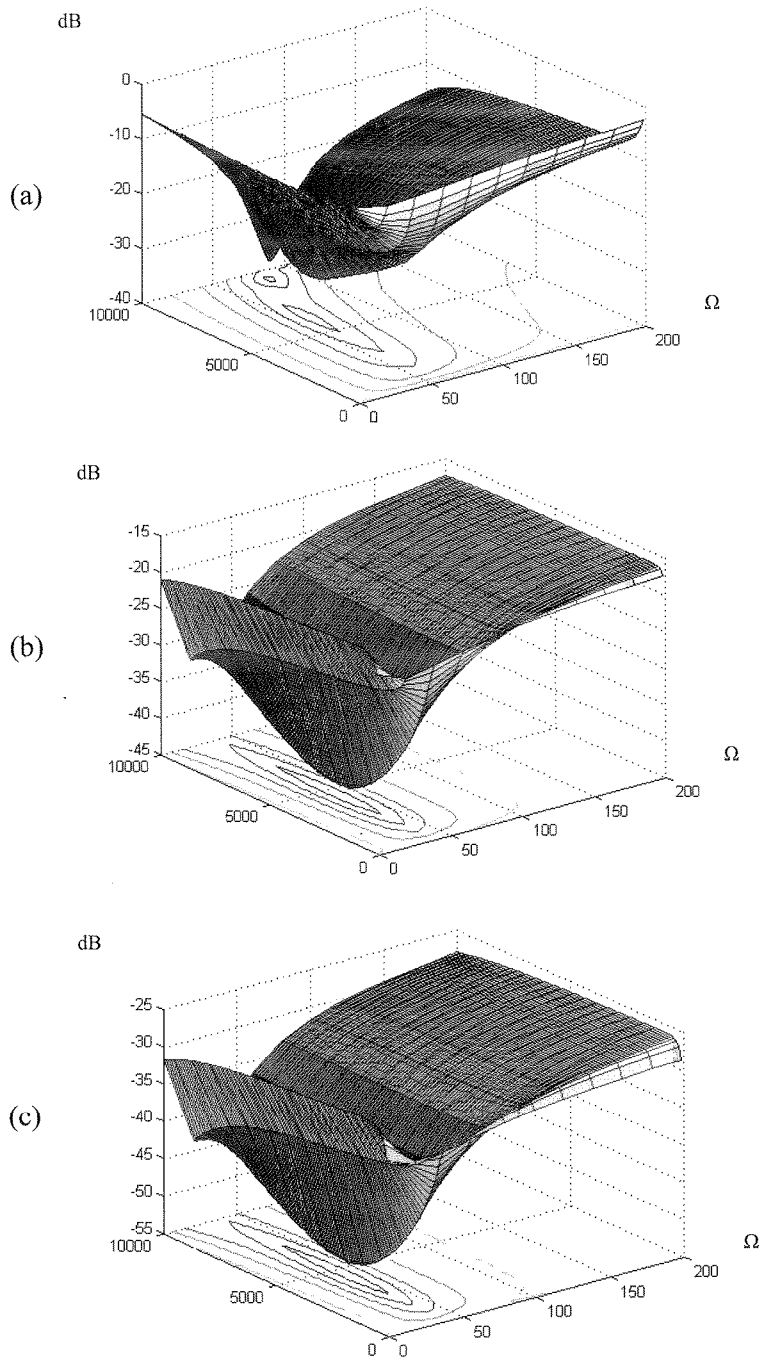

Fig. 10. The influrnce of the initial permeability and ballast resistance RL on parametersTAP (a), OUT-TAP (b) and TAP A-B (c) of the two-way tap

Parameter characteristics, regarding ballast resistor and the initial permeability influence, presented so far, do not illustrate complete relation between these two factors. In order to complete our considerations, 3-D charts of TAP, OUT-TAP and TAP A-B parameters versus ballast resistance R_L and initial permeability at 5 MHz were presented at Fig. 10.

2.3. THE INFLUENCE OF THE CAPACITANCE AND DISSIPATION

In papers [4], [8] it was proved that capacitances of the unidirectional transformer have firmly parasitic character. These capacitances limit working frequency band of the transformer at high frequencies and have negative influence on reflectance and isolation of the transformer. The dissipation coming out of inaccuracy in transformer windings has the similar destructive influence. In order to decrease the influence of parasitic capacitances and dissipation, it is necessary to use proper transformer winding technique, which limits capacitances and dissipation of the transformer. Using smaller ferrite cores is also a good solution.

2.4. CORRECTION CIRCUITS

Similarly to the unidirectional transformer case, there are low frequency correction circuits and high frequency correction circuits. Serial capacitances and circuits with chokes and capacitors at the input, are examples of low frequency correction circuits. However the most economical and also the most effective solution, is placing high value capacitance between transformers in series. This correction circuit is a π-type circuit in fact, because correction circuit is closed by transformer coupling inductances in this case. It is illustrated graphically by Fig. 11.

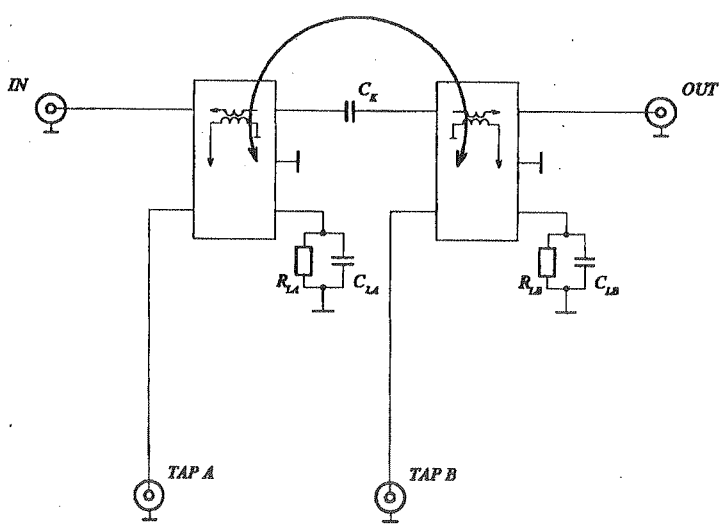

Fig. 11. The π-type correction for low frequencies

OUT-TAP

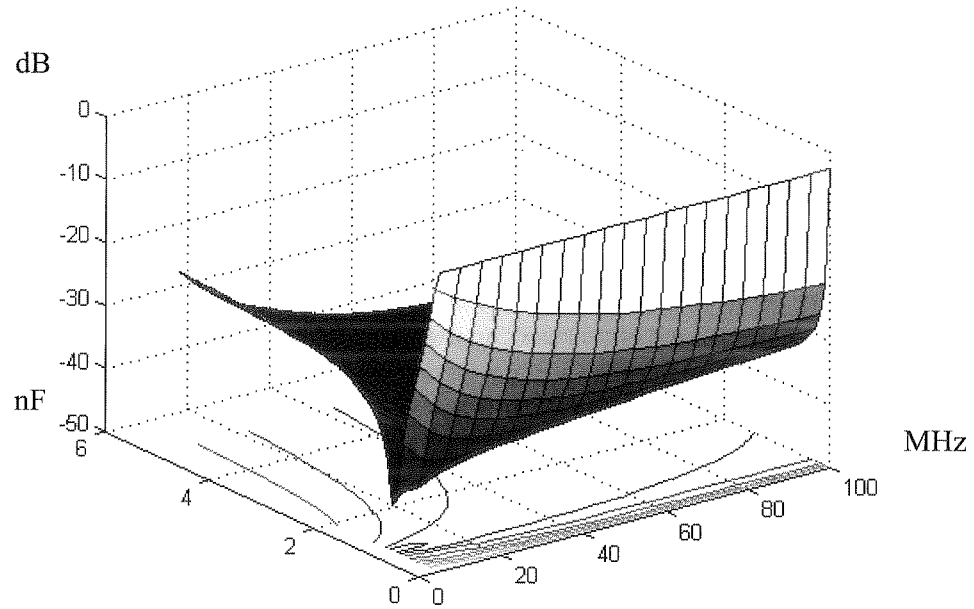

Fig. 12. The influence of the corrective series capacitor on the parameter IN

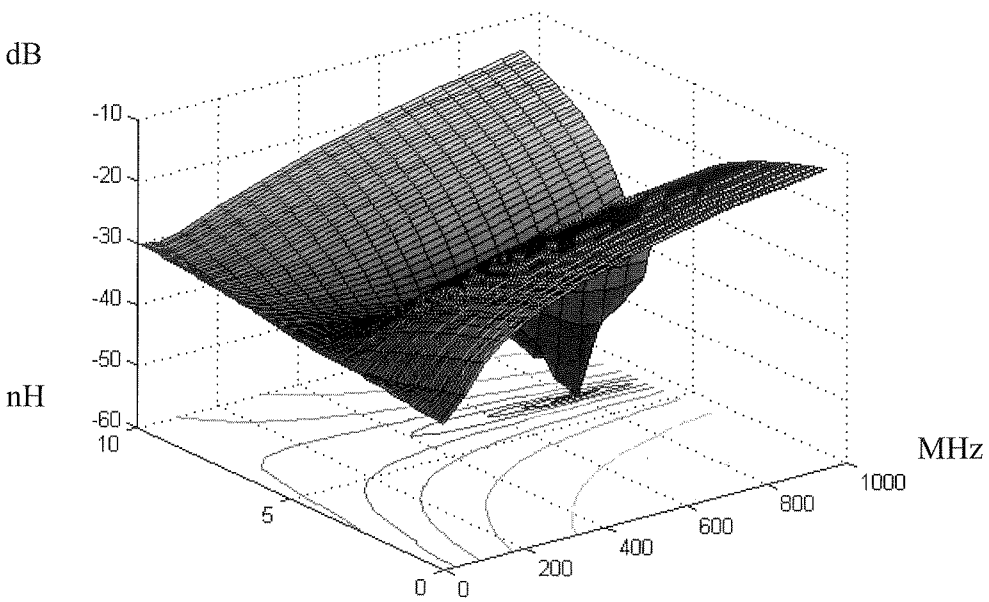

Fig. 13. The influrnce of the corrective inductance on the parameter IN

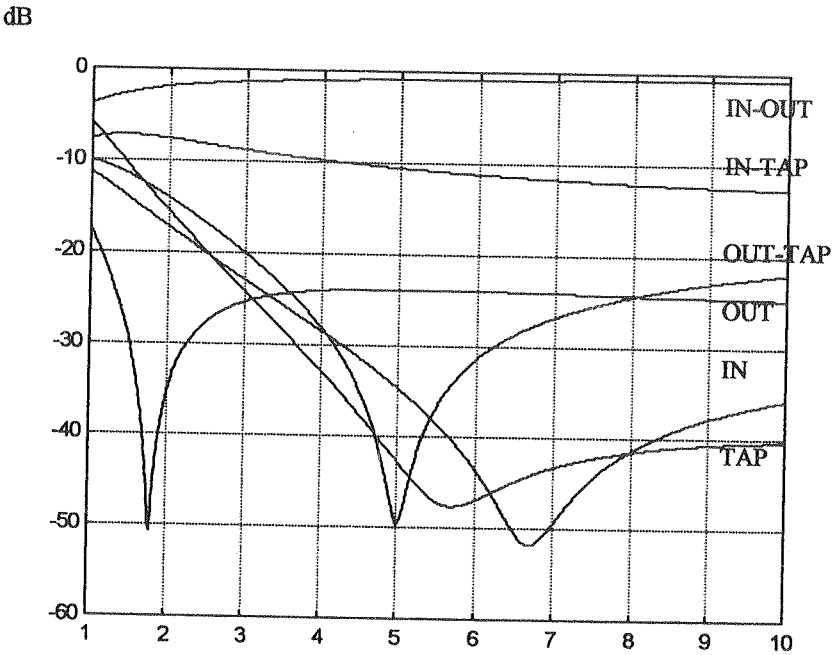

Fig. 14. The influence of the windings L2 on the parameters of the unidirectional transformer, at frequency 65 MHz

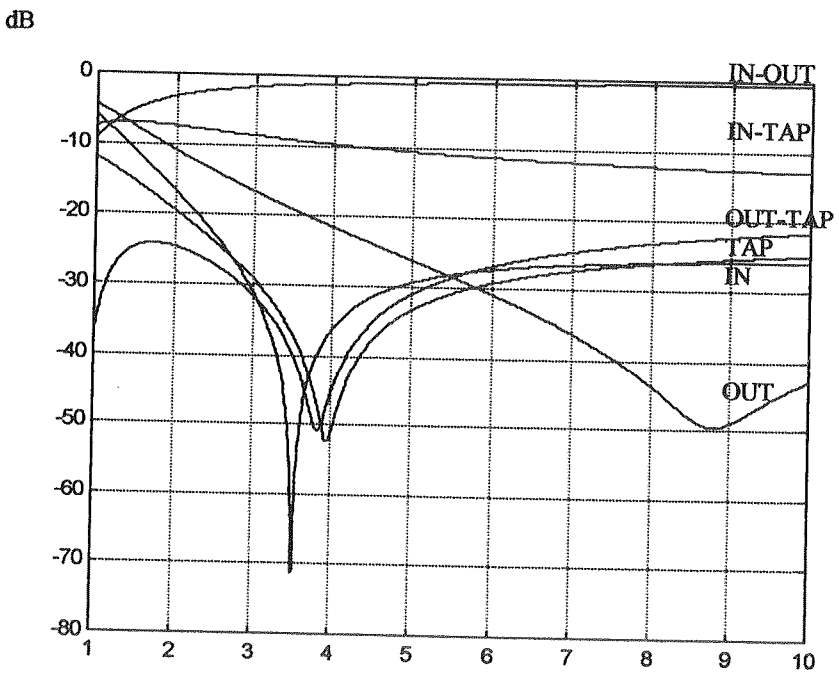

Fig. 15. The influence of the windings L3 on the parameters of the unidirectional transformer, at frequency 65 MHz

LC circuits with low value capacitor and inductor are high frequency correction circuits (the same circuits are utilized by unidirectional transformers [4], [8]).

High and low frequency correction circuits are illustrated by characteristics at Fig. 12, 13.

Fig. 12 presents the influence of the capacitance (placed in series between transformers) on IN parameter. Fig. 13 illustrates influence of the correction inductance on IN parameter, assuming constant correction capacitance.

Moreover, ballast capaciror C_L is also a kind of high frequency corrector. Thanks to ballast capacitor, TAP and OUT-TAP parameters can be improved at high frequencies [4], [8].

2.5. THE CASCADE TAPS WITH COUPLED LINE EQUAL ATTENUATION

The cascade connection of unidirectional transformers in natural way results in differences between branching lines attenuation, namely each subsequent transformer to cascade connection causes stronger branching line attenuation (IN-TAP). In order to obtain the same attenuation level in each branching line, it is necessary to design subsequent transformer of lower than prior transformer attenuation. It can be realized by choosing appropriate winding configuration. Decrease or increase in coil number could be realized by all coils in fact, but L_2, and L_3 changes results in less radical changes of other parameters. With L_2 or L_3 coil number decrease, comes decrease in coupled lines attenuation level, which results in equal attenuation level of coupled lines. Fig. 14, 15 illustrates these cases for 10-dB transformer, which was mentioned previously. These charts present parameters of the 10-dB transformer at 65 MHz.

2.6. THE COMBINED CONFIGURATION

According to presented configuration analysis, following conclusions are obvious: in order to obtain better input reflectance (IN), it is advantageous using basic transformer configuration at the input, whilst in order to achieve better output reflectance (OUT) it is advantageous using transformer in inversed configuration at the output.

In this way combined configuration is obtained. Additionally transformer in inversed configuration at the output ensures good OUT-TAP and TAP A-B isolations.

This configuration is presented in Fig. 16. Moreover, this device includes capacitor C_K for parameters improvement at low frequencies. There is also $L_W C_W$ circuit, which improve cascade tap parameters at high frequencies. It is the optimal solution, which utilizes both advantages of transformer configurations, and correction circuits.

Fig. 18, 19 presents 10-dB and 15 dB characteristics of cascade taps according to diagram presented at Fig. 16.

As a supplement, Fig. 20 presents circular charts for 10-dB cascade tap IN, OUT, TAP reflectances.

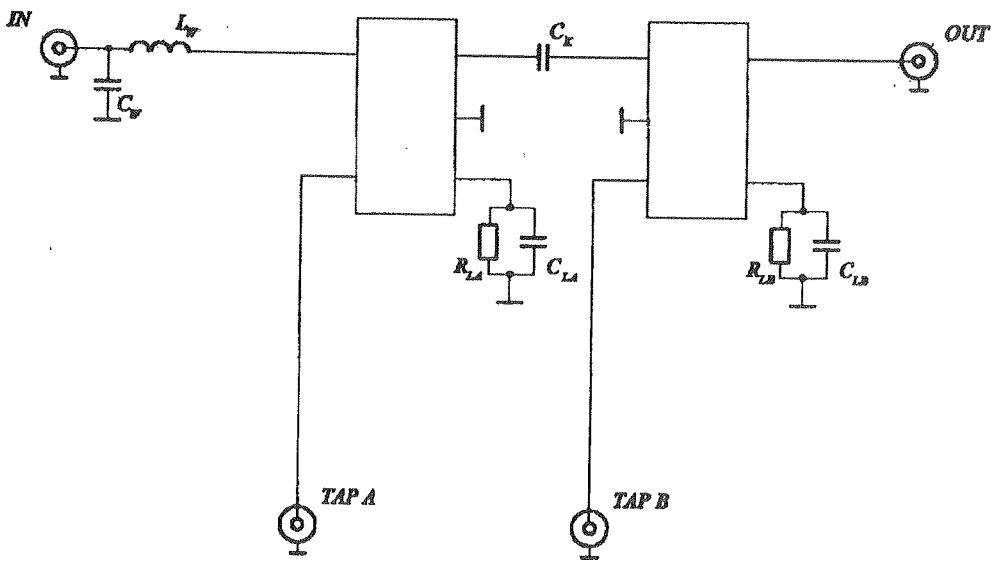

Fig. 16. The combined configuration of the two-way tap

These cascade taps utilize small ferrite cores of 3000 permeability value, according to comments given in points 2.2 and 2.3.

It is necessary to add that inversed configuration provides lower than basic configuration coupled line attenuation (IN-TAP) and because of that fact, second transformer windings correction is not always the must. The same transformers can be used be device, which results in approximately the same coupled line attenuations.

Besides traditional application of autonomous cascade tap, it can be utilized by the wall outlet, which was illustrated by Fig. 17. The wall outlet is a two-way cascade tap in combined

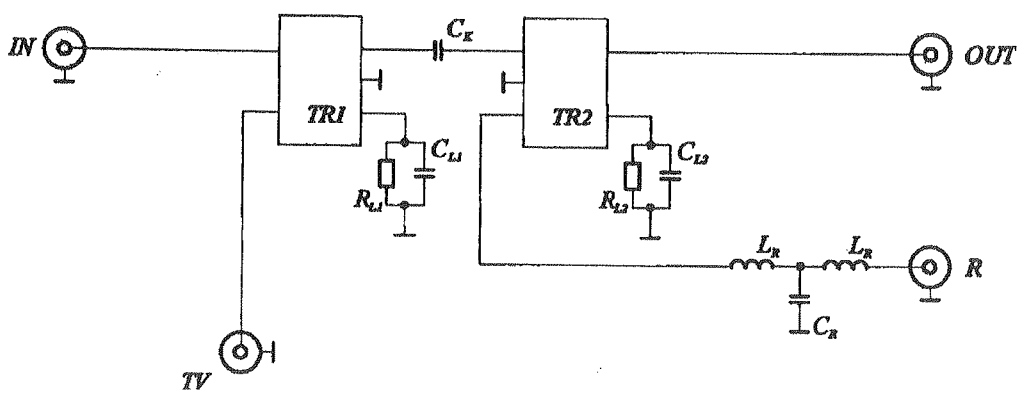

Fig. 17. The wall outlet of tapping type

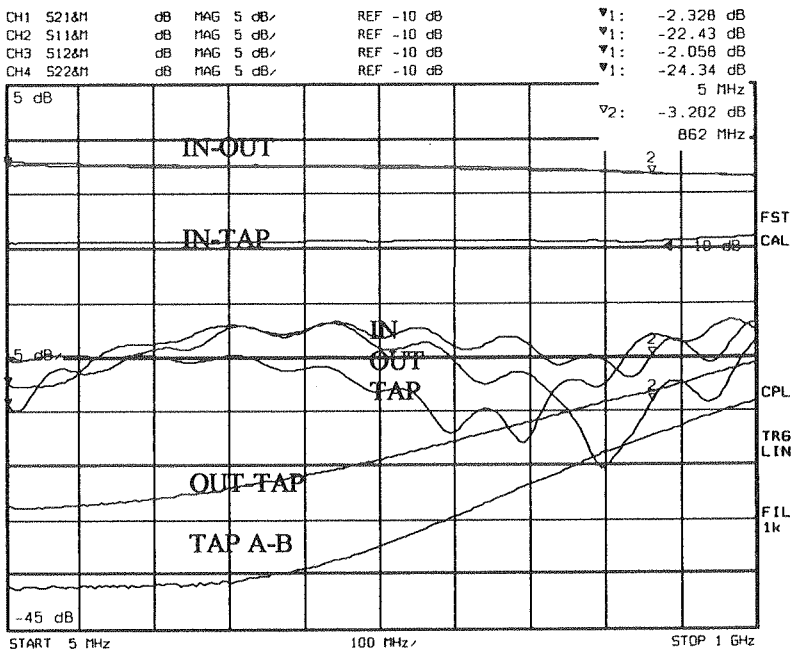

Fig. 18. Frequency characteristics of the 10-dB two-way cascade tap

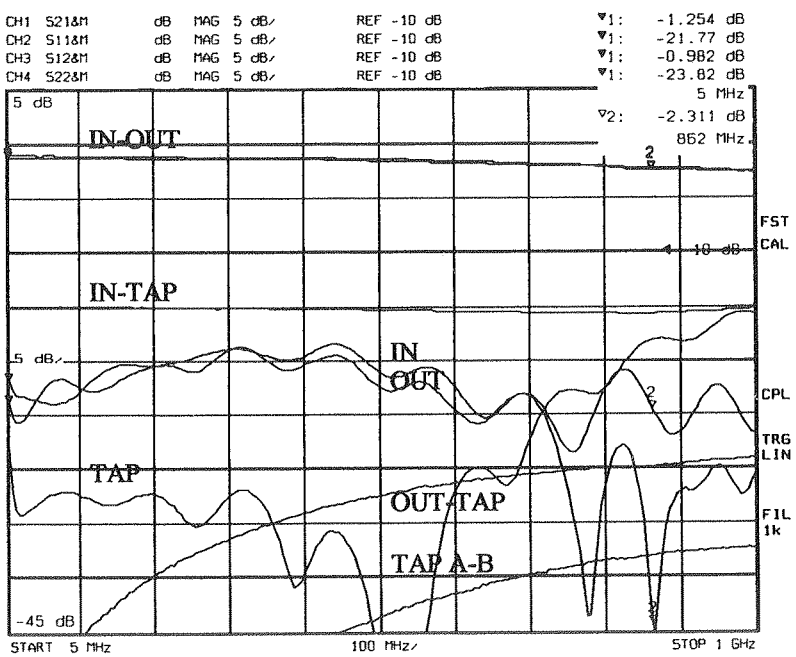

Fig. 19. Frequency characteristics of the 15-dB two-way cascade tap

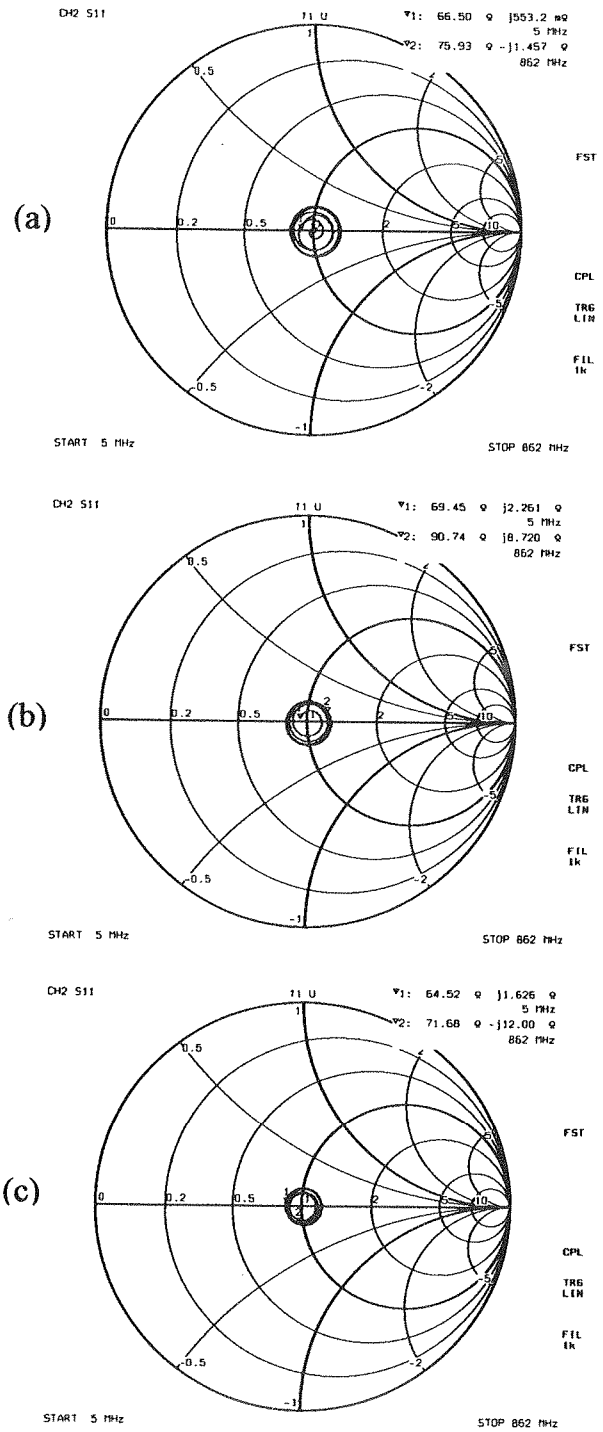

Fig. 20. Smith charts of the reflektances IN (a), OUT (b) and TAP (c) of the 10-dB two-way cascade tap

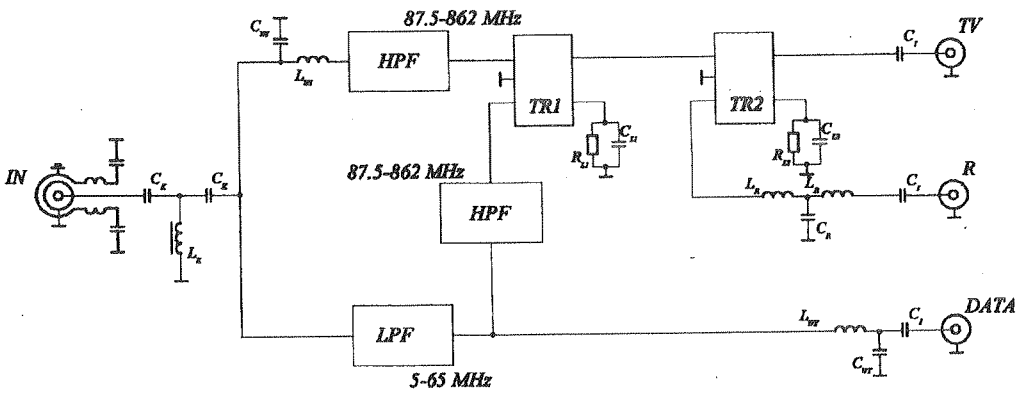

Fig. 21. The schematic diagram of the multimedia wall outlet

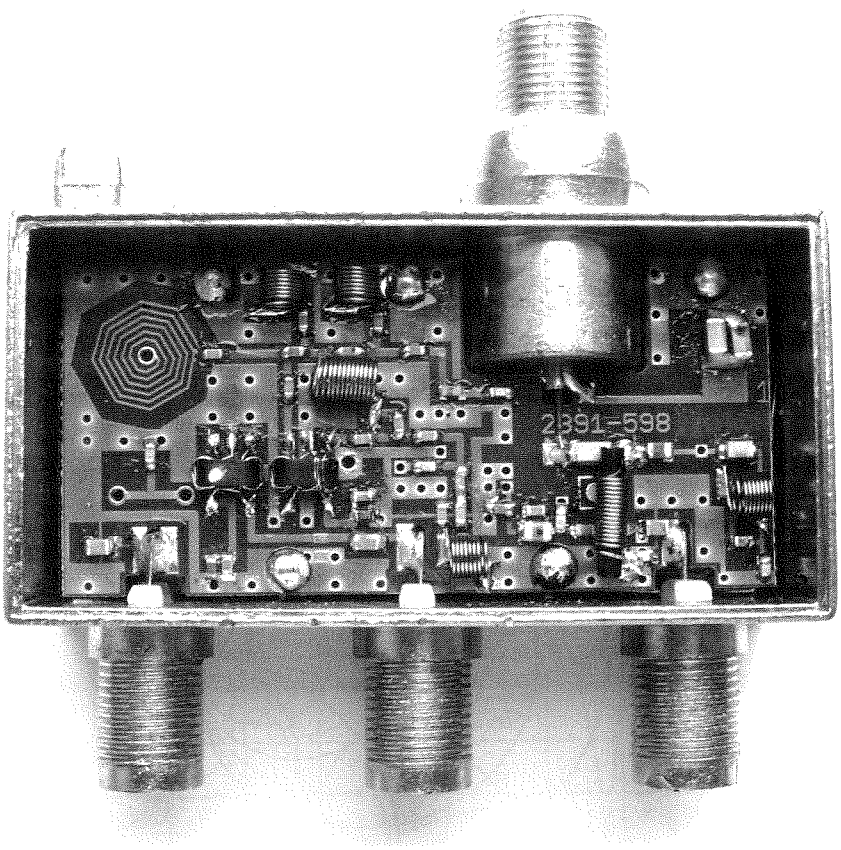

Fig. 22. The photo of the multimedia wall outlet

configuration, in which radio filter limiting working frequency band to 139 MHz is connected to radio circuit.

The wall outlet constructed in this way is called wall outlet of tapping type.

Another example of application of the two-way tap is an advanced tapping multimedia wall outlet [2], [9]. The diagram of the wall outlet is illustrated by Fig. 21 and its photo is presented at Fig. 22. This wall outlet utilizes two-way cascade tap. First transformer is used for "DATA" band selection, whilst second is used for radio "R" band selection. Inversed configuration, which was used in this wall outlet, improves isolations.

In this case, there was no need for combined configuration use, because the characteristic of the input reflectance IN is determined by low (LPF) and high pass (HPF) filters. The wall outlet has following correction circuits: T-type filter (low frequency correction circuit) and LC circuits at input "IN" and at "DATA" output (high frequency correction circuits).

The wall outlet has the isolation between input ground and device ground and the suppresing line, which provides electromagnetic compatibility EMC [9].

Fig. 23. presents basic characteristics of the wall outlet.

It is necessary to add to the above, that it is not possible to achieve identical coupled line attenuations because of no fluency in winding changes. Identical coupled line attenuations can be achieved in the multidirectional transformers, which provide power division between coupled lines in natural way [5], [6], [8]. They have this advantage that using one inductive element can provide equal attenuation characteristics for each transformer. However, relatively weak TAP A-B isolation is a disadvantage of multidirectional transformers. Regarding this parameter, cascade taps are better.

Another way for identical coupled lines attenuation, is utilization of splitterring taps. In these splittering taps, the splitters of appropriate number of ways are connected to unidirectional transformer [7].

3. THE THREE-WAY CASCADE TAPS

Conclusions given so far, are practically applicable to the three-way cascade taps. Transformer configuration use results in analogical effects to two-way cascade taps. Regarding ballast resistance, the distinguishable feature is ballast resistance influences on isolation between branches TAP A-B. The ballast resistor of first transformer influences on isolation of each branching line, whilst the ballast resistor of second transformer influences only on two last branching lines. Third ballast resistor has no influence on any branching line. The optimal range of permeability values is 3000-6000, like previously. Similarly to previous considerations, the influences of capacitance and dissipation have firmly negative character.

Similarly to the two-way cascade taps, following correction circuits are applicable to the three-way cascade taps: for high frequency correction like previously, the best results of low frequency correction are obtained for capacitor placed between first and second transformer. Placing correction capacitor between second and third capacitor is an ineffective correction. It is better using the RC corrector, which improves the IN-OUT characteristic.

(a)

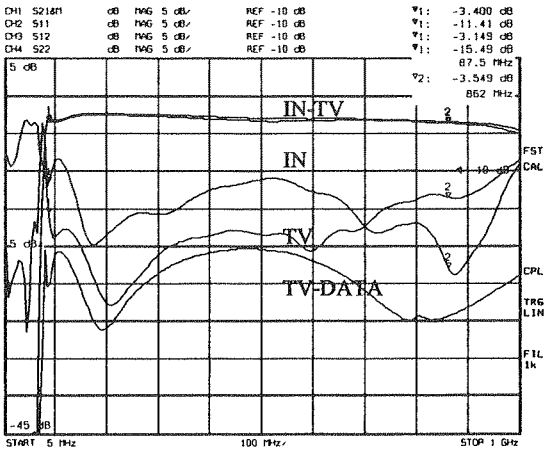

(b)

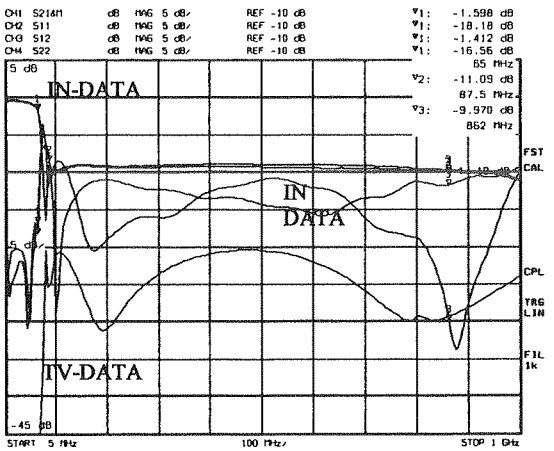

(c)

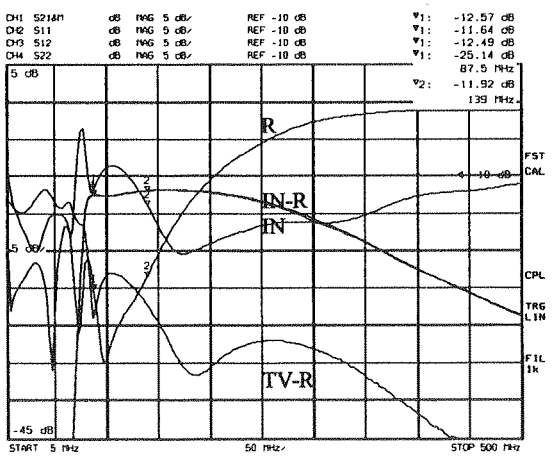

Fig. 23. Main characteristics of the advanced multimedia wall outlet

Fig. 26, 27 present basic characteristics of 14-dB and 18-dB cascade taps fabricated according to diagram illustrated at Fig. 24.

In this case also ferrite cores of 3000 permeability value were used. Similarly to the two-way cascade taps, the three-way cascade taps have various applications. A multimedia wall outlet of tapping type is the example of cascade taps application. High pass filters HPF were placed in RTV lines, for RTV outputs isolation improvement at low frequencies. The diagram of the wall outlet is illustrated by Fig. 25.

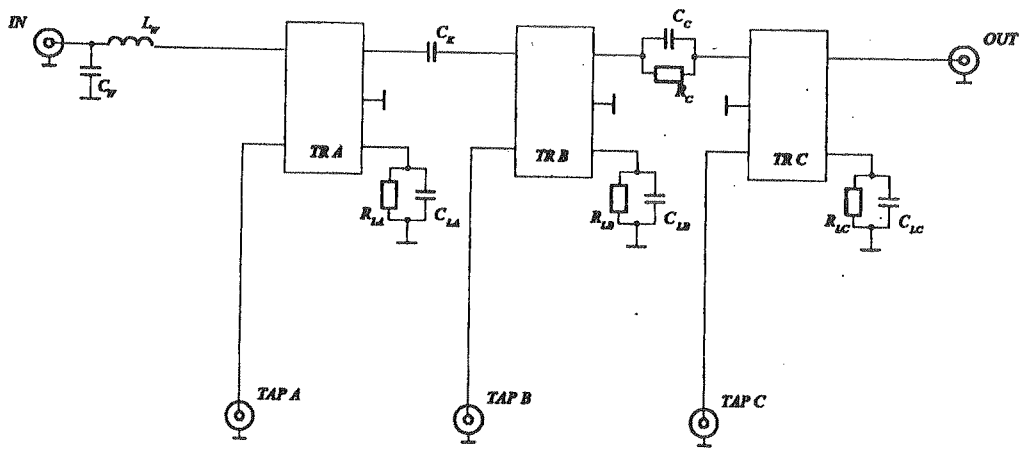

Fig. 24. The three-way tap

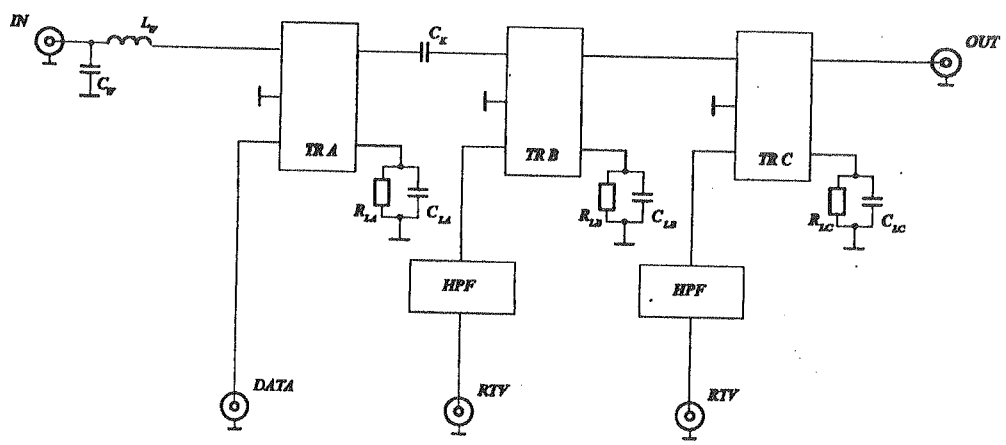

Fig. 25. The multimedia separator

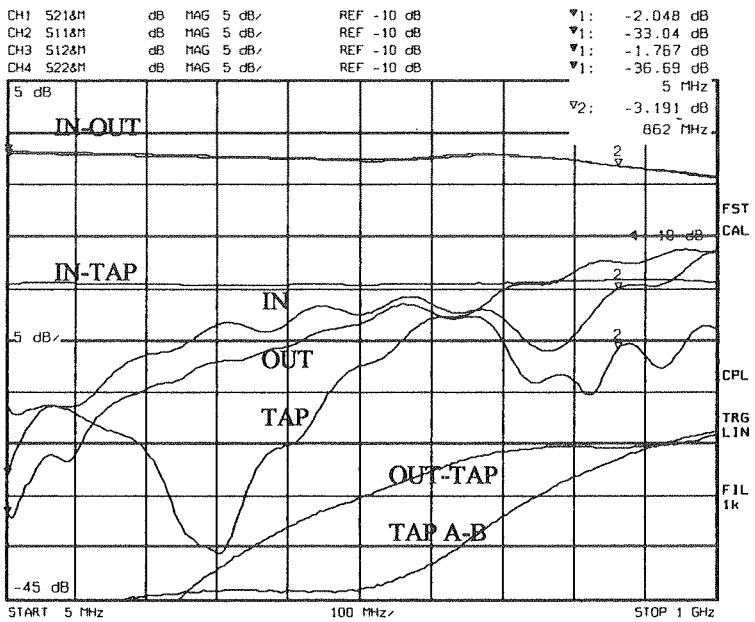

Fig. 26. Frequency characteristics of the 14-dB three-way cascade tap

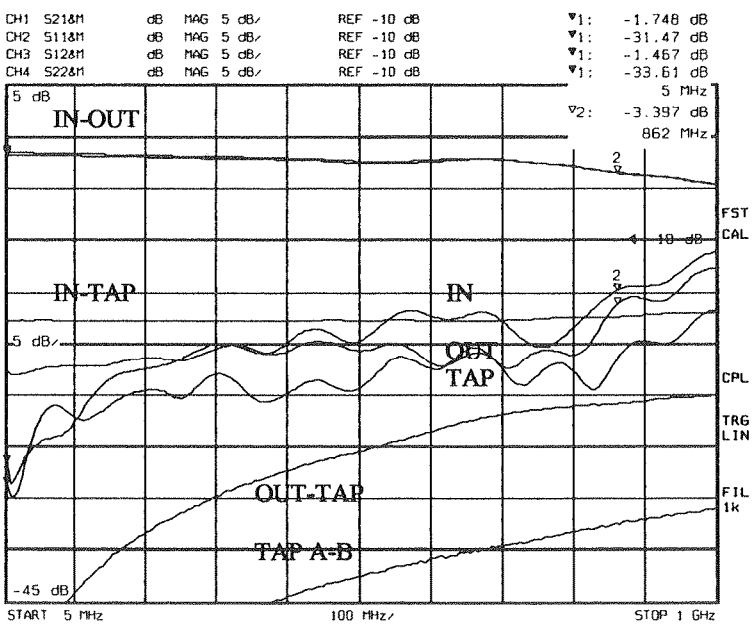

Fig. 27. Frequency characteristics of the 18-dB three-way cascade tap

4. THE FOUR-WAY CASCADE TAPS

Conclusions for the four-way cascade taps are analogical to the two-way and three-way cascade taps. For four-way cascade taps the best effective low frequency correction is achieved for series capacitor placed between first and second, and third and fourth transformer. In this way two π-type correctors are obtained (input and output parameters correction; see also Fig. 11). Similarly to the three-way cascade tap, RC correctors for IN-OUT characteristic improvement are advantageous. Obviously, it is not always necessary to use transformers of equal level of coupled line attenuations. The cascade tap with rising attenuations in coupled lines is a good example. The block diagram is illustrated at Fig. 28, exemplary characteristics are presented by Fig. 29, 30. The basic element of this cascade tap is the same 12-dB transformer. Additionally in coupled lines series capacitors were placed, which with transformer windings create γ-type correctors. These correctors improve TAP characteristics at low frequencies.

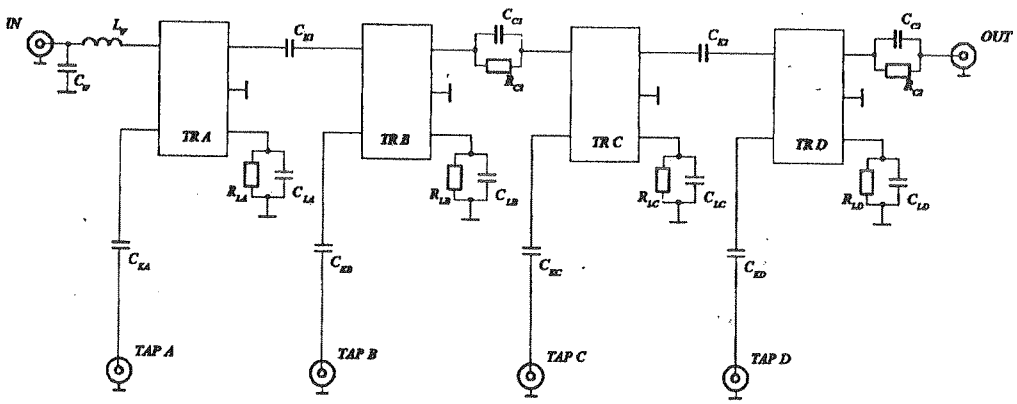

Fig. 28. The four-way cascade tap

5. CONCLUSIONS

In this paper main features of cascade taps were presented. The research considered cascade taps of small number of ways like: the two-way, three-way and four-way cascade taps. These research and experiments provide some proofs that described conclusions are right for cascade taps of higher number of ways. It is results of the fact that the most important element of each cascade tap is a unidirectional transformer, which determines cascade tap features. Because of reasons given in papers [4], [8] mathematical model strays from reality, and it can be assumed that it has about 10 % precession.

To the above it is necessary to add, that cascade tap features depend on project establishments and priorities. Exemplary in point 2.6 in order to achieve maximum OUT-TAP and TAP A-B isolations, device with inversed transformers is more appropriate, than model with combined configurations. However, device with inversed transformers has worse IN parameter.

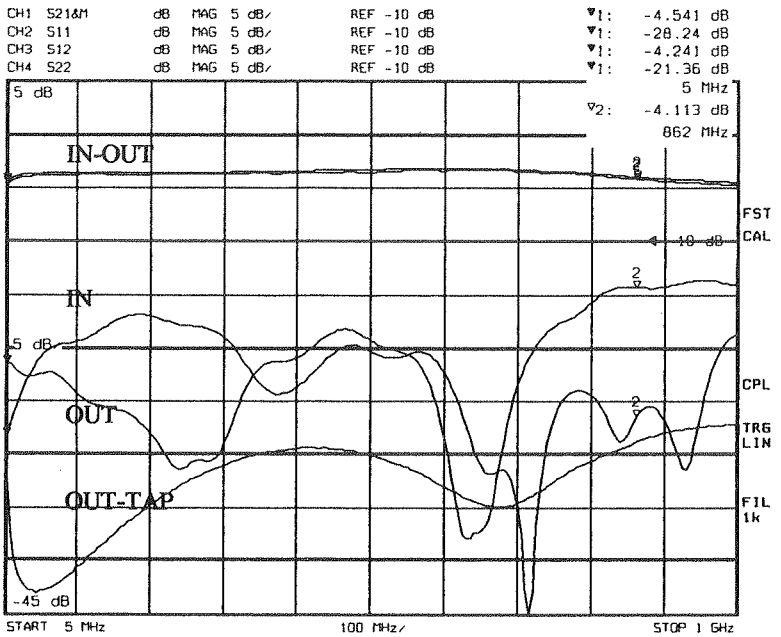

Fig. 29. The IN-OUT frequency characteristic of the four-way cascade tap

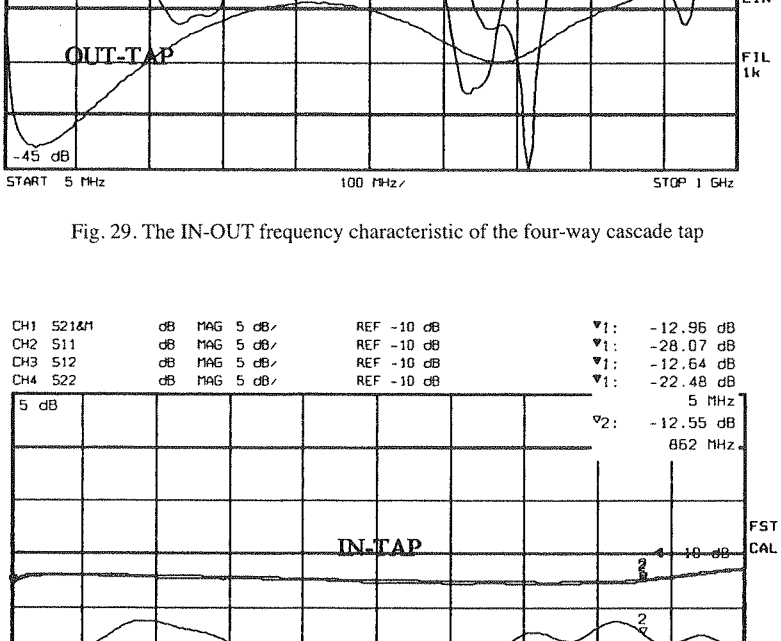

Fig. 30. The IN-TAP frequency characteristic of the four-way cascade tap

The inversed configuration with separatory resistor was derived in papers [4], [8]. This configuration can be utilized instead of inversed configuration, what results in better TAP A-B isolation. It is necessary to remember that inversed configuration with separatory resistor introduces higher coupled line attenuation IN-TAP.

Sometimes it happens that it is necessary to create taps with minimum intermodulation distortion. In this case ferrite cores of the lowest permeability are the most advantageous (3000-6000 permeability values are optimal). However, ferrite cores of low initial permeability introduce worse IN, OUT reflectances at lower frequencies. There, described previously, low frequency correctors are helpful.

Similarly to unidirectional transformer case [4], [8], it is possible to widen cascade tap working frequency band. It is applicable only to few types of transformers. Only for inductors L_1 and L_4 (Fig. 1) of 0.5 coils it is possible. And then only a few transformers are characterized by low inequality in wide frequency band. These transformers have small number of coils, because higher number of coils causes higher transformer self-capacitances, which results in frequency band narrowing. Transformers constructed in this way and microstrip line, use can widen cascade taps working frequency band even to 3 GHz.

The characteristic impedance of the cascade taps were assumed as 75 Ω (standard impedance for transmission lines in CaTV system). It is necessary to remember that change in characteristic impedance value comes with changes in parameters of cascade tap. The increase in characteristic impedance results in higher IN-OUT and IN-TAP attenuation. Reflectances IN, OUT and TAP also decrease their performance with increase in characteristic impedance. Moreover, the fact that changes in characteristic impedance value comes with changes in ballast resistor optimal value for TAP and OUT-TAP parameters, is of high importance.

6. REFERENCES

1. D.I. Kim, M. Takahashi, K. Araki, Y. Naito: *Optimum design of the power dividers with ferrite toroids for CATV and/or MATV systems*. IEEE Trans. On Consumer Electronics, vol. CE-29, no 1, Feb. 1983, pp. 27-38.
2. Y. Naito: *Formulation of frequency dispersion of permeability*. Trans. IECE, vol. 59-c May 1976, pp. 297-304.
3. D. Krzemieniecki: *Advanced tapping multimedia outlets and separators*. National Telecommunication Symposium, Bydgoszcz 2001, vol. A, pp. 401-410 (in polish).
4. D. Krzemieniecki: *Investigation and optimization of the wideband directional transformer*. Electronics and Telecommunication Quarterly, 2005, 51, vol. 1, pp. 105-135 (in polish).
5. D. Krzemieniecki: *Investigation and optimization of the wideband two-directional transformer*. Electronics and Telecommunication Quarterly, 2005, 51, vol. 3, pp. 387-419 (in polish).
6. D. Krzemieniecki: *Investigation and optimization of the wideband four-directional transformer*. Electronics and Telecommunication Quarterly, 2005, 51, vol. 4, pp. 603-637 (in polish).
7. D. Krzemieniecki: *Current posibilities of projecting of the taps arrangements*. National Conference of Radiocommunication, Radio and Television, Poznań 2006, pp. 457-460 (in polish).
8. D. Krzemieniecki: *Modelling and designing of directional transformers*, PhD Thesis, Faculty of Electronics, Telecommunications and Informatics, Gdańsk University of Technology, Poland (in Polish) 2006.
9. D. Krzemieniecki: *Advanced multimedia outlets and separators with full isolation*. National Conference of Radiocommunication, Radio and Television, Gdańsk 2007, pp. 415-418 (in polish).

ELECTRONICS AND TELECOMMUNICATIONS QUARTERLY, 2008, 54, no 2, pp. 203–221

Analysis of the CaTV splitters

DARIUSZ KRZEMIENIECKI, JAKUB JUCHNIEWICZ

Gdańskie Zakłady Teleelektroniczne TELKOM-TELMOR
80-425 Gdańsk ul. Mickiewicza 5/7
e-mail: dariusz.krzemieniecki@telmor.pl
jakub.juchniewicz@gmail.com

Received 2008.03.12
Authorized 2008.05.30

This article presents CaTV splitters. Basic features of splitters and influence of basic factors on crucial parameters were investigated in this article. Additionally, correction circuits for parameters improvement were proposed. The research considered two-way, three-way and four-way splitters. Some examples of applications of splitters in passive devices used in CaTV network were presented.

Keywords: splitter, divider, matching transformer (autotransformer)

1. INTRODUCTION

Splitters are common devices used in CaTV system. They are relatively simple devices, which are used for power division, mostly for equal parts. Splitters are willingly used by CaTV providers, as they are characterized by low attenuation and in opposite to threw type devices, they allow for direct access to subscriber. They are compounded of dividers and matching transformers (autotransformers). In the case of two-way splitter, matching transformer has from 2 to 5 turn ratio. The goal of the use of autotransformer is to improve the reflectance at the input. It was proved in [3]. Splitters are devices with wide working frequency band. Although CaTV networks have the working frequency band in the range 5-862 MHz, the working frequency band of splitters can be widened even to 3 GHz by using relevant techniques (the change in turn ratio).

Fig. 2, 3 illustrate characteristics of divider and autotransformator versus wide band of frequencies.

Splitters are described by following frequency dependent parameters: the input-output attenuation IN-OUT, the reflectance at the input IN and reflectance at the output OUT and isolation between outputs OUT A-B.

Microstrip lines have the characteristic impedance of 75 Ω.

2. THE TWO-WAY SPLITTER

2.1. THEORETICAL ANALYSIS

The node voltage method will be used for theoretical considerations. In the first place analysis of the divider will be carried out.

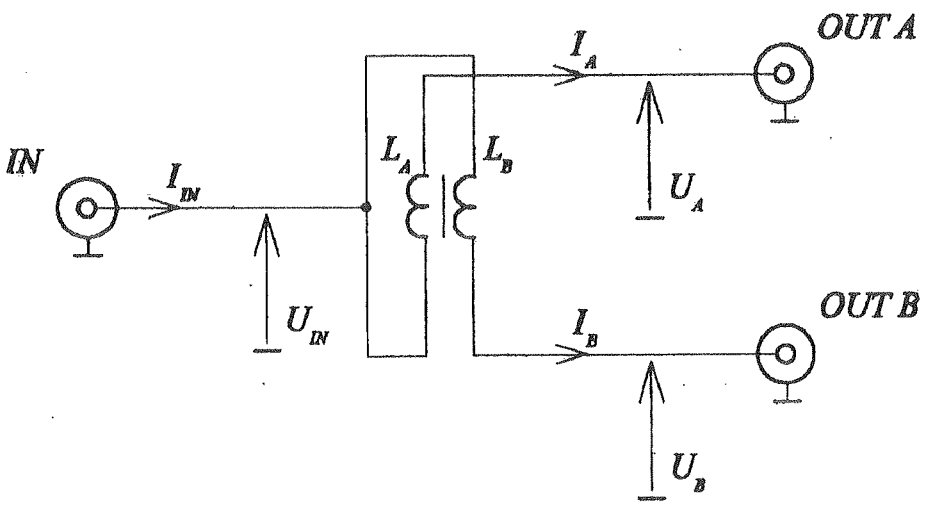

Fig. 1. The nodal model of the divider

According to Fig. 1 we can write voltage equations, then current equations can be written.

$$U_{IN}-U_A = j\omega L_A I_A - j\omega M_{AB} I_B \tag{1}$$

$$U_{IN}-U_B = -j\omega M_{BA} I_A + j\omega L_B I_B \tag{2}$$

$$I_A = (U_{IN}-U_A)\xi_{11} + (U_{IN}-U_B)\xi_{12} \tag{3}$$

$$I_B = (U_{IN}-U_A)\xi_{21} + (U_{IN}-U_B)\xi_{22} \tag{4}$$

A transconductance of the divider is marked as a ξ_{ij} symbol.
According to equations above, node equations can be derived.

For node "IN":

$$U_{IN}y_0 = U_I(\xi_{11}+\xi_{12}+\xi_{21}+\xi_{22}) - U_A(\xi_{12}+\xi_{22}) - U_B(\xi_{11}+\xi_{21}) \tag{5}$$

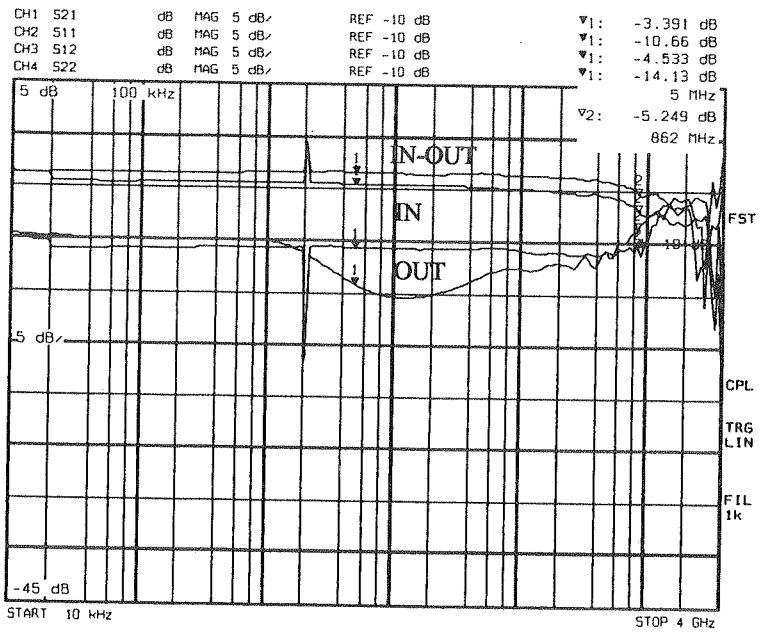

Fig. 2. The IN-OUT characteristic of the simple divider in wideband frequencies

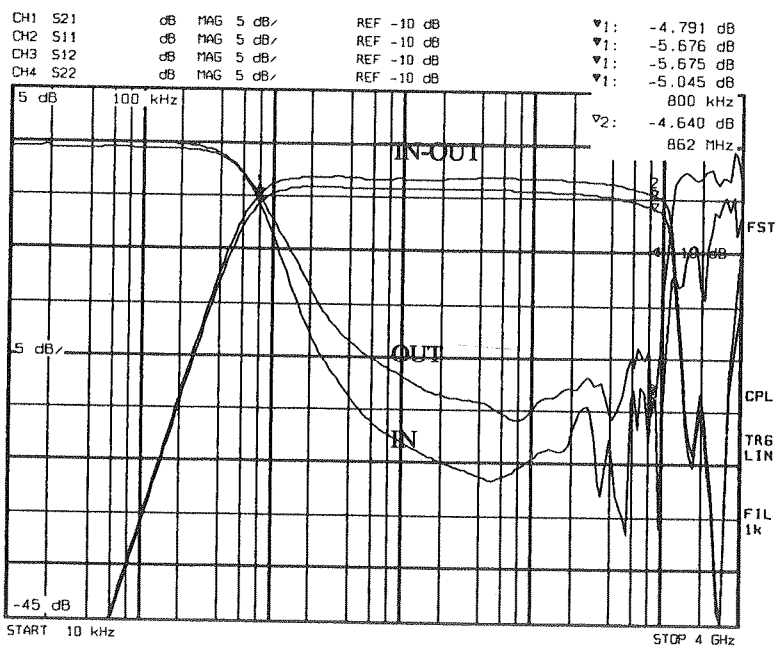

Fig. 3. The IN-OUT characteristic of the assembly: divider and autotransformer in wideband frequencies

For node "OUT A":

$$U_A y_0 = - U_{IN}(\xi_{21} + \xi_{22}) + U_A \xi_{22} + U_B \xi_{21} \tag{6}$$

For node "OUT B":

$$U_A y_0 = - U_{IN}(\xi_{11} + \xi_{12}) + U_A \xi_{12} + U_B \xi_{11} \tag{7}$$

The matching transformer (autotransformer) can be treated in a similar way.
Analysis is carried out using Fig. 4.

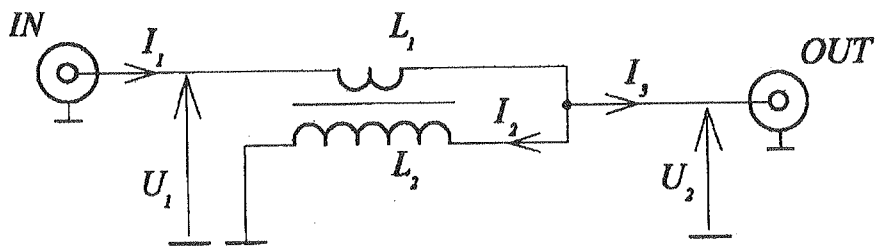

Fig. 4. The nodal model of the autotransformer

$$U_1 - U_2 = j\omega L_1 I_1 - j\omega M_{12} I_2 \tag{8}$$

$$U_2 = - j\omega M_{21} I_1 + j\omega L_2 I_2 \tag{9}$$

$$I_1 = (U_1 - U_2)\xi_{11} + U_2 \xi_{12} \tag{10}$$

$$I_2 = (U_1 - U_2)\xi_{21} + U_2 \xi_{22} \tag{11}$$

Node "IN":

$$U_1 y_0 = U_1 \xi_{11} + U_2(\xi_{12} - \xi_{11}) \tag{12}$$

Node "OUT":

$$U_2 y_0 = U_1(\xi_{21} - \xi_{11}) + U_2(\xi_{11} + \xi_{22} - \xi_{12} - \xi_{21}) \tag{13}$$

The admittance matrix of the autotransformer-divider circuit (Fig. 5) is presented in Table 1.
The scattering matrix and inductances are derived analogically to [5].

Fig. 6 presents measured, whilst Fig. 7 presents theoretical characteristics of the splitter. In order to complete our analysis, Fig. 8 illustrates circular charts of IN and OUT reflectances.

Because of similar reasons given in [5], the mathematical model is characterized by a certain precision, that is way some differences between measured and calculated values can be observed. About 10 % can be assumed as the precision of the model.

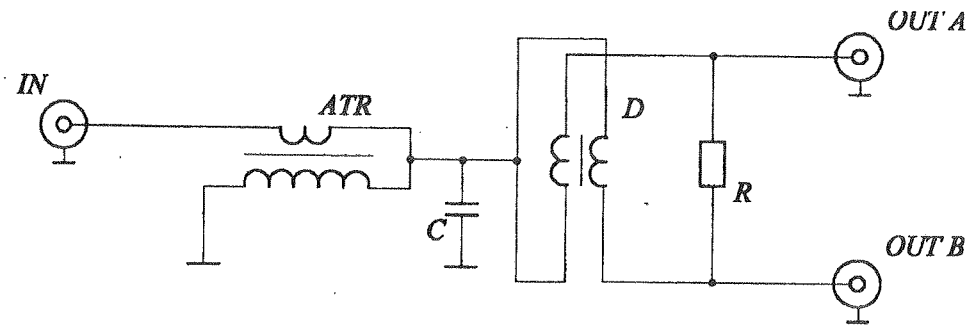

Fig. 5. The two-way splitter

Table 1

Admittance mattrix of the two-way splitter

node	*IN*	-	*OUT A*	*OUT B*
IN	y_{11A}	y_{12A}	*0*	*0*
-	y_{21A}	$y_{22A} + y_{11D} + j\omega C$	y_{12D}	y_{13D}
OUTA	*0*	y_{21D}	$y_{22D} + 1/R$	$y_{23D} - 1/R$
OUTB	*0*	y_{31D}	$y_{32D} - 1/R$	$y_{33D} + 1/R$

2.2. THE INFLUENCE OF THE SEPARATORY RESISTOR

A separatory resistance influences on OUT reflectance at the output and isolation between outputs OUT A-B. It has no influence on IN reflectance. Fig 9, 10 illustrate correlations of reflectance at the output OUT and isolation OUT A-B versus separatory resistance R and frequency respectively.

Main purpose for separatory resistance R use, is the improvement of isolation. The isolation can be additionally corrected at both low and high frequencies, by adding relatively high capacitance and serial small inductance. It is illustrated by Fig. 11.

It is worth to notice that reflectance IN at the input has great influence on isolation. The better reflectance, the better isolation is obtained.

2.3. THE INFLUENCE OF THE INITIAL PERMEABILITY

An initial permeability has a great impact on parameters of the splitter at low frequencies. Fig. 12, 13 present influence on characteristics of the autotransformer and divider respectively,

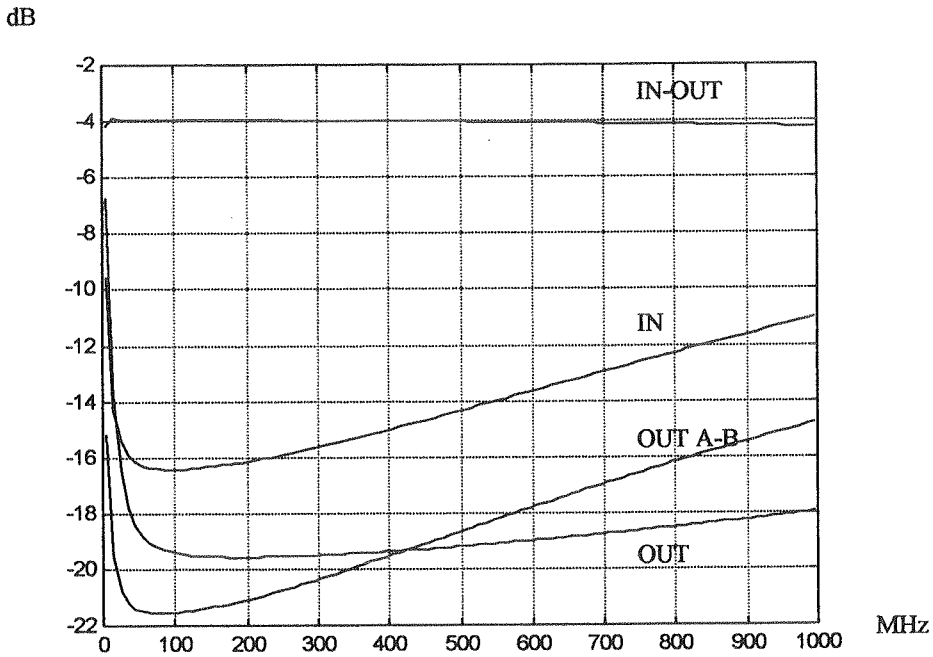

Fig. 6. Calculated frequency characteristics of the two-way splitter

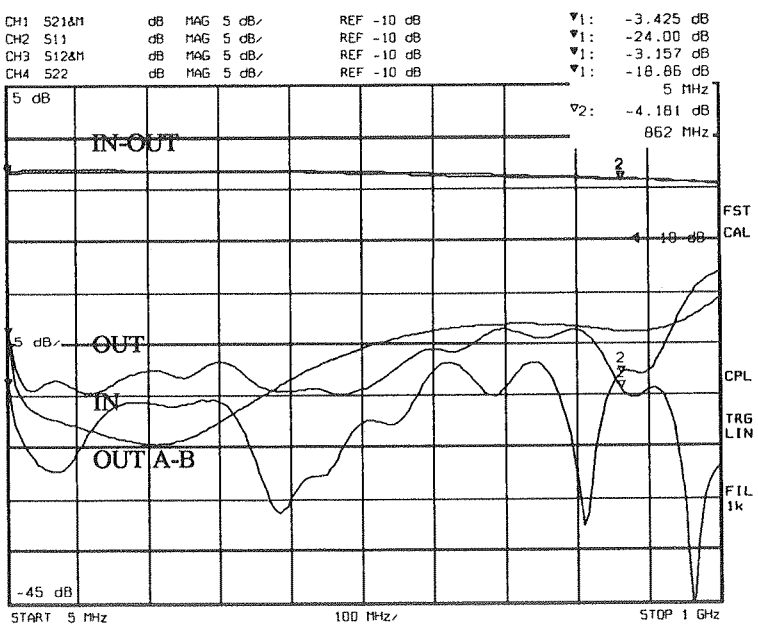

Fig. 7. Measured frequency characteristics of the two-way splitter

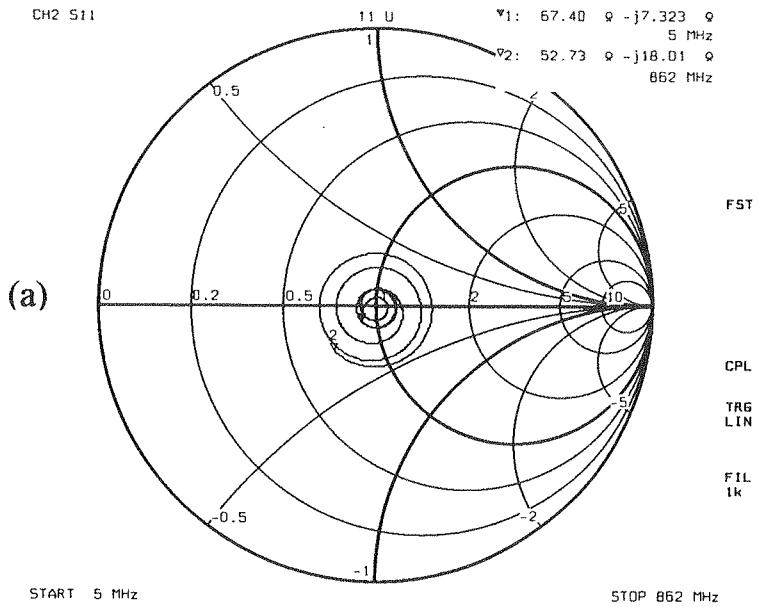

(a)

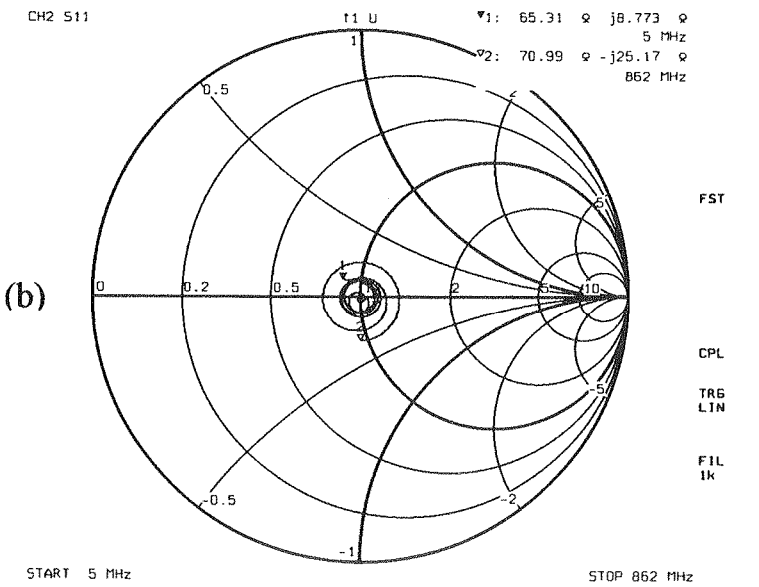

(b)

Fig. 8. Smith charts od the reflectances IN (a), OUT (b) of the two-way splitter

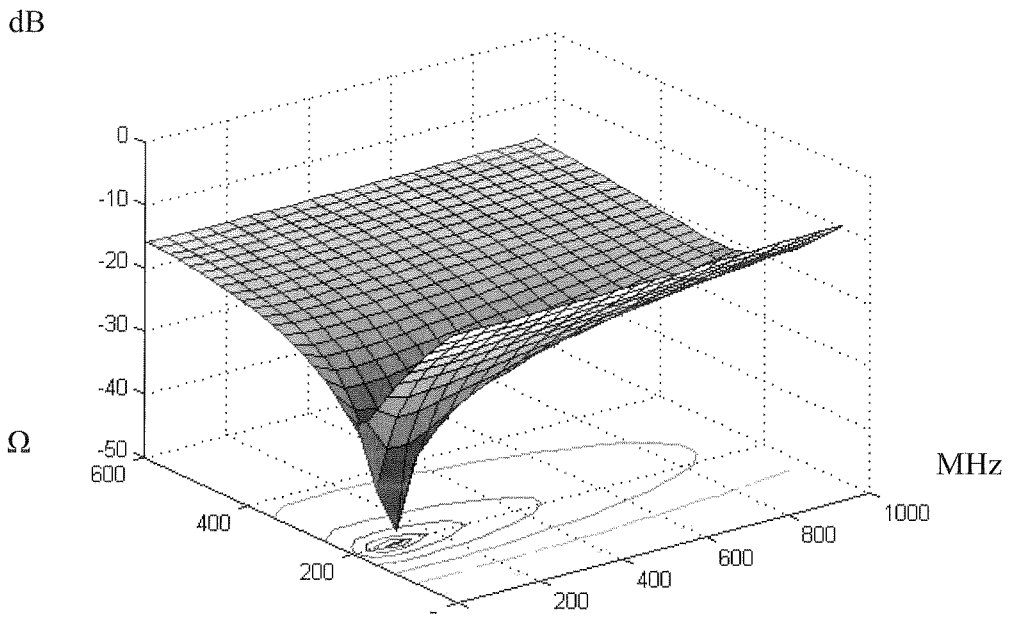

Fig. 9. The influence of the separatory resistance R, on the OUT parameter of the two-way splitter

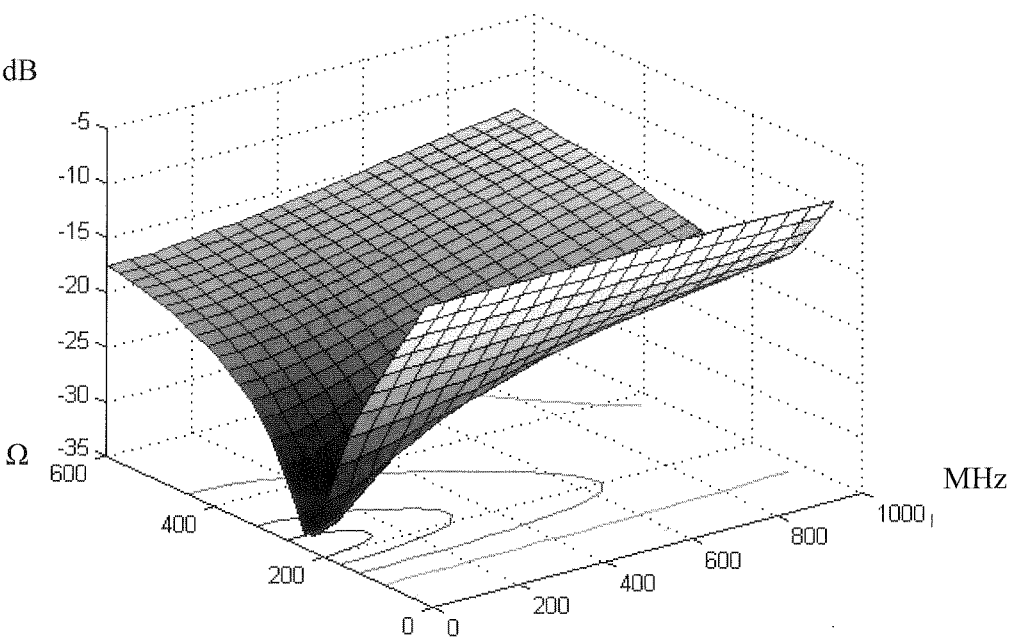

Fig. 10. The influence of the separatory resistance R, on the OUT A-B parameter of the two-way splitter

at frequency 5 MHz. It is noticeable (looking at charts) that because of isolation, which is the crucial parameter, ferrite cores with relatively low permeability are the most advantageous. Of high importance is the fact, that permeability values have relatively weak influence on IN-OUT attenuation characteristic, and that is positive trait.

2.4. THE INFLUENCE OF THE CAPACITANCE AND DISSIPATION

The capacitance and dissipation concern autotransformers. And in this case, similarly to unidirectional transformers [5], the influence of the capacitance and dissipation is firmly negative. These factors introduce low pass frequency band limitation and destructively affect reflectances IN, OUT and isolation OUT A-B. And similarly to unidirectional transformer case, smaller ferrite cores and appropriate turn winding technique, are used in order to improve splitter performance.

2.5. CORRECTION CIRCUITS

Correction circuits for low frequencies, like that which can be used in unidirectional transformers [5], or in splitterring taps [6], aren't applicable to splitters, because they are ineffective. Inductors used for isolation characteristic improvement (the inductance L_R at Fig. 11) and parallel capacitor placed between the autotransformer and divider (the capacitance C at Fig. 11) can be included to high frequency correctors. The C capacitance improves IN-OUT attenuation and reflectance IN characteristics at high frequencies. Utilization of LC circuit can also be helpful at high frequencies, like for unidirectional transformers and splitterring taps [5], [6].

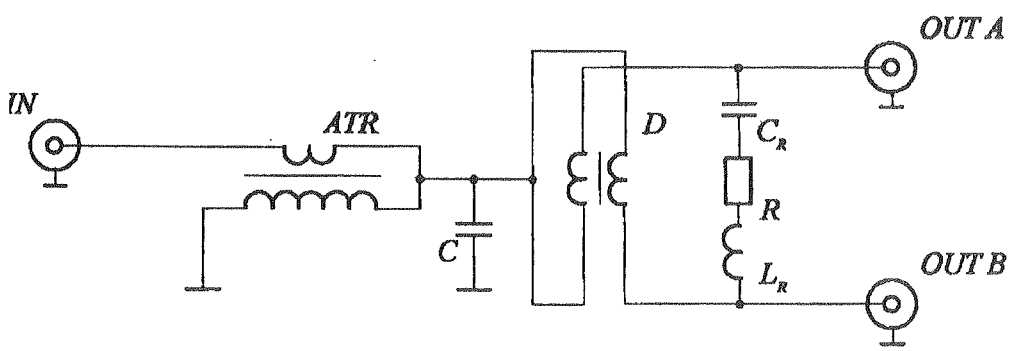

Fig.11. The two-way splitter with correction circuits

2.6. APPLICATIONS

The two-way splitter can be used not only as an autonomous splitter. Different example of its application can be used an advanced multimedia separator type splitter [4], [7]. The splitter is the crucial element of this device. The device is the synthesis of the splitter, high pass HPF and low pass LPF filters. Diagram of the separator is illustrated by Fig. 14 and its lookout is presented by photo at Fig. 15.

The splitter is equipped with isolation between input ground and suppressing line providing electromagnetic compatibility EMC [7].

Fig. 16 present basic characteristics of the separator versus frequency.

3. THE THREE-WAY SPLITTER

Dividers and autotransformers are crucial elements which can be used as a base for multi-way splitters. The three-way splitter is presented by Fig. 17. This device use one symmetrical divider and two nonsymmetrical dividers. A signal at the middle output (OUT B) is a sum of lower power nonsymmetrical divider outputs. The autotransformer has from 3 to 4 turn ratio.

Theoretical analysis will be taken as previously. Fig. 19, 20 illustrate theoretical and measured characteristics of the three-way splitter.

For this splitter configuration none additional separation resistors are utilized because it is ineffective.

Fig. 12.

The best initial permeability value of ferrite core is generally low. Fig. 21 presents examples of isolation characteristics for particular inductors.

Similarly to the two-way splitter, the three-way splitter can use high frequency correctors such as: LC circuit at the input [5] and correction capacitors between autotransformers and nonsymmetrical dividers (capacitor C at Fig. 17).

4. THE FOUR-WAY SPLITTER

Construction of the four-way splitter is similar to the three-way splitter structure (Fig.18). The main difference is that, this structure uses symmetrical dividers and isolated four outputs (in opposition to the three-way splitter there is no sum of signals at the ouput). Different turn ratio is used also (3 to 3).

Fig. 22, 23 illustrate theoretical and measured characteristics of the four-way splitter.

In this case it is advantageous to use isolation resistors connected to the outputs of dividers. It improves TAP A-B isolation. However it is hard to find trade-offs between isolation and reflectance at the input IN and between IN-OUT attenuation. Optimal resistor's value equals about 390 Ω. Generally, low initial ferrite core permeability value provides advantageous performance, what is similar to prior cases (Fig. 24, 25).

Correction circuits can be utilized as in prior splitter constructions.

Fig. 13. T

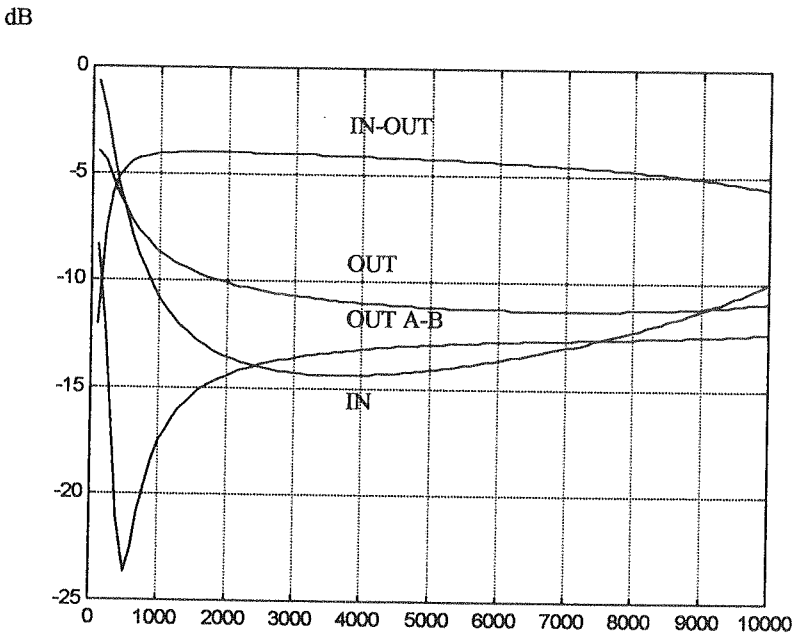

Fig. 12. The influence of the initial permeability of the autotransformer on the parameters of the two-way splitter, at frequency 5 MHz

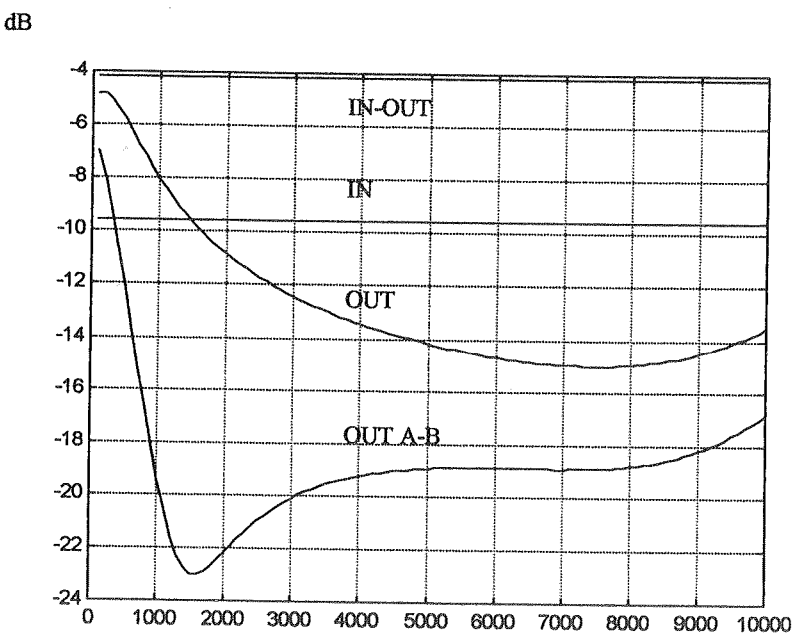

Fig. 13. The influence of the initial permeability of the divider on the parameters of the two-way splitter, at frequency 5 MHz

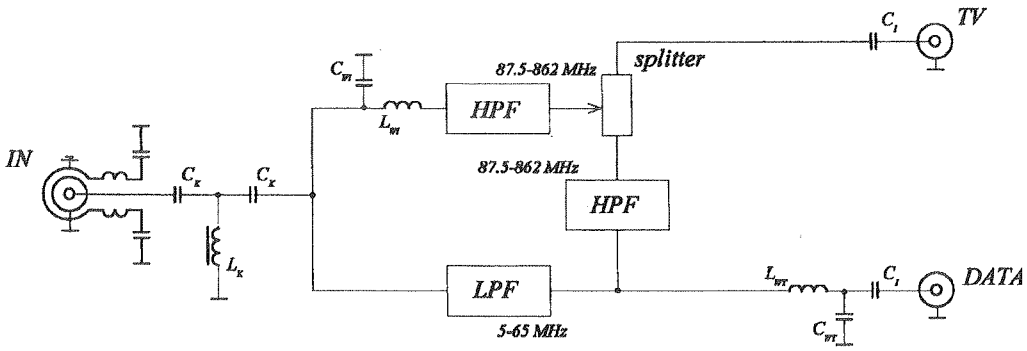

Fig. 14. The schematic diagram of the multimedia separator

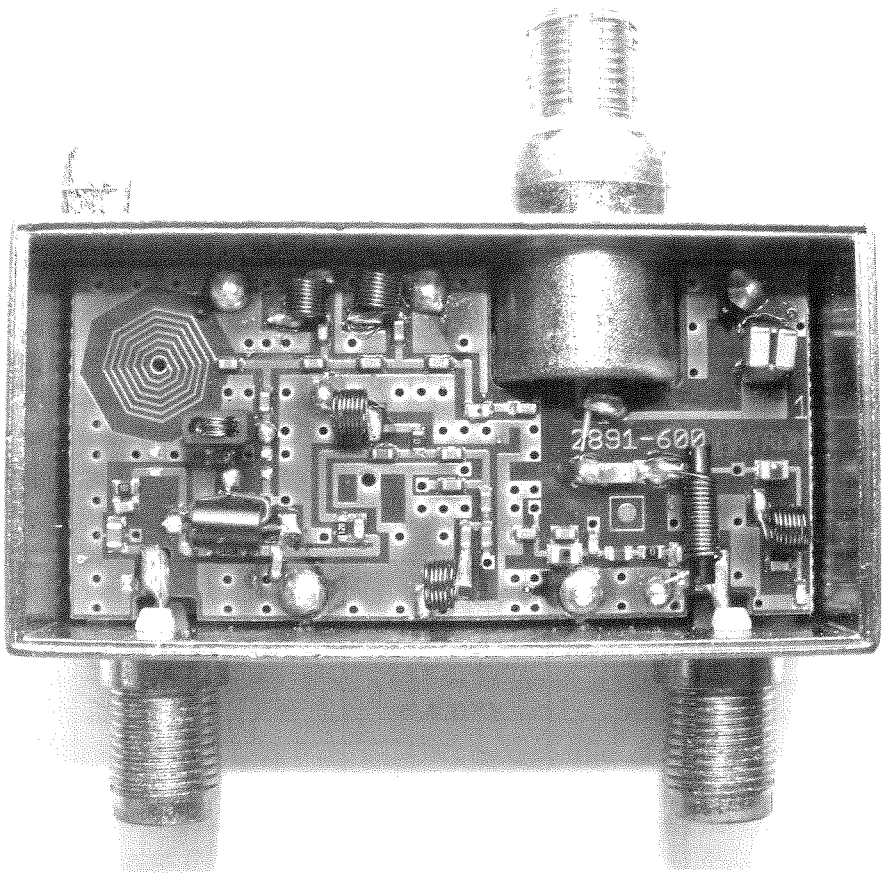

Fig. 15. The photo of the multimedia separator

(a)

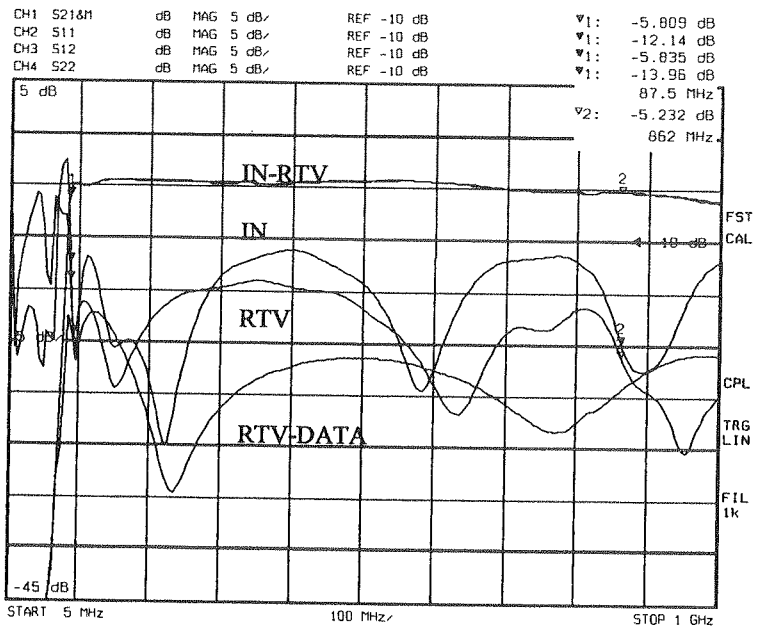

(b)

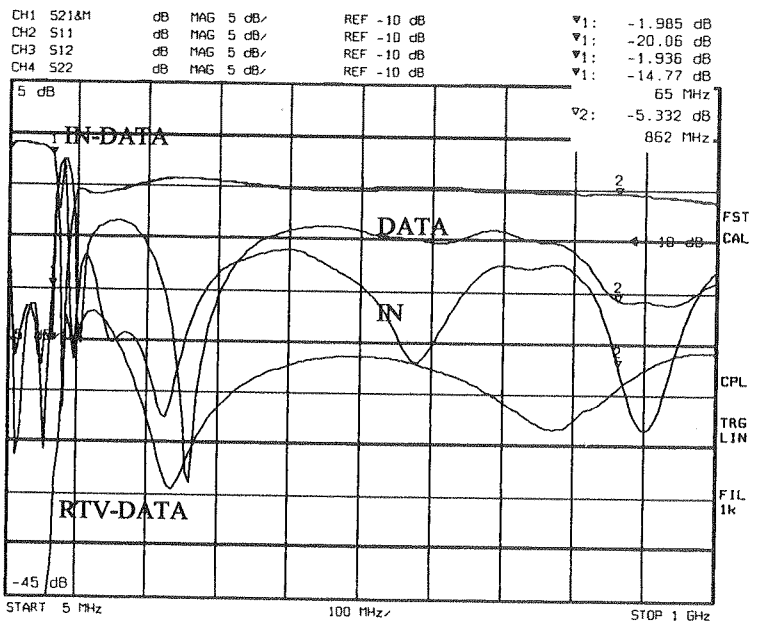

Fig. 16. Main characteristics of the advanced multimedia separator

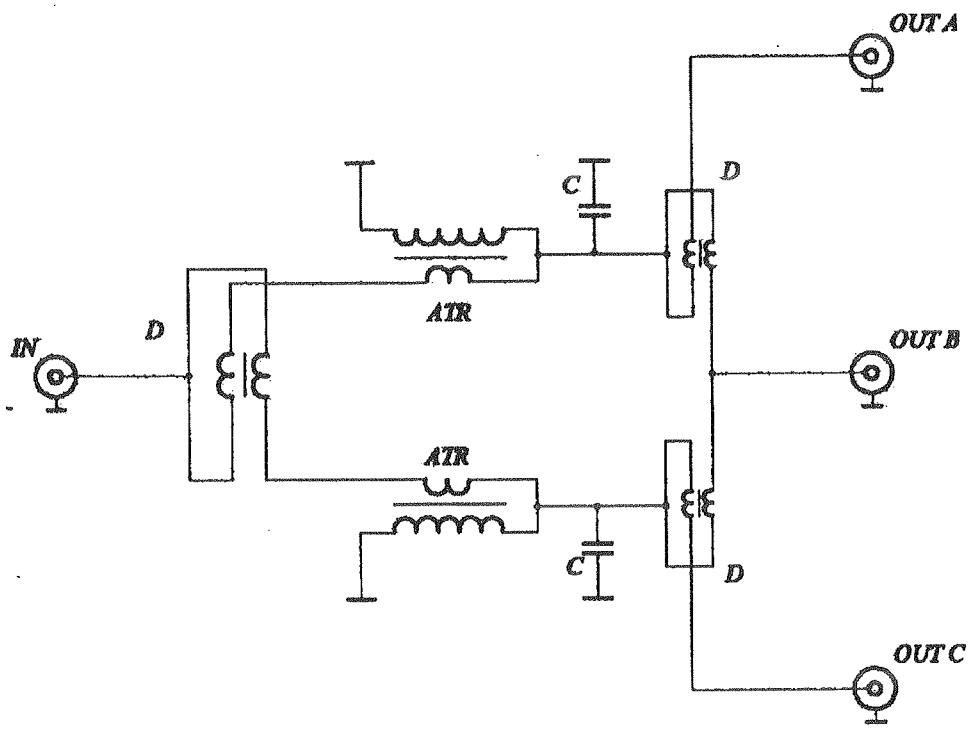

Fig. 17. The three-way splitter

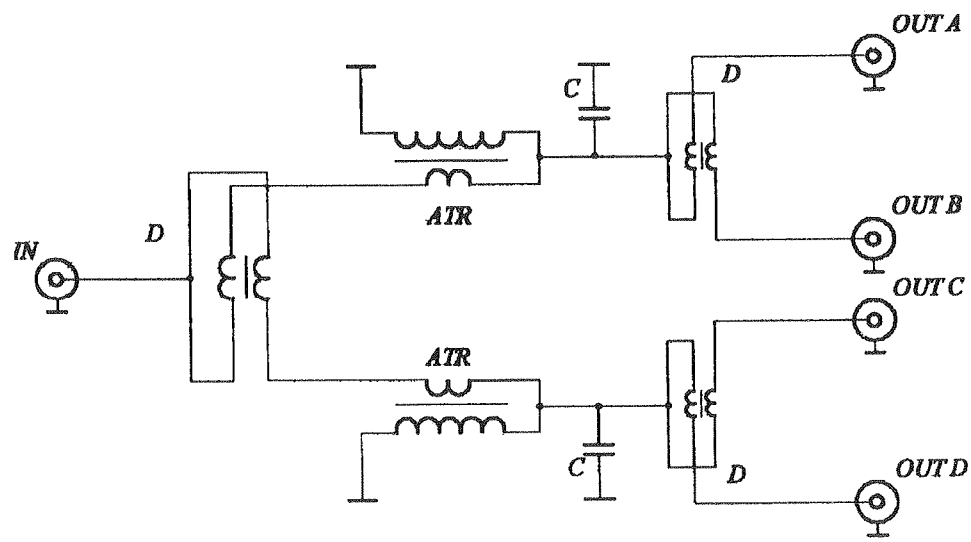

Fig. 18. The four-way splitter

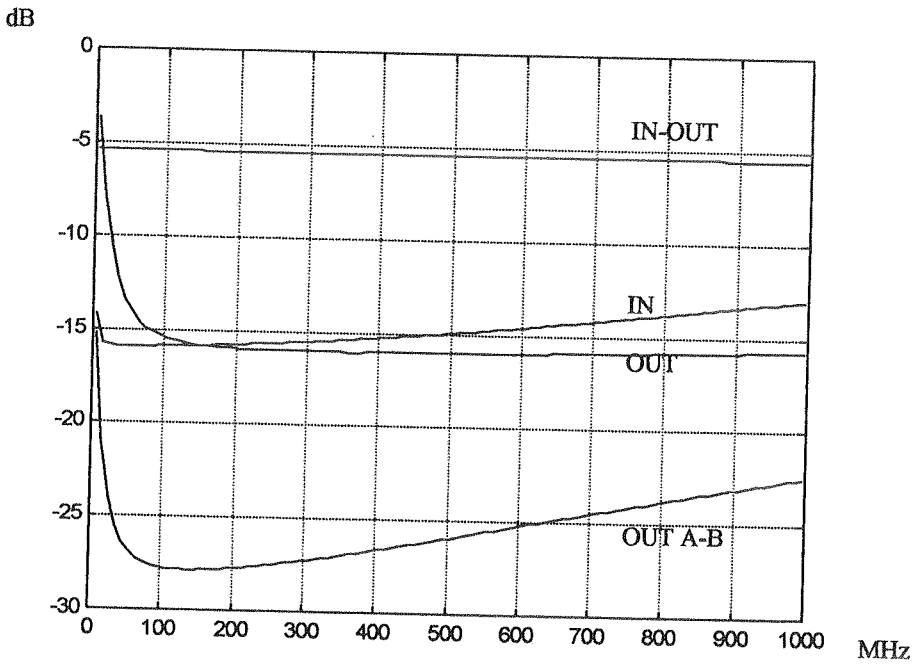

Fig. 19. Calculated frequency characteristics of the three-way splitter

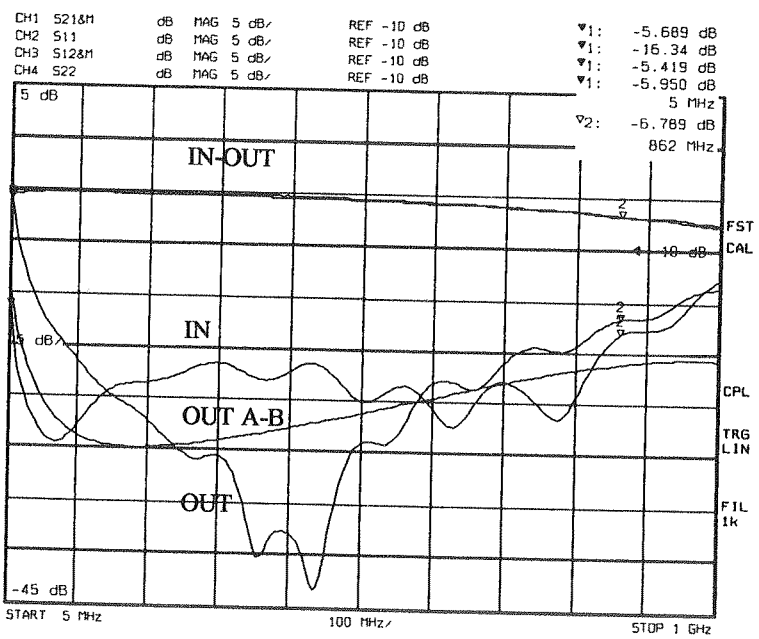

Fig. 20. Measured frequency characteristics of the three-way splitter

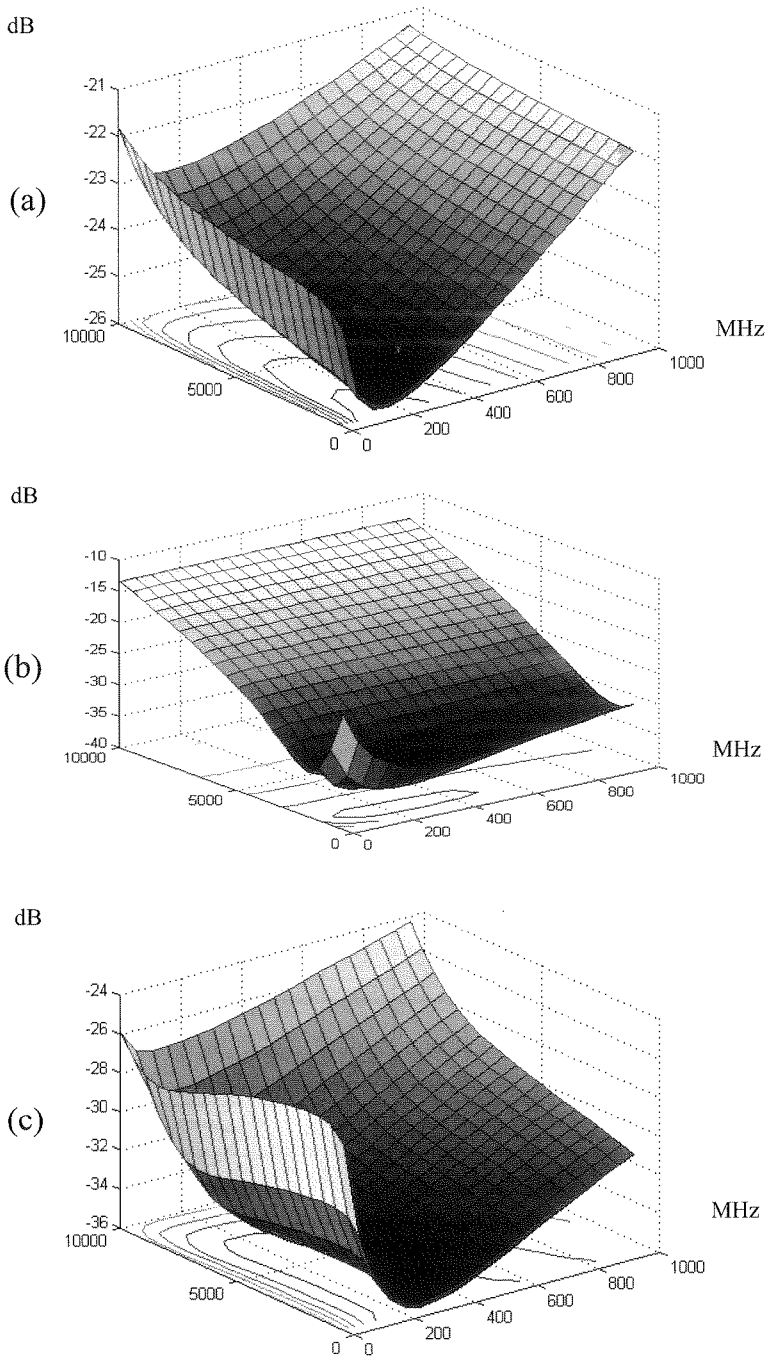

Fig. 21. The influence of the initial permeability of the autotransformer (a), symmetrical divider (b) and unsimmetrical divider (c) on the OUT A-B parameters of the three-way splitter

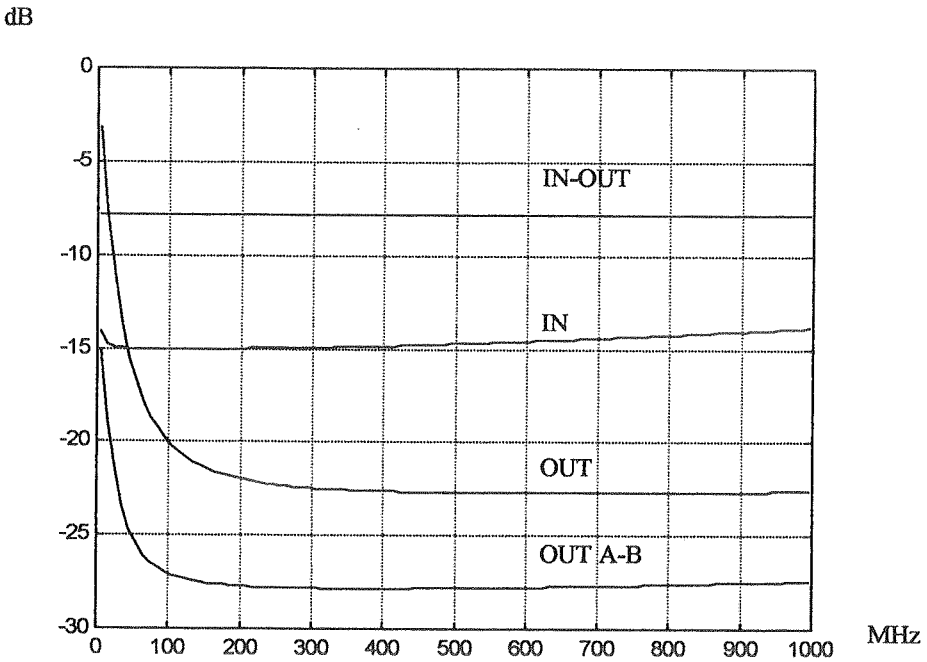

Fig. 22. Calculated frequency characteristics of the four-way splitter

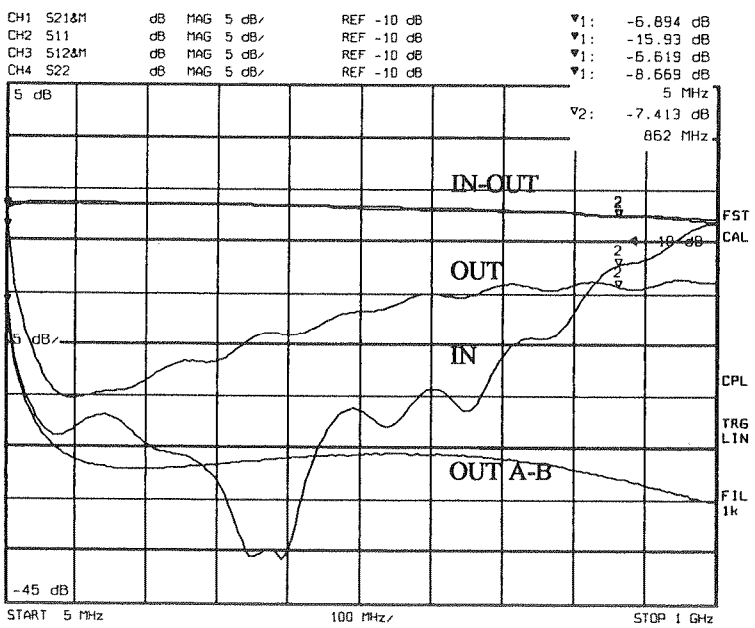

Fig. 23. Measured frequency characteristics of the four-way splitter

nmetrical

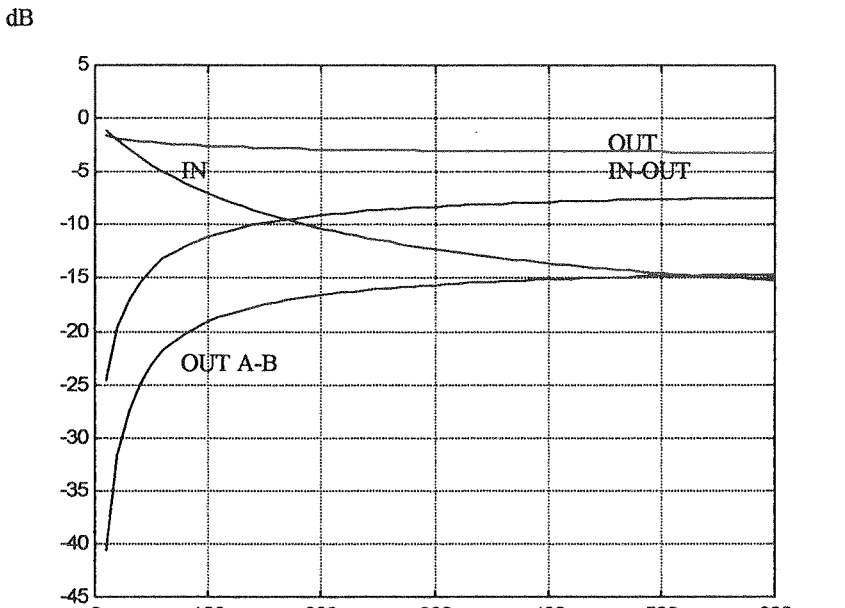

Fig. 24. The influence of the separatory resistor on parameters of the four-way splitter, at frequency 5 MHz

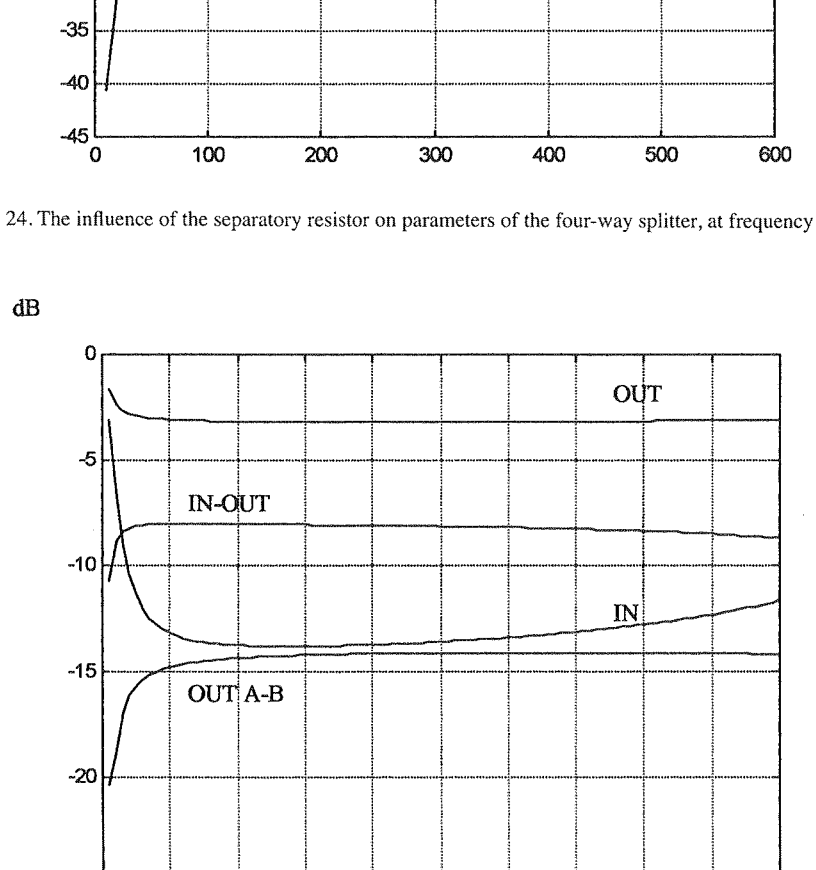

Fig. 25. The influence of the initial permeability of the autotransformer on parameters of the four-way splitter, at frequency 5 MHz

5. CONCLUSIONS

The divider, presented in the introduction part, is a basic element for multi outputs splitter. In order to maintain relevant level of reflectance IN, OUT it is necessary to add matching transformers (autotransformers) [3]. In the two-way splitter matter, utilization of low values of permeability of ferrite core increases isolation between outputs OUT A-B. That low value of permeability has positive influence on intermodulation distortions.

Generally splitters of greater number of outputs have better performance for ferrite cores of low values of permeability, however in some cases, depending on splitter outputs, cores of higher permeability value could be more beneficial.

Splitters are generally wide band passive devices (the autotransformer introduces low frequency limitation, whilst inductances of autotransformers, inductances of dividers and self-capacitances of autotransformers introduce high frequency limitation). Although this paper presents splitters working in CaTV frequency band (5-862 MHz), it is worth to know that lower turn ratio (1:3) and microstrip technique utilization, can widen the working frequency band of the splitter even to 3 GHz. Lower turn ratio decreases self-capacitances what results in wider working frequency band (frequency limitation is passed to higher frequencies). However, it increases attenuation.

The characteristic impedance of splitters was assumed as 75 Ω (standard impedance for transmission lines in CaTV system). It is necessary to remember that change in the characteristic impedance value comes with changes in splitter parameters. The increase of the characteristic impedance results in higher IN-OUT attenuation. Moreover, the increase in the characteristic impedance value causes worse IN and OUT reflectances. This rule is applicable to splitters described in this article.

6. REFERENCES

1. D.I. Kim, M. Takahashi, K. Araki, Y. Naito: *Optimum design of the power dividers with ferrite toroids for CATV and/or MATV systems*. IEEE Trans. On Consumer Electronics, vol. CE-29, no 1, Feb. 1983, pp. 27-38.
2. Y. Naito: *Formulation of frequency dispersion of permeability*. Trans. IECE, vol. 59-c May 1976, pp. 297-304.
3. D.I. Kim, S.W. Jung, Y. Yun: *A high performance transformer-type Wilkinson power splitter with compensating circuit for CATV transmission system and its optimal design method*. IEEE Trans. On Consumer Electronics, vol. 50, no 3, Aug. 2004, pp. 934-940.
4. D. Krzemieniecki: *Advanced splittering multimedia separators*. National Telecommunication Symposium, Bydgoszcz 2001, vol. A, pp. 411-420 (in polish).
5. D. Krzemieniecki: *Investigation and optimization of the wideband directional transformer*. Electronics and Telecommunication Quarterly, 2005, 51, vol. 1, pp. 105-135 (in polish).
6. D. Krzemieniecki: *Current posibilities of projecting of the taps arrangements*. National Conference of Radiocommunication, Radio and Television, Poznań 2006, pp. 457-460 (in polish).
7. D. Krzemieniecki: *Advanced multimedia outlets and separators with full isolation*.. National Conference of Radiocommunication, Radio and Television, Gdańsk 2007, pp. 415-418 (in polish).

An arti
not exc

Basic r
The arti
copies.
should
Layout
– Title
– Autho
– Workp
– Conci
– Main
  • In
  • T
  • N
  • P
  • P
  • ...
  • C
  • A
  • R

Pages sh

Main te
Main tex
that are c
the articl
Text shou
written w

Tables
Tables w
should be
directly b
contain a
be cited i

Mathema
Character
should be
arrows, d
with Arab
symbols s
(Internatio

Referenc
Reference
(without b
book [3] r

INFORMATION FOR AUTHORS OF E.T.Q.

An article published in other magazines can not be submitted for publishing in E.T.Q. The size of an article can not exceed 30 pages, 1800 characters each, including figures and tables.

Basic requirements

The article should be submitted to the editorial staff as a one side, clear, black and white computer printout in two copies. The article should be prepared in English. Floppy disc or a CD with an electronic version of the article should be enclosed.

Layout of the article:

- Title
- Author (first name and surname of author/authors)
- Workplace (institution, address and e-mail)
- Concise summary
- Main text with following layout:
  - Introduction
  - Theory (if applicable)
  - Numerical results (if applicable)
  - Paragraph 1
  - Paragraph 2
  - .....
  - Conclusions
  - Acknowledgements (if applicable)
  - References

Pages should have continuous numbering.

Main text

Main text cannot contain formatting such as spacing, underlining, words written in capital letters (except words that are commonly written in capital letters). Author can mark suggested formatting with pencil on the margin of the article using commonly accepted adjusting marks.

Text should be written with double line spacing with 35 mm left and right margin. Titles and subtitles should be written with small letters. Titles and subtitles should be numbered using no more than 3 levels (i.e. 4.1.1)

Tables

Tables with their titles should be placed on a separate page at the end of the article. Titles of rows and columns should be written in small letters with double line spacing. Annotations concerning tables should be placed directly below the table. Tables should be numbered with Arabic numbers on the top of each table. Table can contain algorithm and program listings. In such cases original layout of the table will be preserved. Table should be cited in the text.

Mathematical formulas

Characters, numbers, letters and spacing of the formula should be adequate to layout of the article. Indexes should be properly lowered or raised above the basic line and clearly written. Special characters such as lines, arrows, dots should be placed exactly over symbols which they are attributed to. Formulas should be numbered with Arabic numbers placed in brackets on the right side of the page. Units of measure, letters and graphic symbols should be printed according to requirements of IEC (International Electronical Commission) and ISO (International Organisation of Standardisation).

References

References should be placed at the main text with the subtitle "References". References should be numbered (without brackets) adequately to references palced in the text. Examples of periodical [1], non-periodical [2] and book [3] references:

1. F. Valdoni: A new milimetre wave satelite. E.T.T. 1990, vol. 2, no 5, pp. 141-148
2. K. Andersen: A resource allocation framework. XVI International Symposium, Stockholm (Sweden), may 1991, paper A 2,4
3. Y.P. Tvidis: Operation and modeling of the MOS transistors. New York, McGraw-Hill, 1987, p. 553

Figures

Figures should be clearly drawn on plain or milimetre paper in the format not smaller than 9x12 cm. Figures can be also printed (preferred editor - CorelDRAW). Photos or diapositives will be accepted in black and white format not greater than 10x15 cm. On the margin of each drawing and on the back of each photo author name and abbreviation of the article title should be placed. Figures captures should be listed on a spearete page. Figures should be cited in the text.

Additional information

On a separate page following information should be placed:
– mailing address (home or office)
– phone (home and/or office)
– e-mail

Author is entitled to free of charge 20 copies of article. Additional copies or the whole magazine can be ordered at publisher at the ones expense.

Author is obliged to perform the athors correction, which should be accomplished within 3 days starting from the date of receiving the text from the editorial staff. Corrected text should be returned to the editorial staff personally or by mail. Correction marks should be placed on the margin of copies received from the editorial staff or if needed on separate pages. In the case when the correction is not returned within said time limit, correction will be performed by technical editorial staff of the publisher.

In case of changing of workplace or home address authors are asked to inform the editorial staff.